CHARACTERISTICS OF GROUND ALFALFA IN RELATION TO STEAM CONDITIONING

A Thesis Submitted to the College of
Graduate Studies and Research
in Partial Fulfillment of the Requirements
for the Degree of Doctor of Philosophy
in the Department of Agricultural and Bioresource Engineering
University of Saskatchewan
Saskatoon

by

Weihua Yang

Spring 1998

PERMISSION TO USE

The author has agreed that the Library, University of Saskatchewan, may make this thesis freely available for inspection. Moreover, the author has agreed that permission for extensive photocopying of this thesis for scholarly purpose may be granted by the professor or professors who supervised the thesis work recorded therein or, in their absence, by the Head of the Department or the Dean of the College in which the thesis work was done. It is understood that due recognition will be given to the author of this thesis and to the University of Saskatchewan in any use of the material in this thesis. Copying or publication or any use of the thesis for financial gain without approval by the University of Saskatchewan and the author's written permission is prohibited.

Requests for permission to copy or to make any other use of the material in this thesis in whole or in part should be addressed to:

Head of the Department of Agricultural and Bioresource Engineering
University of Saskatchewan
57 Campus Drive
Saskatoon, Saskatchewan
CANADA S7N 5A9

ABSTRACT

Conditioning is an intermediate process in alfalfa pelleting designed to make alfalfa grind easier to bind. It is an important step because the quality of the final pellets depends to a great extent on the quality of the conditioned mash. The mash pliability is in turn dictated by the fundamental characteristics of the alfalfa grind such as its morphological attributes, thermal properties, rate of moisture diffusion, and equilibrium moisture relationship. There has so far been a lack of research pertinent to the characteristics imperative to the improvement of mash quality. This study was conceived for such a need, in which physical, morphological, thermal, moisture diffusion, and moisture equilibrium characteristics of alfalfa grind were scrutinized.

The physical properties studied were the density of alfalfa grind as affected by particle size and moisture content, particle size distribution, and particle characterization. The bulk and the solid densities of alfalfa grind ranged from 205 to 257 kg/m^3 and 1218 to 1367 kg/m^3, respectively, at the moisture contents ranging from 0.0057 to 0.47 (w/w, db) and 0.038 to 0.52 (w/w, db), respectively. The bulk and the solid densities of alfalfa grind ranged from 187 to 242 kg/m^3 and 1214 to 1432 kg/m^3, respectively, in the particle undersize range of 150 μm to 1000 μm. Models have been developed to correlate the bulk and the solid densities to moisture content and particle size. The particle size of alfalfa grind distributed log-normally with a median size of 238 μm and a log-normal S.D. of 0.65. The surface area of alfalfa grind particles based on sieving tests was 0.0215 m^2/g, which was much lower than measured by nitrogen sorption that (i.e., 0.75 m^2/g, standard deviation 0.26). The difference was attributed to the pores, cracks and fissures in the particles that could trap nitrogen. The mean particle length, width, area and perimeter of alfalfa grinds were in the ranges of 0.074-0.979 mm, 0.034-0.425 mm, 0.002-0.295 mm^2, and 0.188-2.421 mm, respectively, in the sieve openings from 20 to 850 μm. The overall sphericity (roundness) of alfalfa particles ranged from 0.54 to 0.64.

The thermal properties studied were specific heat capacity, thermal conductivity and thermal diffusivity. The specific heat capacity of alfalfa grind determined by differential scanning calorimetry varied from 0.9 to 2.2 kJ/kg.K at temperatures from 10 to

110°C and moisture contents from 0.0054 to 0.32 (w/w, wb). The thermal conductivity and the thermal diffusivity of alfalfa grind ranged from 0.025 to 0.072 W/m.K and from 1.0×10^{-7} to 1.6×10^{-7} m^2/s, respectively, at temperatures from 9 to 80°C and moisture contents from 0.0054 to 0.32 (w/w, wb). A multiple regression model was developed to correlate the specific heat, thermal conductivity and thermal diffusivity of alfalfa grind to moisture content and temperature.

Moisture diffusion characteristics of alfalfa grind were studied in terms of moisture diffusivity. Based on thin-layer kinetics, the moisture diffusivity of whole dehydrated alfalfa grind was 3.03×10^{-8} m^2/s. The moisture diffusivity of the fractionated and the sun-cured dehydrated alfalfa grind ranged from 3.13×10^{-8} to 2.19×10^{-7} m^2/s and 5.19×10^{-8} to 4.11×10^{-7} m^2/s, respectively, in the particle undersize range of 0.149 to 1.4 mm. There was a significant difference in moisture diffusivity between the dehydrated and the sun-cured alfalfa grinds (α=0.05). From the "ring stack" diffusion tests, a mean diffusivity of 8.55×10^{-8} m^2/s resulted for the whole dehydrated grind. The moisture diffusivity of the fractionated dehydrated alfalfa grind ranged from 1.43×10^{-8} to 5.86×10^{-8} m^2/s in the particle undersize range of 0.149 mm to 1.0 mm. The moisture diffusivity of alfalfa grind ranged between 9.15×10^{-10} to 8.55×10^{-8} m^2/s in the packing density range of 240 to 1395 kg/m^3, following a power relationship with packing density. It was also found that the relationship between the moisture diffusivity of alfalfa grind and particle undersize could be best described by the Gaussian function.

Moisture equilibrium characteristics of alfalfa grind included moisture sorption isotherms and hysteresis behavior. The equilibrium moisture content (EMC) values of alfalfa grind ranged from 0.035 to 0.44 (w/w, db) in the equilibrium relative humidity (ERH) range of 0.123 to 0.925 at 9°C, from 0.039 to 0.35 (w/w, db) in the ERH range of 0.154 to 0.909 at 25°C, and from 0.031 to 0.33 (w/w, db) in the ERH range of 0.163 to 0.998 at 50°C. A best-fit model was developed for describing the isotherms of alfalfa grind. The magnitude of the hysteresis of alfalfa grind ranged from 0.028 to 0.058 (w/w, db), 0.014 to 0.031 (w/w, db), and 0 to 0.018 (w/w, db) at 9°C, 25°C, and 50°C, respectively, in the relative humidity range of 0.123 to 0.998. A hypothesis was proposed to account for the origin of sorption hysteresis. Based on the hypothesis a mathematical

model was developed to quantify the magnitude of hysteresis loops. The applicability of the model developed has been verified by the hysteresis data of alfalfa grind.

Pilot-scale steam conditioning tests of alfalfa grind have been conducted in this study. Semi-empirical models have been developed for describing the meal temperature and moisture content trends in a steam conditioner. The goodness-of-fit of the models were verified with the pilot-scale steam conditioning test results.

ACKNOWLEDGEMENT

I would like to extend my heartfelt gratitude to Dr. Shahab Sokhansanj, my supervisor for his support in every phase of this thesis.

Many thanks to my thesis examination committee (Dr. D.I. Norum, Dr. E.M. Barber, Dr. R.L. Kushwaha, and Dr. G. Strathdee) and my external examiner, Dr. L. Correia, for their constructive criticism and comments.

Thanks are also due to Wayne Morley (electronic technologist), Louis Roth (mechanical technologist) and Russ Bikner (equipment coordinator) of the Department of Agricultural and Bioresource Engineering for their assistance in experimental setup.

I would also like to thank Dr. P.M. Huang, Department of Soil Science, for allowing me to use his Autosorp-1 Nitrogen sorption device, Dr. S. Yanoccopolis, Department of Mechanical Engineering, for permitting me to use his DSC unit, Dr. S. Rohani, Department of Chemical Engineering, for permitting me to use his Gilsonic Autosiever, and Mr. Yukio Yano, Department of Biology, for his assistance in Scanning Electron Microscopy.

Many thanks to my colleagues in the BPEG, specifically, Mr. Bill Crerar, Mr. Maurice Romaniuk, Mr. Phil Winter, Dr. R. Patil, Dr. L. Tabil, Jr., Dr. H. Koshtaghaza and Mr. K.K. Krishna for their assistance in the instrumentation, image processing and experiments.

Thanks also go to the College of Graduate Studies and Research, University of Saskatchewan for providing me with the graduate scholarship during my Ph.D. program, and Natural Science and Engineering Research Council (NSERC) and Canadian Dehydrators Association (CDA) for their financial support in the experiments.

I am also greatly indebted to my employer, International Business and Engineering Corporation, for their support in my thesis writing and defence.

I would like to thank my beloved wife, Tianyu Liu, for her help in data collection and analyses and my friends and relatives for their moral support.

TABLE OF CONTENTS

LIST OF FIGURES

LIST OF TABLES

NOTATIONS

Symbols

a - model constant
a_w - water activity
A - model constant; projection area of a particle; cross-sectional area
A' - model constant
A_{cs} - cross-sectional area of nitrogen molecule
b - model constant
B - model constant
c - specific heat; model constant
c_p - specific heat
C - model constant; vapor concentration
d - nominal sieve opening; model constant
D - overall effective diffusion coefficient; diameter
E - enthalpy
ΔE - enthalpy due to sorbate-sorbent interactions
f - voidity of the meal bulk
g - the magnitude of the energy of a spherical source
GF - Green's function
h - the amount of redistributed sorbate in either adsorption or desorption; screw flight height
H - overall hysteresis either inside or outside the spherical source (with subscript); total hysteresis in the entire material (without subscript)
I - electric current
k - thermal conductivity; drying or rewetting constant
L - latent heat of vaporization or condensation; enthalpy due to phase change
m - the mass of sorbate; moisture content
M - molecular weight of adsorbate; moisture content
MR - moisture ratio
n - number of sieves + 1
N - molar number; Avogadro's number; number of particles in a charge; rotation speed
P - pressure of a system; perimeter of a projected area
p - vapor pressure of water; partial pressure of adsorbate
p_o - vapor pressure of water (or adsorbate) at saturation
q - heat transfer rate
r - the radius in spherical or cylindrical polar coordinates
r_o - radius of a continuously distributed spherical energy source
RH - relative humidity (interchangeable with a_w)
R - universal gas constant; roundness; electric resistance
S - geometric standard deviation; specific surface area; slope
S_t - total surface area
t - time
t_o - the time at which the energy of spherical energy source pulses

T - temperature
u - meal flow velocity
U - particle undersize
V - molar volume of the sorbate
w - mass of adsorbate; channel width
W - sample mass or mass retained on a sieve
α - thermal diffusivity; slope; proportionality constant; screw flight inclination angle
β - a coefficient between 0 and 1; intercept; shape factor
θ - angle of contact
ρ - density
σ - surface tension; distribution spread index
m - chemical potential; median particle size
d - the Dirac delta function
f - surface potential or spreading pressure; sphericity
Γ- an intermediate temperature

Subscripts

a - pure sorbent; adsorption
A - air; gas phase
b - sorbate in sorbent; bulk; conditioner surface
ave - average
b,c - pertinent to boundary condition
c - mean; container
d - desorption
e - equilibrium
i - pertinent to initial condition; within spherical source
g - pertinent to internal generation
gw - geometric mean by mass
ln - log-normal distribution
m - monolayer; meal
p - point source
pa - sorbent containing sorbed water
s - the whole material (sorbent plus sorbate); sorbate vapor; shape; surface; solid
t - total
T - pertinent to a temperature T
v - pertinent to volume
w - sorbate in liquid state; water
θ - outside spherical source
Γ- at an intermediate temperature Γ
o - initial; equilibrium; pertinent to spherical source; saturation
1 - local; altered; pertinent to temperature T_1; sorbed water

Chapter 1

INTRODUCTION

Forages are dried, ground and pelleted for animal feed. Ground forage like alfalfa grind is usually steam conditioned in practice before entering the subsequent pelleting process. Figure 1.1 is a diagram showing a typical steam conditioning process. Following size reduction in a hammer mill or grinder, alfalfa grind is introduced into the conditioner through a feeder such as the vibratory feeder shown in Figure 1.1. Alfalfa grind is conveyed from the intake to the discharge end of the conditioner by a rotating paddle, while mixed with steam injected into the conditioner. The conditioner is insulated to reduce heat loss. External heaters are sometimes used to provide supplemental heat to the mash to facilitate temperature rise and moisture dispersion. After a prescribed residence time, the conditioned alfalfa grind is discharged from the outlet to the pelleter.

Research work and industrial practice have led to the consensus that conditioning is one of the operations in a pelleting process that most affect the quality of pellets. During conditioning, dry or saturated steam is normally added to ground forage like alfalfa grind as heat and moisture source. The inclusion of steam would induce many complex thermal and physical processes. For super-heated steam, it may involve vapor diffusion through the inter-particular voids of the mash when discharged from the pressured steam line. It may also involve condensation of vapor on the surface of the mash to give out sensible and latent heat. The mash undergoes a rewetting process that results in an increase in moisture content of the mash. This diffused moisture will change the physical and thermal properties of the mash as conditioning proceeds.

Research work done so far in this particular area of feed mash conditioning has been briefly reviewed by Sokhansanj and Wood (1990). A critical review on steam conditioning and its effect on pellet durability were given by Tabil and Sokhansanj (1992; 1993). Early elucidation of the factors in conditioning pellet mash and the effect of steam on pellet durability dates back to Smith (1959) and Bartikoski (1962).

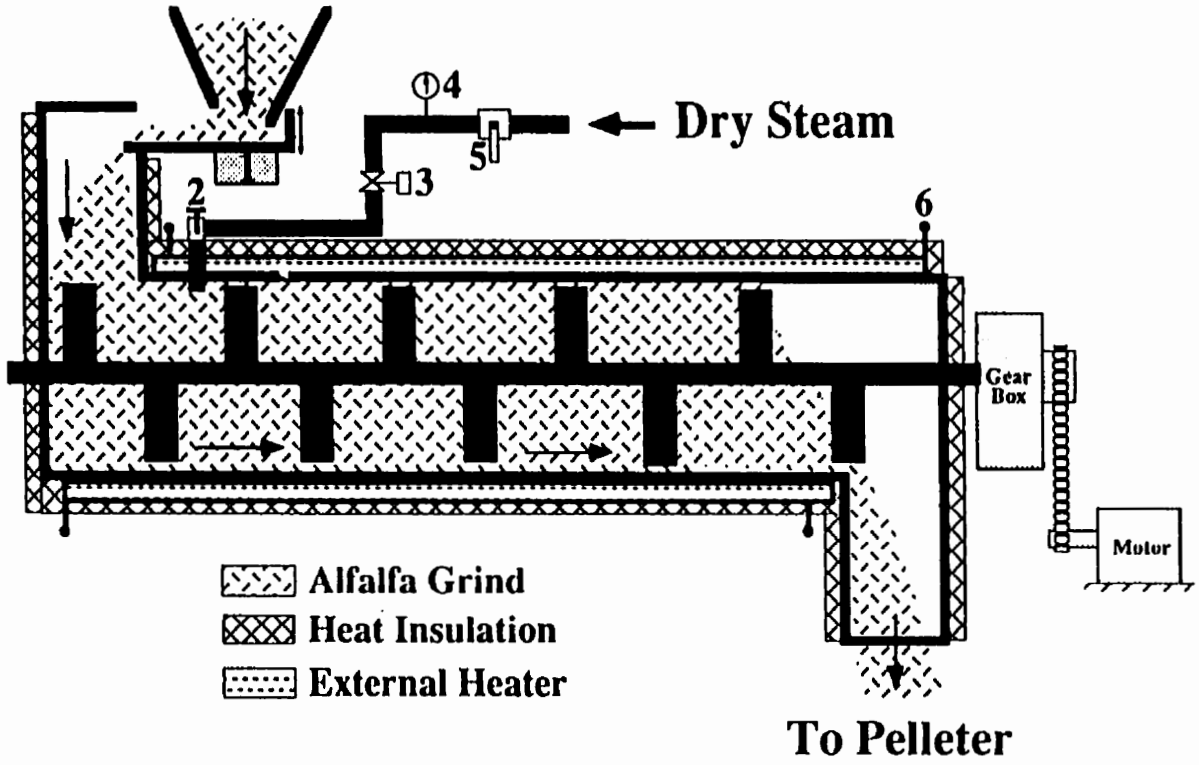

1 - Vibratory Feeder 2 - Steam Temperature Sensor
3 - Differential Pressure Transducer 4 - Pressure Gauge
5 - Steam Flow Switch 6 - Heater Extension Line

Figure 1.1: A diagram showing the steam conditioning process of alfalfa grind

Dobie (1959) appraised a hay pelleting operation and found that meal moisture condition was critical to the operation. It was noticed that throughput decreased at 10% hay moisture content. At moisture contents between 12% and 16%, both the pelleting operation and output were satisfactory. Beyond 18% moisture content, it was hard to produce pellets of high durability due to difficulty in fine grinding of the hay. Dobie (1959) also found that the density and pelleting capacity were proportionate to the fineness of hay grinds. The effect of steam-conditioning rate on pelleting variables was studied by Skoch et al. (1981) using a poultry layer-diet containing soya meal, yellow corn and sorghum. Winowiski (1985) tested the conditioning temperatures for a variety of feed rations and gave tips on how to optimize the feed temperature during the conditioning process prior to pelleting. Hill and Pulkinen (1988) found that 3.5% to 8% meal moisture content prior to steam conditioning did not affect pellet durability, but the power consumption of the pelleter decreased by one-fold with an increased moisture content, due possibly to the lubrication effect of moisture. Increasing the mash temperature from 60°C to 104°C increased the durability and reduced power consumption. These authors also reached the same conclusion as did Dobie (1959) in terms of the effect of particle size on pellet durability who suggested that the size of the screen in a hay grinder should be no more than the diameter of the pelleting die.

Most recently, Maier and Gardecki (1993) evaluated industrial conditioning process through a survey of pellet mill problems categorized by steam supply, steam regulation, and conditioner maintenance. They found that only 22.7% of 88 mills evaluated were fully functional. Most pellet mills had one or more problems with steam supply, regulation or conditioner maintenance. It was concluded that there was a need for improved educational out-reach to train feed manufacturers in steam supply, regulation and conditioning.

The effect of particle size distribution on pellet durability and the inclusion of natural binders in alfalfa conditioning were studied by Tabil and Sokhansanj (1993; 1994). Based on his work on the binding characteristics of alfalfa, Tabil (1996) made the following recommendations for further study of the steam conditioning of alfalfa grind: 1) Characterization of the moisture sorption of alfalfa particles, 2) Determination of the physical properties, thermal properties, particle size distribution of alfalfa grind, and 3) A

detailed study of the steam conditioning process.

It was noted from a review of the literature that although steam conditioning of feed particulates has been practiced for decades, it is still more an art than a science. Most work hitherto done in steam conditioning of feed materials has been centered around examining the effect of conditioning parameters on pellet quality indices such as durability and color. Little research has been done to determine the fundamental characteristics of a mash like alfalfa grind that are pertinent to the improvement and/or enhancement of the quality of the final mash. There is still a lack of answers to questions such as 1) how much moisture can be absorbed by alfalfa grind to reach its maximum capacity at a given relative humidity? 2) what the moisture diffusion rate of alfalfa grind can be expected in the presence of steam? 3) how the particle size of a regular commercial alfalfa grind is distributed and what the physical and thermal properties of alfalfa grind are in relation to temperature and moisture content? 4) what the isotherms and hysteresis loops of alfalfa grind look like? and 5) what the meal temperature and moisture content trends are and how they can be mathematically modeled? A research that could provide the fundamental information on the steam conditioning process would prove pragmatic in terms of the status quo of steam conditioning technology. This study was conceived for such a need.

Chapter 2

OBJECTIVES

The overall goal of this research was to study the interaction of moisture and temperature, in an unsteady state and/or in equilibrium conditions, with the particles of the ground alfalfa, referred to as alfalfa grind hereinafter, during steam conditioning. To achieve the overall goal, the following objectives were set:

1. To characterize alfalfa grind in terms of the following physical and morphological characteristics: bulk and solid densities as affected by particle size and moisture content, particle size distribution pattern, and particle size and shape related parameters;
2. To investigate the following thermal characteristics of alfalfa grind: specific heat capacity, thermal conductivity, and thermal diffusivity as affected by temperature and moisture content;
3. To examine the moisture diffusion characteristics of alfalfa grind during steam conditioning, which comprise the following components: moisture diffusivity under steam condensation at various particle sizes and compaction degrees, and moisture sorption kinetics of the whole and fractionated grinds;
4. To study moisture the equilibrium characteristics of alfalfa grind, which includes measurement of the moisture sorption isotherm and hysteresis at various temperatures, examination of the applicability of the newly released ASAE (1996a) standardized isotherm equations in search of the best-fit model for alfalfa grind, and characterization and modeling of moisture sorption hysteresis.
5. To develop heat and mass transfer models for describing the relationships of meal temperature and moisture content versus time in a steam conditioner, and verify the models with pilot-scale test results.

Chapter 3

PHYSICAL AND MORPHOLOGICAL ATTRIBUTES OF ALFALFA GRIND

3.1 Overview

Alfalfa grind is an intermediate product derived after hammer milling the dehydrated alfalfa. The size of alfalfa grind varies with the size of screen used in a hammer mill. It also changes with other factors such as moisture content of alfalfa chops, type of blade assembly, screen wear and hammer rotational speed (Sokhansanj et al., 1992; Pulkinen, 1994).

Information on the size and shape of alfalfa grind is important. When evaluating a hammer mill, particle size distribution reflects on the performance of the mill. Particle size distribution data are also required for the design of pneumatic conveyors and cyclones. For the steam conditioning of alfalfa grind prior to pelleting, basic material properties such as specific surface area, particle density, and particle shape factors determine the rate of steam application. Particle size and shape also highly relate to the feed intake, digestion, and metabolic products of ruminants (Troelsen and Campbell, 1968; Woodford and Murphy, 1988; Luginbuhl et al., 1989).

The international standard ISO 2591-1 (ISO 1988) and its equivalent ASAE S319.2 (ASAE 1996c) specify test methods for measuring particle size distribution by sieving tests. Finding particle size and shape through other means, such as projector and image analysis (Patil and Sokhansanj, 1992), have also been reported. Scanning electron microscope (SEM) also provides an excellent alternative for examining size and shape for finer particles.

Although the alfalfa grind used in this study was from one alfalfa pelleting plant (The Tisdale Dehy Ltd.), it was generally believed to be representative of most alfalfa grinds in terms of particle size, shape, and composition. This is because most alfalfa pelleting plants are, after years of practice and exchange of information, well aware of the particle size range in which good-quality pellets can be produced, since there is only a certain size range that results in durable pellets (Dobie, 1959; Hill and Pulkinen, 1988).

The equipment such as blade assembly in a grinder, the size of the screen, the depth of chop inlet, etc. are often adjusted accordingly so that particles fall within the optimal size range. Therefore, the alfalfa grind collected from different plants would generally tend to be similar in size distribution, although exceptions may exist, e.g., blade worn out, screen holes partially plugged, etc. which could result in larger particles and smaller particles, respectively.

3.1.1 Particle densities and size distribution

Particle densities refer to two terms in this chapter: bulk density for a collection of alfalfa particles loosely deposited together and solid density for individual alfalfa particles. Bulk density is usually determined by measuring the mass of the material held in a container of predetermined volume. Solid density measurement requires a density bottle or air/gas comparison pycnometer (Woodcock and Mason, 1986).

There are a number of methods such as sieving, Coulter counter, laser diffraction spectrometry, sedimentation, elutriation, optical microscopy, and electron microscopy for determining particle size distribution of particulate and loose materials. Woodcock and Mason (1986) listed approximate range of application of these methods in terms of the magnitude of the particles. For alfalfa grind of which the particle sizes are within the range of 50 μm - 100 mm, sieving method is most appropriate for determining its particle size distribution. ASAE S319.2 (ASAE, 1996c), ISO 2591-1 (ISO, 1988) and British Standards BS 1796 (BSI, 1989) are good references in this regard. In ISO 9276-1 (ISO, 1990), particle size distribution can be represented by histogram, cumulative curve and density function in normal, logarithmic or log-probabilistic coordinates. In ASAE S319.2, the size of particles is reported in terms of geometric mean diameter and geometric standard deviation, as calculated by:

$$d_{gw} = \log^{-1}\left[\frac{\sum_{i=1}^{n}(W_i \log \overline{d_i})}{\sum_{i=1}^{n} W_i}\right] \qquad (3.1)$$

$$s_{ln} = \left[\frac{\sum_{i=1}^{n} W_i (\log \overline{d_i} - \log d_{gw})^2}{\sum_{i=1}^{n} W_i} \right]^{\frac{1}{2}} \tag{3.2}$$

$$S_{gw} = \frac{1}{2} d_{gw} \left[\log^{-1} S_{ln} - (\log^{-1} S_{ln})^{-1} \right] \tag{3.3}$$

where

d_i nominal sieve openings of the i^{th} sieve (mm)

d_{i+1} nominal sieve openings in next larger than i^{th} sieve (just above in a set) (mm)

dgw geometric mean diameter or median size of particles by mass (mm)
geometric mean diameter or median size of particles on i^{th} sieve (mm)
$(d_i \times d_{i+1})^{1/2}$

S_{ln} geometric standard deviation of log-normal distribution by mass

S_{gw} geometric standard deviation of particles by mass (mm)

W_i mass on i^{th} sieve (g)

n number of sieves +1 (pan)

S_{ln} can, in addition to Equation 3.2, also be determined by graphic method as:

$$S_{ln} = \log\left(\frac{d_{84}}{d_{50}}\right) = \log\left(\frac{d_{50}}{d_{16}}\right) \tag{3.4}$$

where

d_{84} particle diameter at 84% probability

d_{50} particle diameter at 50% probability

d_{16} particle diameter at 16% probability

3.1.2 Particle specific surface area, sphericity and number of particles per unit mass

The most popular method for measuring surface area of a particulate material is the BET method (Brunauer et al., 1938) with nitrogen sorption. According to the BET theory, the partial pressure of a sorbate, relates to its amount of sorption as:

$$\frac{1}{w\left(\frac{p_0}{p}-1\right)}=\frac{1}{w_m C}+\frac{C-1}{w_m C}\left(\frac{p}{p_0}\right) \tag{3.5}$$

where:

w	mass of sorbate in the material (g),
p	partial pressure of sorbate (Pa),
p_o	saturation pressure of sorbate (Pa),
w_m	mass of the sorbate formed in monolayer (g), and
C	a constant.

For most substances, linearity results if $\frac{1}{w(\frac{p_0}{p}-1)}$ is plotted against relative pressure, p/p_0 ($0< p/p_0 <0.3$). The resultant slope, α, and intercept, β, are:

$$\alpha=\frac{C-1}{w_m C} \quad \text{and} \quad \beta=\frac{1}{w_m C}$$

Rearranging these expressions gives:

$$w_m = 1/(\alpha+\beta) \tag{3.6}$$

The total surface area is then calculated as:

$$S_t = w_m N A_{cs}/M \tag{3.7}$$

where:

N	Avogadro's number (6.023×10^{23} molecules/mole),
M	molecular weight of adsorbate (nitrogen), and
A_{cs}	cross-sectional area of nitrogen molecule (0.162 nm^2 at 77 K).

Thus, specific surface area can be obtained as:

$$S = S_t/W_t \tag{3.8}$$

where W_t is the sample mass.

Based on the determined median size and its standard deviation, the surface area of particles per unit mass can be calculated using Equation 3.9 (ASAE, 1996c):

$$S = \frac{\beta_s W_t}{\beta_v \rho \mu} \exp\left[0.5(\ln \sigma)^2\right] \tag{3.9}$$

where:

S	surface area of sample (m^2),
β_S	shape factor for the surface area of particles (cubical, β_S=6; spherical, β_S=π),
β_v	shape factor for the volume of particles (cubical, β_V=1; spherical, β_V=π/6),
ρ	solid density of material (kg/m^3),
μ	median size of particles (m),
σ	distribution spread index (standard deviation), and
W_t	mass of a charge (kg).

Based on the measured and calculated surface area at the same mass or volume, the sphericity (ϕ) of the particles can be calculated using Equation 3.10 (Woodcock and Mason, 1986):

$$\phi = \frac{\text{surface area of sphere (calculated by Equation 3.9)}}{\text{surface area of particle (measured with Autosorb} - 1)} \tag{3.10}$$

Based on the determined median size and its standard deviation, the number of particles per unit mass can be calculated using Equation 3.11 (ASAE, 1996c):

$$N_t = \frac{W_t}{\beta_v \rho \mu^3} \exp\left[4.5(\ln \sigma)^2\right] \tag{3.11}$$

where N_t is the number of particles in a charge.

3.1.3 Particle projection parameters

The major article projection parameters included: mean particle projection length, width, area, perimeter and roundness.

The mean particle projection length, width, area, perimeter, and roundness can be determined using SEM and the image analysis system (Patil and Sokhansanj, 1992). Particle length and width were defined as the length and width of a rectangular box circumscribing the projected area of a particle and oriented along the major and minor axis. Particle roundness can be calculated as

$$R = \frac{4\pi A}{P^2} \tag{3.12}$$

where:

R roundness of the projected area of a particle (between 0 and 1),
A projection area of a particle, and
P perimeter of the projected area of a particle.

3.2 Material and methods

3.2.1 Material and preparation

The material used in this section was alfalfa grind. It was obtained from Tisdale Dehy Ltd., Tisdale, Saskatchewan and transported to the university campus in polybags within 24 hours. The initial moisture content of the dehydrated alfalfa grind was 7.01 % db (dry basis) or 0.070 (w/w, db). The moisture content is mostly expressed in fraction format and dry basis throughout the text. However, moisture contents in percentage or wet basis will occasionally appear in some chapters in case of need, such as quoting other researchers' published results that had moisture contents in percentage or wet basis, preparing right data format for regression so that the numbers will not be too small to handle at ease in computation, etc.

Pre-treatments including tempering, drying and sieving were taken to condition the material to higher and lower moisture contents and to separate the particles of the

alfalfa grind into different size ranges for a particular experiment. The moisture content ranged from 0.005 (w/w, db) to 0.51 (w/w, db). The particle undersize ranged from 150 μm to 1000 μm.

To temper to the targeted moisture content, a specific quantity of alfalfa grind was sampled from the material bulk and a predetermined amount of deionized water was sprayed with tumbling to the sample. The rewetted sample, held in a Ziplog bag, was then stored at about 8°C in a refrigerator for 24 hours in order for the moisture content to be uniform through the sample. During storage, the sample was stirred from time to time to expedite moisture equilibration.

To dry to a targeted moisture content, a specific quantity of alfalfa grind was sampled from the material bulk and dried at 75°C in an air-ventilated oven to a predetermined mass. The dried sample was transferred to an air-tight Ziploc bag and stored at room temperature for 24 hours for moisture to equilibrate. During storage, the sample was also stirred from time to time to expedite moisture equilibration. Similar tempering and drying methods were followed in other experiments, which will be described later.

The ASTM standard test sieves of 215-mm frame diameter were used to sieve the whole alfalfa grind into various portions of the particle undersize ranging from 150 μm to 1000 μm. The sieving procedure followed the ASAE Standard S319.2 (ASAE, 1996c). A Ro-tap sieve shaker was used as shaking equipment. The alfalfa grind was separated into 7 portions in terms of its particle sizes by sieving in a nest of 7 sieves. The sieves had the following nominal apertures based on the supplementary size R40/3 as specified in the ISO sieving standard ISO 3310-1: 150 μm, 212 μm, 300 μm, 425 μm, 600 μm, 850 μm and 1000 μm plus a pan. The sieves were corresponding to #100, #70, #50, #40, #30, #20 and #18 sieves in ASTM E11: 87 sieve series. Therefore, the 8 separated portions were in the following particle size ranges: 150 μm and under, 150-212 μm, 212-300 μm, 300-425 μm, 425-600 μm, 600-850 μm, 850-1000 μm and 1000 μm and above.

The following table summarizes the materials used in the experiments, number of observations, and other related information on the sample specifications:

Test Item	Material	Observation	Comments
1. Bulk density vs. MC	Dehy*	27	Three replicates
2. Solid density vs. MC	Dehy	30	Three replicates
3. Bulk density vs. size	Dehy	35	Five replicates
4. Solid density vs. size	Dehy	21	Three replicates
5. Size distribution	Dehy	60	Three replicates**
6. BET surface area	Dehy	6	Six replicates
7. Projection parameters	Dehy	2130	200-300 / opening

* Dehy - dehydrated ** Some with duplicate samples.

3.2.2 Experimental procedures

Measurement of bulk and solid densities

Bulk density of alfalfa grind was measured with a conventional bulk density measuring device that consisted of a fixed-volume container (0.5 L), a funnel and a balance (accurate to 0.01 g). During bulk density measurement, alfalfa meal equilibrated to various moisture contents was poured into the container through the funnel until it overflowed. The heap was leveled to line up with the container edge. The filled container was weighed. Bulk density was expressed as the ratio of net meal weight over the volume of the container.

Solid density of alfalfa grind was measured using a helium-operated multipurpose pycnometer (Quantachrome MVP-2, Quantachrome Corp., Boynton Beach, FL). The principle of this method is described in Appendix A.

Measurement of particle size distribution

The particle size distribution of alfalfa grind was measured in a Gilsonic autosiever (model GA-6) using a series of 100-mm-in-diameter sieves of 20-1700 μm apertures. The ASTM sieves of 215-mm frame diameter were not used for this test due to two reasons: 1) the quantity of alfalfa grind involved in the test of size distribution was small and hard to handle in 215-mm sieves, and 2) the sieves with a Gilsonic autosiever had more intermediate sieve divisions than the 215-mm sieves available in this study. An

analytical balance accurate to 0.0001 g was used to take the sample masses. A charge of 45 g was loaded to the autosiever that ran for 42 min before each sieve was unloaded and weighed. The material in the pan was transferred to next sieving operations with test sieves of finer openings. Size distribution was expressed by both the mass percentage retained on each sieve and the cumulative percent undersize against sieve openings. The median size and its standard deviation of the particles were determined from the distribution data by the method of parameter estimation using various distribution functions.

Specific surface area and particle number per unit mass

Specific surface area of alfalfa grind was measured in a device called Autosorp-1 (Quantachrome Corp., Syosset, NY). This device is capable of automatically determining surface area, porosity and isotherms and carrying out pore structure analysis for powders. The procedure involved the following steps: 1) weighing (accurate to 0.0001 g) and loading a sample of 0.2-0.3 g into a sample bulb, 2) out-gassing under 1.33 Pa vacuum for 22 h with insertion of a steel rod on top of the sample to prevent it from elutriation during evacuation, 3) automatic isotherm measurement at low relative pressure range (5-point BET procedure), and 4) programmed data reduction. The system was connected to a CompuAdd-810 computer and the resultant specific surface area was printed out automatically at the end of a test. Before the trial, the device was calibrated as per the operator's manual. Six replications were made.

Specific surface area of alfalfa grind was also calculated using Equation 3.9 incorporating the median size and standard deviation of particles obtained through sieving tests. The number of particles per unit mass was calculated following Equation 3.11 using the median size and standard deviation of particles.

The sphericity of alfalfa particles was obtained by Equation 3.10.

Particle characterization by SEM and image analysis

A scanning electron microscope (Philips SEM 505, Eindhoven, The Netherlands) was used to capture the image of alfalfa particles retained on the sieves at the aperture sizes ranging from 20 to 850 μm. Sample preparation involved spreading adhesive tape used specially for SEM analysis on top of a sample-holding button and inserting the button into the bulk of samples for the surface of the adhesive tape to collect particles. Extra layers of adhered particles were removed with a soft brush in order for the button to form a single layer of separate particles. During microscopic examination, the image of the particles was video taped, which was later subjected to image analysis. The image analysis system consisted of a Panasonic VCR that played back the video tape and a Macintosh IIfx computer that run an image analysis software (MacRail 7.2, Automatix, Inc., Billerica, MA). Since the video taped alfalfa particles from SEM examination was too noisy for the image analysis program to capture the particles exactly, the image of particles was manually traced to facilitate image analysis. This was done by printing the played-back image on a laser printer and then tracing out the printed image of particles on a transparent drawing paper put on top of the printed image using a drawing pen of fine tip. The traced image was in turn subjected to the image processing system for analysis. The parameters examined were mean particle projection length, width, area, perimeter, and roundness. These parameters were correlated to the nominal sieve openings statistically.

3.3 Results and discussion

3.3.1 Bulk and solid densities

Both the bulk density and solid density of alfalfa grind were found to vary with moisture content and particle size.

Table 3.1 lists the mean bulk density of alfalfa grind calculated from triplicate measurements in relation to moisture content. The bulk density of alfalfa grind ranged from 205 kg/m^3 to 257 kg/m^3, with a mean of 229 kg/m^3 and a standard deviation of 20 kg/m^3, at the moisture contents ranging from 0.0057 (w/w, db) to 0.47 (w/w, db). The

bulk density of alfalfa grind increased with moisture content until about 0.22 (w/w, db) moisture content when it peaked before it declined as moisture content further increased (Figure 3.1). The relationship was a convex curve. This was probably because at low moisture content alfalfa grind particles had lighter weight and at high moisture content alfalfa grind particles had increased volume due to the swelling effect of the moisture content. Both factors rendered the bulk density of alfalfa grind rather low at the two extremities of the moisture content range as compared to that in an intermediate moisture

Table 3.1: Bulk density of dehydrated alfalfa grind at various moisture contents.

Moisture Content (w/w, db)	Mean Bulk Density* (kg/m^3)
0.0057	210
0.0067	210
0.064	242
0.070	240
0.087	242
0.096	247
0.25	255
0.45	211
0.47	205

* Average of three replications. S.D. of bulk density ranged from 0.9 to 2.3 kg/m^3.

content. Polynomial regression by the commercial regression package TableCurve 2D yielded Equation 3.13 to correlate between the bulk density (ρ_b) and the moisture contents (M) (α=0.01), which is also plotted in Figure 3.1 to compare against the measured data. As can be seen, Equation 3.13 approximated very well the ρ_b vs. M relationship in the above-mentioned moisture content range.

$$\rho_b = 206.6 + 614.9\,M - 2121.9\,M^2 + 1740.8\,M^3 \qquad (n=27,\ R^2=0.99) \qquad (3.13)$$

where ρ_b is in kg/m^3 and M is in fraction db.

Table 3.2 gives the measured bulk density of alfalfa grind as a function of the particle undersize of the alfalfa grind at 0.070 (w/w, db) moisture content. The bulk density of alfalfa grind ranged from 187 kg/m^3 to 242 kg/m^3 in the seven listed particle size fractions within the 150 μm to 1000 μm envelope. The bulk density of alfalfa grind followed such a relationship with the particle undersize that it decreased with the particle undersize until around 600 μm when it reached the minimum before it picked up again (Figure 3.2). The relationship resembled a concave parabola. Higher bulk density at smaller particle undersize (e.g., 150-212 μm fraction) could be attributed to the fact that particles at this size tended to stay more compacted in a bulk to result in a higher bulk density because of their smaller size. To explain why bulk density was also higher at larger undersize (e.g., 1000 μm and over fraction), visual observations were made to the physical appearance of the particles in this fraction and the bulk formed by these particles using a magnifying lens. It was observed that the particles at this size fraction consisted

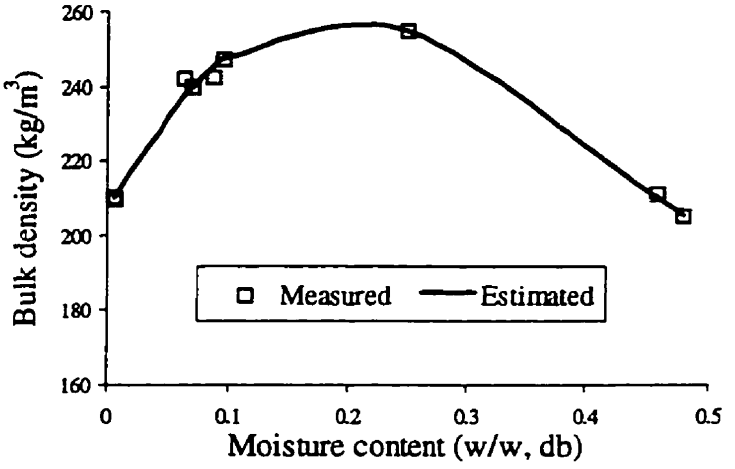

Figure 3.1: The measured and the model estimated mean bulk density of alfalfa grind in relation to moisture content.

of mostly alfalfa stem fragments. Their surfaces were quite smooth. They stayed fairly close to one another, more than was originally believed. Two particular hypotheses based on the observations might cast some light on the phenomenon. One hypothesis was that it was hard for such particles to arch in the bulk to generate voids, because the

Table 3.2: Bulk density of the dehydrated alfalfa grind in relation to particle undersize.

Particle Undersize* (μm)	ASTM Sieve Number	Average Bulk Density (kg/m^3)	Standard Deviation** (kg/m^3)
150	100	226	1.8
212	70	220	0.9
300	50	203	1.2
425	40	193	2.0
600	30	186	1.9
850	20	194	1.1
1000	18	240	5.9

* Supplementary size R40/3 in ISO 3310-1. ** Calculated from five replicates.

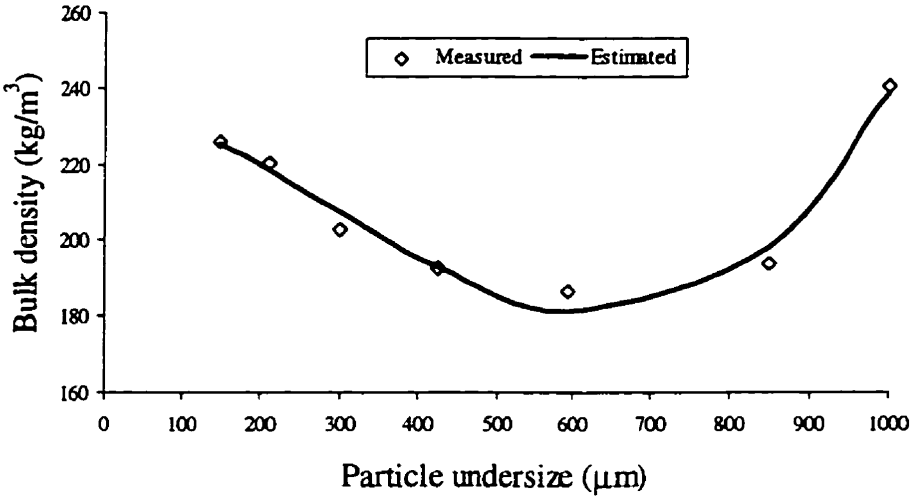

Figure 3.2: The measured and the model estimated mean bulk density of alfalfa grind in relation to particle undersize.

heavier body (density) of these particles rendered it rather hard for bridging to occur on their smooth surfaces. Even though there was arch occasionally formed inside the bulk, such an arch would be short-lived under even a slightest vibration or shock because of smooth or slippery surface. Another hypothesis was that the absence of finer particles, which were mainly from leaf fragments, within the particles of this fraction made it even more difficult for particles to arch. This was because the finer particles coming from leaf fragments usually tended to be more electrostatic and to act more as "cornerstones" in an

arch. Based on the same principle of these two hypotheses, lower bulk densities at intermediate particles sizes could also be explained. It was found after regression that Equation 3.14 could approximate fairly well the relationship between the bulk density (ρ_b) in kg/m^3 and the particle undersize (U) in μm (α=0.01). Such a relation is also depicted in Figure 3.2 in comparison with the measured data.

$$\rho_b = 237.7 - 5.2\text{x}10^{-2}\,U - 2.5\text{x}10^{-4}\,U^2 + 3.1\text{x}10^{-7}\,U^3 \quad (n=35,\ R^2=0.97) \qquad (3.14)$$

Table 3.3 shows the experimental data of the solid density of alfalfa grind at the moisture contents ranging from 0.038 (w/w, db) to 0.52 (w/w, db). The solid density of alfalfa grind ranged from 1218 kg/m^3 to 1367 kg/m^3 in this moisture content range. The solid density of alfalfa grind decreased as moisture content increased. An exponential function (Equation 3.15) was found to approximate fairly well the relationship between the solid density (ρ_s, kg/m^3) and the moisture content (M, w/w db) of alfalfa grind.

$$\rho_s = 1216.1 + 175.3\exp(-7.1\,M) \qquad (n=30,\ R^2=0.90) \qquad (3.15)$$

The solid density values estimated by Equation 3.15 are plotted in Figure 3.3 in contrast to the measured data. The exponential decrease of the solid density with the increase of moisture content could be attributed to 1) volume increase during moisture sorption. Volume swelling during moisture sorption was a commonly observed phenomenon for alfalfa products. For example, Tabil (1996) reported a some 18% volume increase for alfalfa pellets when moisture content increased to about 14%, and the pellet volume tended to increase more as moisture content further increased. Patil (1995) also observed an increased dimension in alfalfa components (e.g., leaf area, stem diameter, and stem projection area) with the increase of moisture content to a level above 12.5 % wb. 2) the density difference between the dry solid particle of alfalfa grind and water. The density of water is usually smaller than the dry solid density of alfalfa particle. With increased water in alfalfa, solid density tended to decrease.

Table 3.3: Solid density of the dehydrated alfalfa grind at various moisture contents.

Moisture Content (w/w, db)	Solid Density (kg/m^3)	Standard Deviation* (kg/m^3)
0.038	1367	30.4
0.043	1319	6.0
0.050	1340	7.3
0.073	1318	8.3
0.099	1332	1.9
0.14	1274	5.0
0.16	1260	15.4
0.19	1254	9.2
0.32	1245	6.4
0.52	1218	3.2

* Calculated from three replicates.

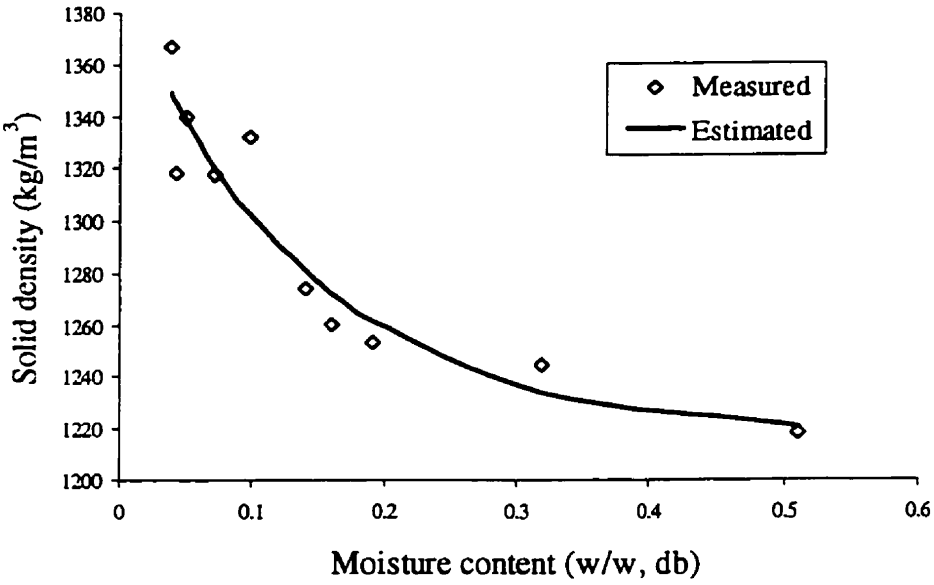

Figure 3.3: The measured and the model estimated mean solid density of alfalfa grind in relation to moisture content.

Table 3.4 presents the solid density of alfalfa grind at different particle undersize. As can be seen, the mean solid density of alfalfa grind ranged from 1214 kg/m^3 to 1432 kg/m^3 in the particle undersize range of 150 μm to 1000 μm. It was found that the solid

density of alfalfa grind decreased linearly with the increase of particle undersize. Such a relationship (Figure 3.4) can be expressed by Equation 3.16 where solid density ρ_s is in kg/m^3 and particle undersize U is in μm.

$$\rho_s = 1468.5 - 0.2\,U \qquad (n=21,\ R^2=0.99) \qquad (3.16)$$

The pattern of solid density vs. particle undersize was quite different from that of bulk density vs. particle undersize. The former exhibited a straight line with negative slope, while the latter exhibited a concave parabola shape. As discussed earlier, higher bulk density at smaller particle undersize in the latter case was because particles at this size tended to stay more compacted in a bulk to result in a higher bulk density because of their smaller size, while higher bulk density at larger particle undersize in the latter case was because most particles in these fractions were comprised of stems that had smooth surface and heavier body weight to disallow them to arch. The predominant reason for the former case was the collection of lighter and more porous fragments which contain more fiber than protein and other constituents in their composition. Most such fragments came from stems, and tended to collect in the sieve fractions of larger undersize. This caused the solid density to decline as particle undersize increased.

Table 3.4: Solid density of the dehydrated alfalfa grind in relation to particle undersize.

Particle Undersize* (μm)	ASTM Sieve Number	Average Solid Density (kg/m^3)	Standard Deviation** (kg/m^3)
150	100	1432	2.6
212	70	1412	14.9
300	50	1393	27.4
425	40	1361	11.9
600	30	1318	1.7
850	20	1253	2.7
1000	18	1215	0.7

* Supplementary size R40/3 in ISO 3310-1. ** Calculated from three replicates.

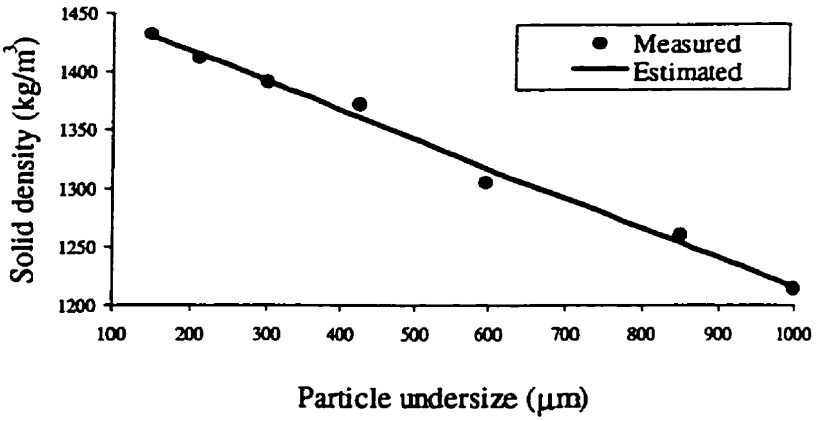

Figure 3.4: The measured and the model estimated mean solid density of alfalfa grind in relation to particle undersize.

3.3.2 Particle size distribution

Figure 3.5 shows the distribution of the percent mass retained on each test sieve in relation to the nominal sieve openings for three repeated trials (no measurement was taken between 850 μm and 1700 μm sieve openings). It shows the skew in shape that is typical of ground grains and their derivatives such as flour, soybean meal and corn meal (Pfost and Headley, 1976). Most particles were in the range of 200 μm to 400 μm. Figure 3.6 shows particle size distribution when the abscissa was transformed to the logarithmic scale. The corresponding cumulative undersize curve (mean of three replications) was also calculated and plotted in Figure 3.6.

The experimental data of Figure 3.5 were used to estimate constants in 19 distribution functions. A log normal distribution function, i.e., Equation 3.13, was found to be the best fitted equation among all (R^2=0.81). Equation 3.13 is plotted as 'estimated' in Figure 3.6.

$$Y = 11.74 \exp\left\{-0.5\left[\frac{\ln\left(\frac{x}{238.01}\right)}{0.65}\right]^2\right\} \qquad (3.13)$$

where Y is mass percentage retained on sieves, and X is nominal sieve openings (μm). The fitted curve in Figure 3.6 did not show a sharp peak to cover the uppermost three

data points. This was probably due to the fact that no intermediate data were available to force the curve to go through these points. The data on the peak were the result of three repeated measurement at the same conditions. As seen in Figure 3.6, the data stay close to one another, indicating good precision of measurement. The most responsible factor may be the way of the ISO (or ASAE or ASTM) sieve sizes are arranged that does not specify half-sized sieve openings in the vicinity of the top three points. If such sieves are available, the fitted curve can be expected to go through the peak points.

The median size and the standard deviation for the log-normal distribution were found to be 238 μm and 0.65, respectively. The standard deviation of the particle size was calculated at 166 μm based on the formula proposed by Sokhansanj and Yang (1996).

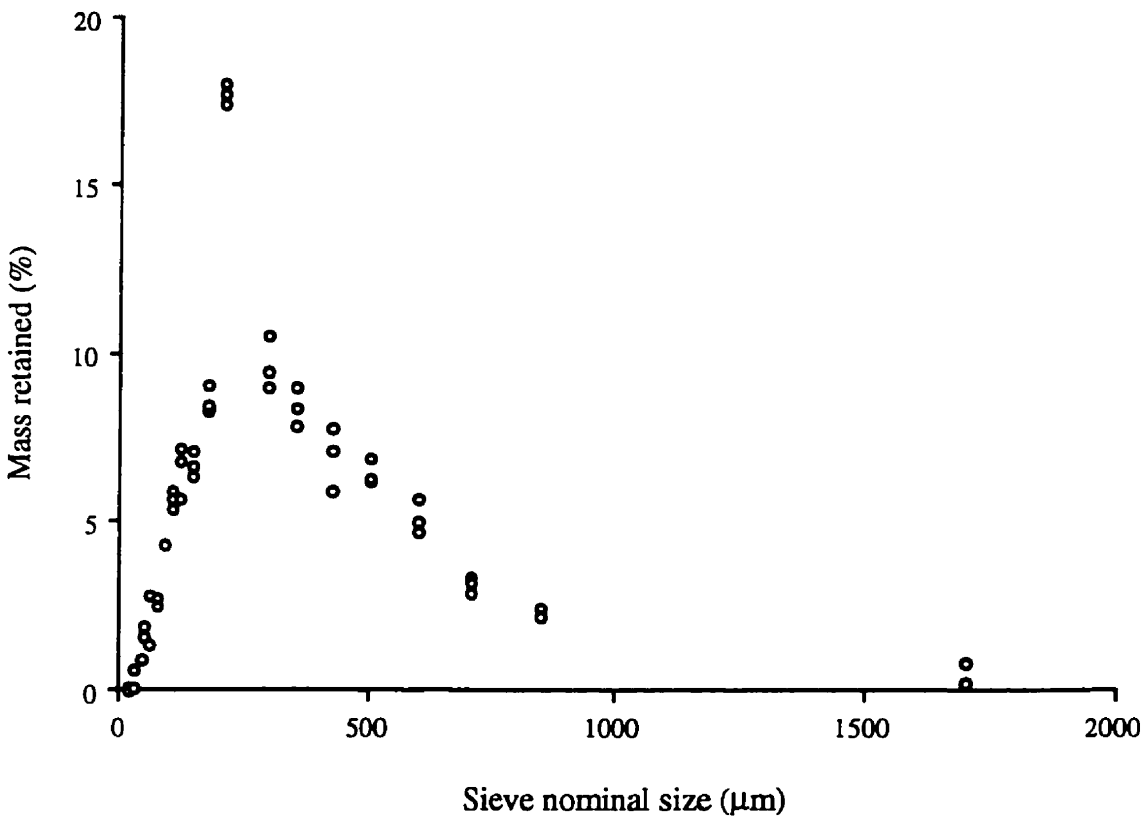

Figure 3.5: The distribution of percent mass retained in relation to sieve undersize for the dehydrated alfalfa grind.

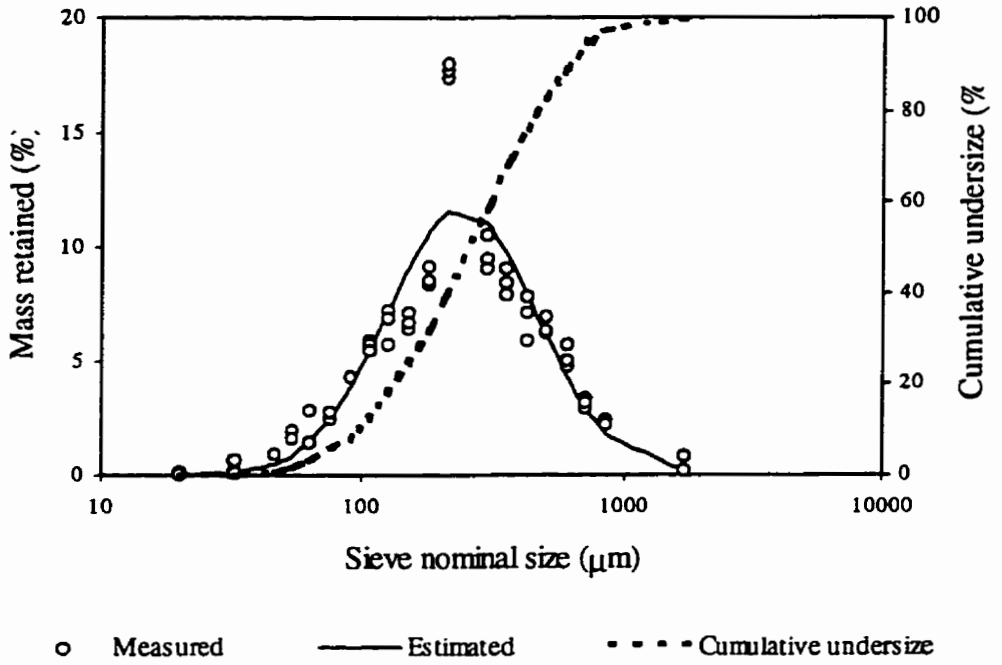

Figure 3.6: Logarithmic particle size distribution of alfalfa grind with both normal and accumulative curves.

3.3.3 Morphological properties

Figure 3.7 shows, as an example, the projected image of the particles retained on a sieve. The measured data of morphological properties based on the image analysis are presented in Table 3.5, where five parameters including the mean particle projection length, width, area, perimeter, and particle sphericity (roundness) retained on individual sieves were given. The length, width, area and perimeter were in the ranges of 0.074-0.979 mm, 0.034-0.425 mm, 0.002-0.295 mm^2, and 0.188-2.421 mm, respectively, in sieve apertures from 20 to 850 μm. The measured and calculated specific surface areas were 0.750 m^2/g and 0.021 m^2/g, respectively. The number of particles per gram charge was calculated to be approximately 652,000 (spheres) and 342,000 (cubes) using Equation 3.11.

Figure 3.7: A SEM micrograph showing the alfalfa grind particles retained on a sieve.

Table 3.5: The measured projection parameters of the dehy alfalfa grind.

Undersize (μm)	Length (mm)	Width (mm)	Area (mm^2)	Perimeter (mm)	Sphericity (Roundness)
20	0.074	0.034	0.002	0.188	0.568
45	0.098	0.045	0.003	0.246	0.609
63	0.144	0.066	0.006	0.363	0.602
90	0.242	0.104	0.016	0.591	0.594
125	0.274	0.145	0.028	0.717	0.612
180	0.268	0.150	0.031	0.885	0.540
300	0.350	0.194	0.044	0.934	0.638
425	0.510	0.234	0.071	1.328	0.549
600	0.780	0.346	0.187	1.927	0.619
850	0.979	0.425	0.296	2.421	0.597

The specific surface area is known to increase if a geometric shape deviates from a sphere, since a sphere has the minimum specific surface area of all geometric configurations. Thus, the calculated specific area assuming that alfalfa particles were

spherical should be less than the measured value. However, the measured specific surface area (0.750 m^2/g) was substantially higher than the calculated value (0.021 m^2/g). The possible reason was that the particles of alfalfa grind were porous in nature and full of cracks and fissures on their surface because of the abrasion and shear during size reduction. The measured surface area should therefore be understood as the total surface area that included the external surface area plus that of the internal pores, cracks or fissures. The calculated area accounted for only the external surface area of geometric particle shape. To study this further, Equation 3.9 and Equation 3.11 were re-derived and the same results as presented in ASAE standard were reached. Examination was also taken to the data of some soil samples that had been measured in the Autosorp-1, such as those by Violante and Huang (1992) and Dynes and Huang (1995), and found that they experienced similar results, i.e., the measured values were higher than the calculated ones. The six replications of alfalfa sample yielded the surface area ranging from 0.266 to 1.072 m^2/g. It seemed unlikely that the deviation was due to the inaccuracy of the Autosorp-1. Despite the above discussion, the true reasons for the deviation need further investigation. The finding on the deviation between the measured and the calculated surface areas of alfalfa grind suggested that Equation 3.10 might give erroneous results if a sorption method is followed for surface area measurement unless the particles were non-porous. Cautions should be exerted in using Equation 3.10 to obtain sphericity for porous particles. The mean roundness obtained from the analysis of the SEM image of randomly sampled particles might be a better approximation to the overall sphericity of the particles.

Regression analysis showed that the particle projection parameters followed linear relationship with sieve openings (R^2 ranging from 0.96 to 0.99). The data showed that particles over each sieve had similar mean sphericity (roundness) (in the range of 0.54-0.64), although other parameters varied widely. The average sphericity (roundness) calculated from a total of about 2130 particles retained on all sieves was 0.601 (standard deviation 0.044).

3.4 Summary

Physical and morphological properties of alfalfa grind were important characteristics to examine, because they are closely related to the rate of steam inclusion and heat and mass transfer during steam conditioning process. They also affect the final quality of the pellets and even the feed intake, digestion, and metabolism of ruminants. The physical properties studied were bulk density, solid density and their relationships with moisture content and particle size. The morphological properties examined in this study included particle size distribution, specific surface area, number of particles per unit mass, and particle projection parameters by SEM.

The bulk density of alfalfa grind was measured by the conventional method, and the solid density of alfalfa grind was measured by gas comparison method in a helium-operated pycnometer. Results showed that the bulk density of alfalfa grind ranged from 205 kg/m^3 to 257 kg/m3 at the moisture content ranging from 0.0057 (w/w, db) to 0.47 (w/w, db). The relationship between the bulk density of alfalfa grind and moisture content could be closely approximated by a 3-order polynomial function in relation to moisture content. The bulk density of alfalfa grind ranged from 187kg/m^3 to 242kg/m^3 in the particle undersize range of 150 μm to 1000 μm. The relationship between the bulk density and the particle undersize was closely approximated by a 3-order polynomial function. The solid density of alfalfa grind was in the range of 1218.1 kg/m^3 to 1367.0 kg/m^3 in the moisture range from 0.038 (w/w, db) to 0.52 (w/w, db). The relationship between the solid density and the moisture content of alfalfa grind could be approximated by an exponential function. The solid density of alfalfa grind ranged between 1213.5 kg/m^3 to 1431.6 kg/m^3 in the particle undersize range of 150 μm to 1000 μm. Linear relationship existed between the solid density and the particle undersize.

Particle size distribution of alfalfa grind was measured by sieving method in a Gilsonic autosiever. The particle size distribution of alfalfa grind could be best described by a log-normal function. The median size of the alfalfa grind was found to be 238.01 μm with a long-normal standard deviation of 0.65. The surface area of alfalfa grind particles calculated based on the sieving tests was 0.0215 m^2/g, which was much lower

than that measured by the Nitrogen sorption method (i.e., 0.750 m^2/g, standard deviation 0.259). The difference was attributed to the pores, cracks and fissures in the particles of alfalfa grind that could trap Nitrogen molecules.

Major morphological characteristics of alfalfa grind were studied by means of scanning electron microscopy and image processing. It was found based on SEM and computer image analysis that the mean particle length, width, area and perimeter of alfalfa grind were in the ranges of 0.074-0.979 mm, 0.034-0.425 mm, 0.002-0.295 mm^2, 0.188-2.421 mm, respectively, in the sieve openings from 20 μm to 850 μm. These parameters followed fairly good linear relationship with sieve openings. The sphericity (roundness) of alfalfa particles ranged from 0.54 to 0.64. The mean sphericity calculated from 2132 particles was 0.601 with a standard deviation of 0.044. The sphericity remained relatively constant over all sieve openings involved.

Chapter 4

THERMAL CHARACTERISTICS OF ALFALFA GRIND

4.1 Overview

Thermal conductivity, thermal diffusivity and specific heat capacity are three important thermal attributes of a material. These parameters are especially essential in heat-transfer related modeling and design. Thermal properties of a number of agricultural and food products have been compiled by Polley et al. (1980) and ASAE (1996d). However, the thermal conductivity and thermal diffusivity data of alfalfa grind are not available in literature.

Specific heat capacity of a material can be determined in several ways, such as by the traditional method of mixtures, through guarded-plate apparatus, or by comparison calorimeter, adiabatic calorimeter and DSC (Mohsenin 1980). It can also be obtained indirectly from measurement of thermal conductivity (k), thermal diffusivity (α) and bulk density (ρ) through the relation: $c_p=k/(\rho\alpha)$. As a rough estimation, specific heat of a material can also be estimated from the specific heats of its contained solid and water based on Siebel's equation or from the composition of this material using the correlation equations as suggested by Toledo (1991) and Singh and Heldman (1993). Among the published methods for specific heat measurement, differential scanning calorimetry (DSC) has so far been the most accurate and rapid method. Yang et al. (1995b) presented a detailed report on the DSC procedure for the specific heat measurement of borage seeds, a model to correlate the specific heat with temperature and moisture content, and the factors that affected the DSC measurement. The specific heat of borage seeds varied from 0.57 to 2.48 $kJ.kg^{-1}.K^{-1}$ in 5-80°C temperature range and 0.5-30.3 % wet basis moisture content range.

The major factors that affect the specific heat measurement are moisture content and temperature (McMillin, 1969; Koch, 1969; Chakrabarti and Johnson, 1972; Murata et al., 1987; Tang et al., 1991). DSC is especially useful in revealing these effects.

Tang et al.(1991) examined the effect of sample thickness, pan seal condition and heating rate on the specific heat of lentil seeds measured with DSC. It was found that sample thickness and seal condition had significant effect on the values of specific heat. An increase in sample thickness from 0.8 mm to 2.4 mm resulted in a 0.25 $kJ.kg^{-1}.K^{-1}$ reduction in value for specific heat, while the value for specific heat of the completely unsealed samples was about 1.1 to 2.5 times that of completely sealed samples at the temperatures between 10 and 80°C. Based on a heat transfer analysis, Tang et al. (1991) suggested a heating rate of 5 K/min to minimize measurement error and in the meanwhile maintain a reasonable signal to noise ratio. In addition to the above-mentioned factors, thermal compensation for the pan that holds the sample, known as blank compensation, is another important aspect to be considered for accurate measurement of specific heat by DSC (Mettler Instrumente AG, 1984).

Thermal conductivity (k), thermal diffusivity (α) and specific heat capacity (c_p) each can be estimated by a number of well established methods as described by Mohsenin (1980), but measuring any two of them would lead to the third through the relationship $\alpha = k/(\rho c_p)$, where ρ is bulk density. It is a more general practice to measure thermal conductivity, specific heat capacity and bulk density before thermal diffusivity is calculated. This approach was also used in the current study.

Methods to estimate thermal conductivity can be classified into two broad categories: steady- and transient-state heat transfer methods (Mohsenin, 1980). The latter have been found more suitable for biological materials which are generally heterogeneous and contain high moisture content, whereas, the steady-state method requires a long time to reach the steady-state and moisture migration may introduce significant measurement errors (Mohsenin, 1980; Kazarian and Hall, 1965; Dutta et al., 1988). The most widely used transient-state method is the line source method that uses either a bare-wire type apparatus or a thermal conductivity probe. In principle, the heat transferring rate (q) from a hot-wire is:

$$q = I^2 R \tag{4.1}$$

where I is electric current in amperes and R electric resistance per unit length in Ω/m. For a long cylindrical sample where the end effects can be neglected, the generated heat conducts in radial direction as governed by the following relationship (in cylindrical coordinates), assuming that k stays constant with position:

$$\frac{\partial T}{\partial t} = \alpha\left(\frac{\partial^2 T}{\partial r^2} + \frac{1}{r}\frac{\partial T}{\partial r}\right) \tag{4.2}$$

where T is the sample temperature in °C, t time in second (s), r the radial axis in meter (m), and α the thermal diffusivity in m^2/s. The solution to Equation 4.2 is (Hooper and Lepper, 1950):

$$T = \frac{q}{2\pi k} F(r * n) \tag{4.3}$$

where:

$$F(r * n) = A - \ln(r * n) + \frac{(r * n)^2}{2} - \frac{(r * n)^4}{8} + \bullet\bullet\bullet \tag{4.4}$$

$$\text{and } n = \frac{1}{2}(\alpha t)^{-\frac{1}{2}}$$

where A is a constant. If the product of r and n is very small, namely, a negligibly small r or a large t, Equation 4.4 can be approximated by the first two terms:

$$T = \frac{q}{2\pi k}\left[A - \ln(r * n)\right] \tag{4.5}$$

or,

$$T = \frac{q\,A}{2\pi k} - \frac{q}{2\pi k}\ln\left(\frac{1}{2} r \alpha^{-\frac{1}{2}}\right) + \frac{q}{4\pi k}\ln(t) \tag{4.6}$$

Equation 4.6 shows the linear relationship between T and ln(t) with the slope $S=q/(4\pi k)$. The thermal conductivity can be calculated from the slope, S:

$$k = \frac{I^2R}{4\pi S} \tag{4.7}$$

However, because of non-ideal conditions, such as non-zero mass and volume of the hot wire, existence of particle-air interface, heterogeneous and anisotropic behavior of biological materials, finite sample size, and axial heat flow (Mohsenin, 1980; Suter et al., 1975; Wang and Hayakawa, 1993), the relationship of temperature vs. ln(t) does not always exhibit linearity, which calls for correction during data reduction. The most used method of correction in early days was the time correction factor method (Van der Held and Van Drunen, 1949), which was to minimize the non-linearity of the T-ln(t) curve by subtracting a factor from the time elapsed. Murakami and Okos (1988) proposed a maximum r^2 method for correction, which searched for a maximum linear portion of the curve by successive linear regression using correlation coefficient as a criteria for the maximum linearity. Most recently, Wang and Hayakawa (1993) have verified both theoretically and experimentally the maximum slope method for correction that was first used by Asher et al. (1986). This method was to calculate the thermal conductivity using the maximum slope identified around the plateau of the local slope vs. ln(t) plot.

4.2 Material and methods

4.2.1 Material and preparation

The dehydrated alfalfa grind at 0.065 (w/w, wb) initial moisture content was used in the study of thermal properties. Five moisture contents of the alfalfa grind, i.e., 0.0054, 0.065, 0.088, 0.20 and 0.32 (w/w, wb), were involved in this study. The samples at the moisture contents below 0.065 (w/w, wb) were prepared by drying a predetermined amount of the alfalfa grind in a convective air oven at 75°C. The samples at the moisture

contents above 0.065 (w/w, wb) were obtained following the conventional grain rewetting method, i.e., spraying a predetermined amount of distilled water on the alfalfa grind followed by intermittently tumbling the samples to facilitate mixing. The conditioned samples were placed in plastic bags and stored at 4°C for at least 12 hours before testing.

The following summarizes the materials used in the experiments, number of observations and other related information on the specifications of the samples:

Test Item	Material	Observation	Comments
1. Specific heat capacity	Dehy*	44	Duplicate at each temp**
2. Thermal conductivity	Dehy	15	Triplicate at each MC
3. Thermal diffusivity	Dehy	N/A	Calculated from k and α

* Dehy - dehydrated ** Three replicates for 0.065 wb and 0.088 wb MCs.

4.2.2 Experimental procedures

Measurement of specific heat capacity

DSC was used to determine the specific heat capacity of alfalfa grind at the five moisture contents as mentioned earlier for the temperatures ranging from 10°C to 110°C. The tests were carried out mostly in triplicates (some in duplicates), following a similar experiment procedure as described by Yang et al. (1995b). A Mettler TA 3000 system (Mettler Instrumente AG, Switzerland) consisting of Model TC10 thermal analyzer and DSC30 cell was used to measure the specific heat of alfalfa grind. A sample of 5-10 mg of alfalfa grind was weighed (accurate to ±0.001 mg). It was then hermetically sealed in a 40 μL standard aluminum crucible and loaded in the DSC cell. The measurements were made between 10°C and 110°C temperature at a heating rate of 5 K/min against a pre-recorded blank compensation curve. A blank curve was obtained in advance by inserting a sealed blank pan as a sample and the data were stored in the memory.

Measurement of thermal conductivity

The bare-wire transient-state method (Sweat, 1986) was used in this study for estimating the thermal conductivity of alfalfa grind. Tests were conducted in triplicates at the initial temperatures of 9°C, 22°C, 40°C and 80°C for the five moisture contents: 0.0054 (w/w, wb), 0.065 (w/w, wb), 0.088 (w/w, wb), 0.20 (w/w, wb) and 0.32 (w/w, wb).

Figure 4.1 shows a schematic diagram of the equipment used. It consisted of a bare-wire thermal conductivity apparatus (A), a ϕ80 mm cylindrical air duct (B), a fan (C) connected to the air duct by a wooden plenum (D), a data acquisition system (E) comprised of a Campbell 21X Micrologger (Campbell Scientific Inc., Logan, Utah) as well as a personal computer, and a dual-tracking DC power supply (F). The bare-wire thermal conductivity apparatus included a ϕ58.6 mm by 240 mm brass circular sample tube with a movable rubber top cover and a fixed rubber bottom lid and a ϕ0.254 mm hot wire (G) connected to the DC power source. In the paper on borage by Yang et al. (1996a), a hot-wire support frame made of ϕ2 mm stainless steel line, a horizontal thin copper string to support a pre-calibrated type T thermocouple (H) (for sensing the core temperature) that connected to the data acquisition system by a thermocouple extension wire, and a pre-calibrated type T thermocouple for monitoring the outer surface temperature of the sample tube were used. Innovation was made in this study to get rid of the frame, so that the hot-wire stretched directly through both ends of the tube. The thermocouple for measuring core temperature was tied to the hot-wire by epoxy resin and made sure that the hot-wire and the thermocouple tip were well separated. The hot-wire had a constant electric resistance per unit length (10.07 Ω/m). An electric current constant at 1.000 ± 0.004 A was generated by the DC power supply and applied to the hot-wire.

In the literature, most researchers kept the sample holder in a constant temperature bath to maintain the surface temperature of the sample holder to be constant at its initial temperature. In this study, the surface temperature was maintained constant by blowing air over the outer surface of the sample tube at a high velocity. The air velocity in the

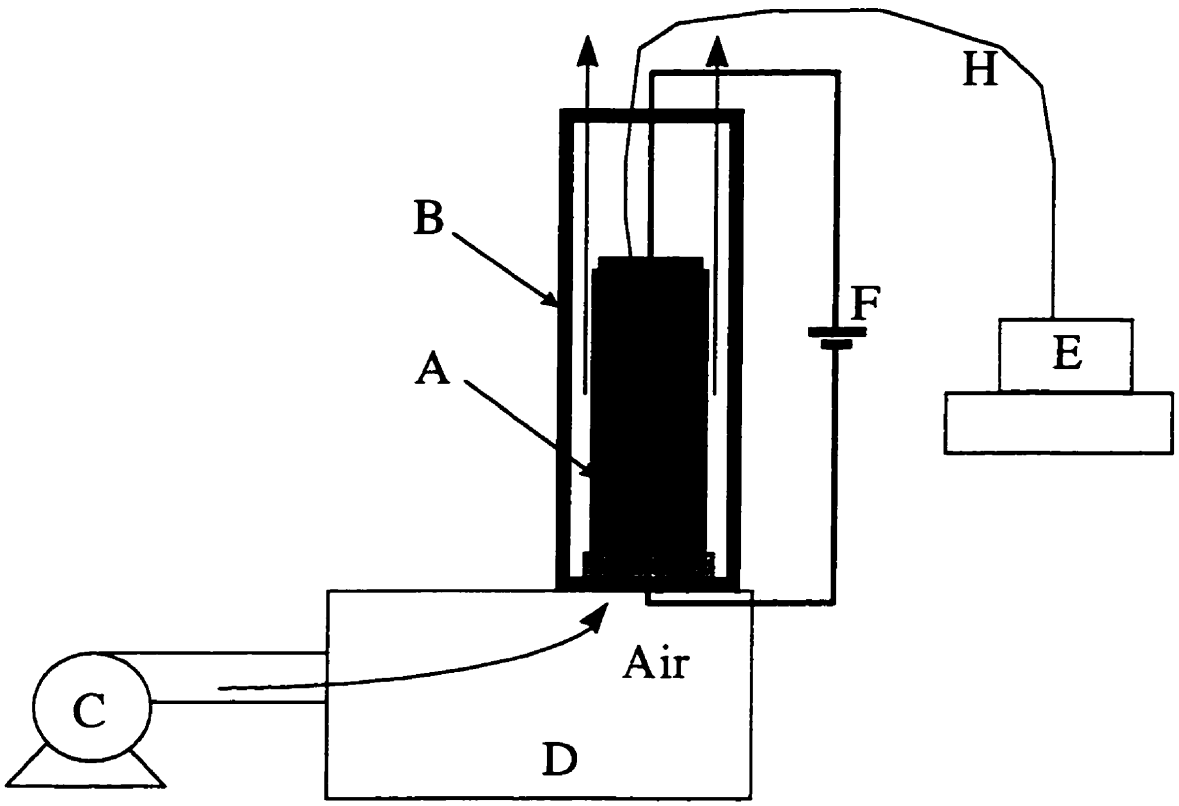

A - Bare-wire apparatus B - Air dut C - Fan D - Air plenum
E - Data acquisition system F - DC power supply G - Hot wire

Figure 4.1: Schematic of the apparatus used in this study for thermal conductivity measurement.

annular space between the sample tube and the air duct was about 27 m/s which was high enough to eliminate the effect of heat transfer boundary layer about the surface on the magnitude of surface temperature. This method has been proven satisfactory by Yang et al. (1996a) in keeping the tube surface temperature constant during thermal conductivity measurement for borage seeds. They found that the average surface temperatures were: 6.6±0.2°C, 10.4±0.4°C and 20.9±0.8°C, corresponding to the initial temperature of 6°C, 10°C and 20°C, respectively. The variation in temperature was mostly within 1°C except for a few cases (between 1 and 2°C), and the temperatures remained almost constant at the initial values throughout the test periods.

Before loading into sample holder, the samples were brought from the refrigerator and equilibrated in an environmental chamber for 5-12 hours to the designated initial temperatures. For a test, the sample tube was filled through a funnel with alfalfa grind until the level was near the upper edge of the tube. The net mass of the filled sample was recorded with a balance for bulk density calculation. The temperatures of the sample core (about 1 mm from the hot wire), sample tube surface and the chamber were recorded at an interval of 10 s.

Instead of applying the traditional method of time correction factor for data reduction, the maximum slope method (Wang and Hayakawa, 1993; Asher et al., 1986) was used to determine the maximum slope for thermal conductivity calculation. The maximum slope was in turn used to calculate the thermal conductivity using Equation 4.7.

Thermal diffusivity magnitude

Thermal diffusivity was calculated according to:

$$\alpha = \frac{k}{\rho c_p} \tag{4.8}$$

where ρ is the averaged bulk density of alfalfa grind (in kg/m^3) obtained by dividing the sample mass recorded each time upon completion of sample loading by the volume of the sample tube.

4.3 Results and discussion

4.3.1 Specific heat capacity

Figure 4.2 depicts the specific heat (c_p) data of alfalfa grind measured at temperatures from 10°C to 110°C (denoted by symbols). The c_p values of alfalfa grind

ranged from 0.9 to 2.2 $kJ.kg^{-1}.K^{-1}$ in the temperature and moisture content ranges prescribed in this study.

The c_p data obtained in this study were also used to develop a model to correlate the specific heat to temperature and moisture content. Interaction terms T*M, T^2*M and $T*M^2$ were applied in multiple regression by SAS (1985). F tests were conducted to determine the significance of the interaction terms on c_p (α=0.01). It was found that the effect of the terms T^2*M and $T*M^2$ were not significant. The resultant multiple regression model is:

$$c_p = 0.6 + 4.3x10^{-2}\,M - 3.9x10^{-4}\,M^2 + 1.7x10^{-2}\,T - 7.0x10^{-5}\,T^2 - 1.2x10^{-4}\,T*M \qquad (R^2=0.94) \qquad (4.9)$$

where M is moisture content in percent wet basis and T is temperature in °C. Figure 4.2 also gives the c_p values calculated using Equation 4.9 (denoted by curves) in contrast to the measured data (denoted by symbols). As can be seen, Equation 4.9 approximated the relationship of c_p vs. T and M fairly well in the full temperature range for moisture

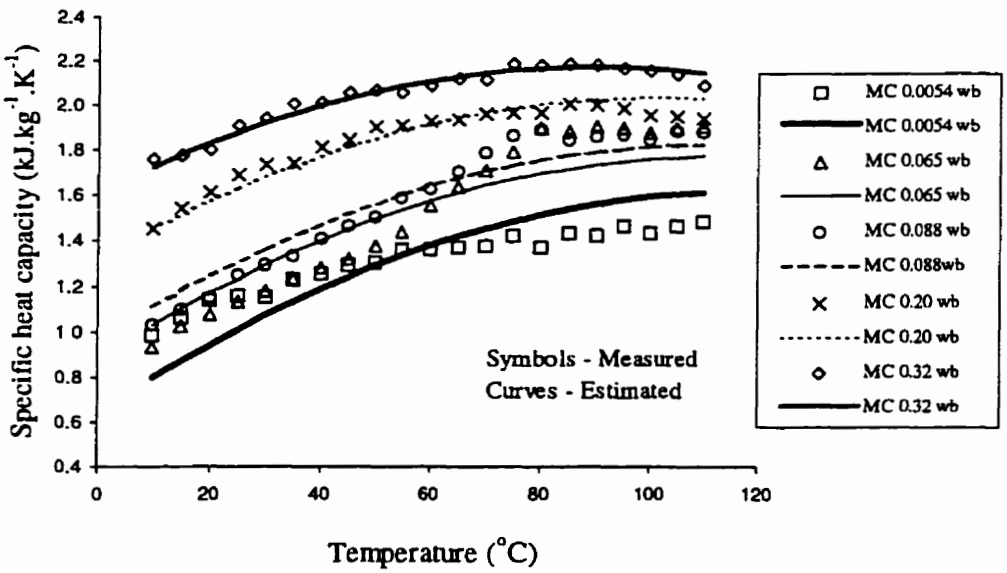

Figure 4.2: The relationship between the specific heat capacity of alfalfa grind and temperature at five moisture contents.

contents 0.20 and 0.32 (w/w, wb) and in 10-60°C temperature range at 0.0054, 0.065 and 0.088 (w/w, wb). It is noted that in the temperature range of 60°C to 110°C the measured specific heat capacity at 0.0054 (w/w, wb) moisture content curved down a little bit from its previous course, while those at 0.065 (w/w, wb) and 0.088 (w/w, wb) moisture content, respectively, curved up a little bit from their original trends. Tang et al. (1991) and Yang et al. (1995b) observed similar digression from the main course of the cp vs. T relationship for lentil and borage samples of low moisture contents. The reasons are still unknown, but it is unlikely due to experimental error, as evidenced by Tang et al. (1991), Yang et al. (1995b) and the replicated data obtained in this study (refer to Appendix B). For example, the data collected in this study showed that digression appeared in every single repeated measurement in the same way as other replication and at the same temperature range. The observed phenomenon of digression might signify a certain unknown transition taking place in the sample during c_p measurement. Nevertheless, the magnitude of digression (i.e., the difference between the measured and the model estimated c_p values over the measured values) was quite small (about 5.7% in an average) in the temperature range of 60°C to 110°C, which might have insignificant effect on the magnitude of c_p in the related temperature and moisture content ranges.

4.3.2 Thermal conductivity

Figure 4.3 shows the mean thermal conductivity data of alfalfa grind as a function of moisture content at 9°C, 22°C, 40°C and 80°C initial temperatures. The averaged thermal conductivity of alfalfa grind varied from 0.025 $W.m^{-1}.K^{-1}$ to 0.072 $W.m^{-1}.K^{-1}$. It was much smaller than that of alfalfa cube (0.31 to 0.48 $W.m^{-1}.K^{-1}$ in the 4.4°C to 58.4°C temperature range) as reported by Khoshtaghaza et al. (1995). The thermal conductivity of alfalfa grind was also smaller than those of grains and oilseeds, such as the whole rapeseed that has a thermal conductivity in the range of 0.108 to 0.155 $W.m^{-1}.K^{-1}$ at moisture contents from 0.061 wb to 0.13 wb and temperatures from 4.4°C to 31.7°C (Mohsenin, 1980). The difference could be attributed to the difference in density, since less dense material had more voids of air that has a very low thermal conductivity.

Multiple regression by SAS (1985) was performed to fit the first, the second and the third order response functions with interaction term between temperature (T) and moisture content (M) to the thermal conductivity data. Tests of the hypothesis concerning

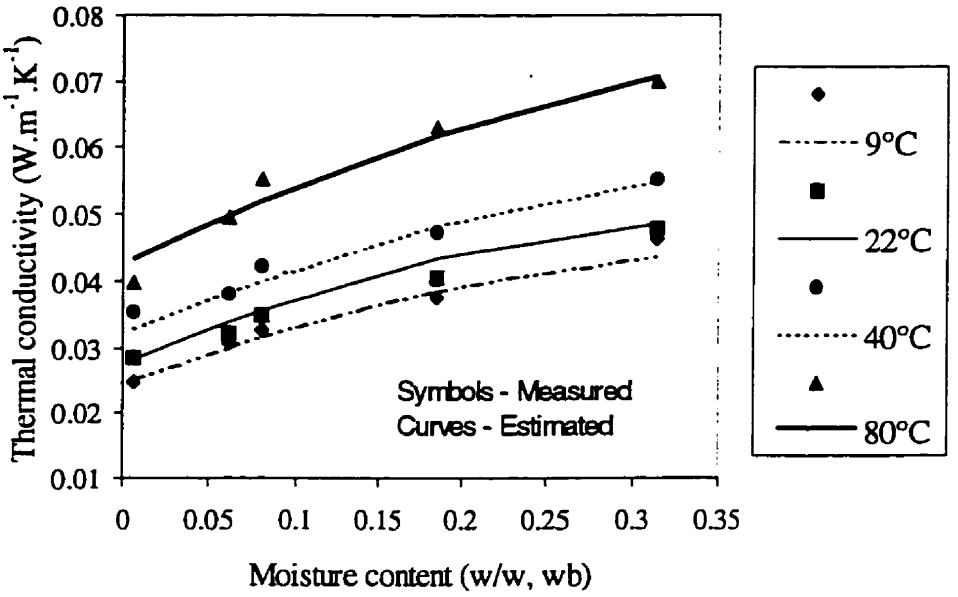

Figure 4.3: Thermal conductivity of alfalfa grind as a function of moisture content at the temperatures of 9°C, 22°C, 40°C and 80°C.

the regression coefficients (Neter et al., 1985) were conducted (α=0.01) to discriminate among equations of different terms. It was found, based on the statistical parameters: the mean percent relative deviation (P) and standard error of the residuals (S.E.), that the second-order response function with T*M interaction was sufficient to describe closely the relationship of k vs. T and M without any higher-order response functions (α=0.01). Therefore, the resultant equation is:

$$k = 0.02 + 9.1\times10^{-4}\,M - 1.1\times10^{-5}M^2 + 2.2\times10^{-4}\,T$$
$$+3.4\times10^{-7}\,T^2 + 4.1\times10^{-6}\,T*M \qquad (R^2=0.99) \qquad (4.10)$$

where T is the initial temperature in °C and M the sample moisture content in percent wet basis. The estimated values by Equation 4.10 are plotted in Figure 4.3 in comparison to

the measured data. Figure 4.3 showed good approximation of Equation 4.10 to the thermal conductivity data of alfalfa grind in the above-mentioned temperature and moisture content ranges.

4.3.3 Thermal diffusivity

Calculation of the thermal diffusivity of alfalfa grind, α, necessitates the data on its bulk density, which were, as described earlier, obtained by dividing the mass of alfalfa grind by the volume of the tube.

Similar to the data of k, the calculated α values were also fit to a second-order multiple regression model using SAS. The resultant equation to represent α -M-T relationship was:

$$\alpha = (1.6 - 7.5 \times 10^{-3} T + 6.4 \times 10^{-5} T^2 - 0.05 M + 1.15 \times 10^{-3} M^2 + 2.1 \times 10^{-4} T^* M) \times 10^{-7} \qquad (R^2=0.98) \qquad (4.11)$$

where α is in m^2/s, M is in percent wet basis, and T in °C.

Figure 4.4 presents the calculated thermal diffusivity values as a function of moisture content at temperatures 9°C, 22°C, 40°C and 80°C, respectively. The α values ranged from 1.0×10^{-7} m^2/s to 1.6×10^{-7} m^2/s in the temperatures and moisture contents tested in this study. Most thermal diffusivity values of alfalfa grind were close to that of water (1.47×10^{-7} m^2/s) and much less than that of air (2.35×10^{-5} m^2/s) (Jiang et al., 1986). Ott and Hurbut (1964) reported that the thermal diffusivity of baled alfalfa was 1.6×10^{-7} m^2/s at 8.2 % wb moisture content at 342 kg/m^3 bulk density. The thermal diffusivity of alfalfa grind at the temperature and moisture content ranges prescribed in this study was close to that of baled alfalfa. Khoshtaghaza et al. (1995) measured the thermal diffusivity of alfalfa cube, which was found to range between 3.99×10^{-7} m^2/s at 4.8°C and 2.55×10^{-7} m^2/s at 57.0°C. The thermal diffusivity of alfalfa cube was generally 2 to 3 times that of alfalfa grind at similar temperatures and moisture content, but they were all

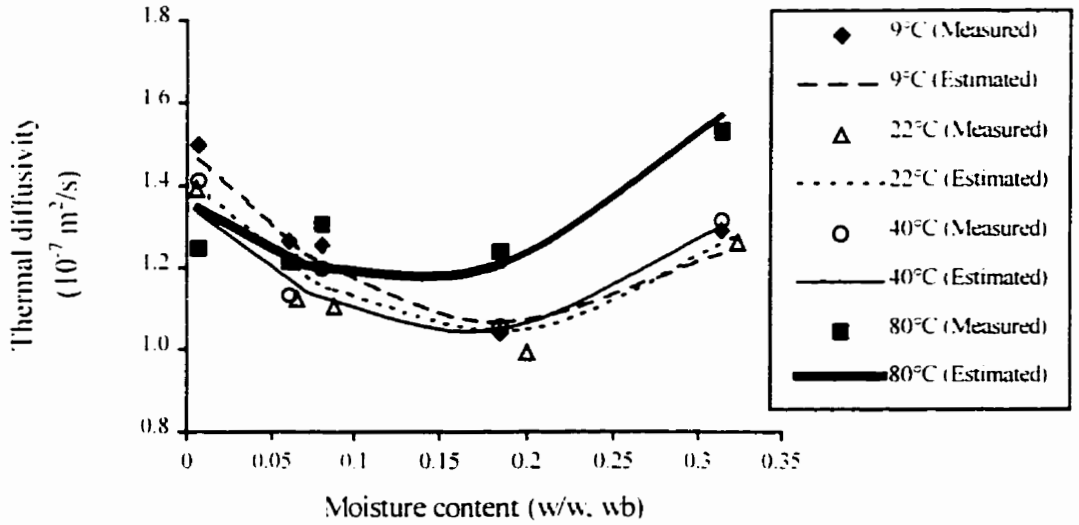

Figure 4.4: Thermal diffusivity of alfalfa grind vs. moisture content at four temperatures.

in the same order of 10^{-7} m^2 s. The difference in the thermal diffusivity among the alfalfa grind, alfalfa bale and alfalfa cube could, as mentioned by Khoshtaghaza et al. (1995), be attributed to their densities. For example, the thermal diffusivity alfalfa bale at 342 kg/m^3 bulk density at 8.2 % wb moisture content (i.e., 1.6 x 10^{-7} m^2/s) was slightly higher than that of alfalfa grind at 242 kg/m^3 bulk density and 8.1 % wb moisture content (i.e., approximately 1.2 x 10^{-7} m^2/s), while the thermal diffusivity of alfalfa cube at 803 kg/m^3 bulk density, 5.2 % wb moisture content and 9.7°C temperature (i.e., 3.5 x 10^{-7} m^2/s) was much higher than that of alfalfa grind at 210 kg/m^3 bulk density and similar moisture content and temperature (i.e., around 1.3 x 10^{-7} m^2/s).

The pattern of α-M relationship was in a concave parabola shape. It has been noted that three shapes of α-M curves were generally observed: ascending (e.g., gram (Dutta et al., 1988)), descending (e.g., haylage (Jiang et al., 1986)), and convex or concave (e.g., alfalfa grind). This is because the magnitude of α depended on the combined effects of k, ρ and c_p according to Equation 30. In the case of marginal increase in k with moisture content and substantial variation in bulk density, such as haylage, thermal diffusivity could follow a descending trend with moisture content. For the material where k increases faster than ρ and c_p in the same temperature and moisture

ranges like gram, thermal diffusivity could end up assuming an ascending trend with moisture content. For alfalfa grind, the concave shape in the α-M curve might attribute to the convex pattern of the ρ-M relationship of alfalfa grind as mentioned before, given the findings that k-M and c_p-M relationships all followed a steadily-increasing pattern.

The α values estimated by Equation 4.11 (in curves) were also shown in Figure 4.4 in comparison with the α values calculated by Equation 4.8 (in symbols). It seemed from Figure 4.4 that Equation 4.11 fit well to the α values in the prescribed temperature and moisture content ranges. Multiple regression statistical parameters also indicated that Equation 4.11 was a model accurate enough in estimating α values for a problem of engineering nature.

4.4 Summary

Thermal properties are another important characteristics of alfalfa that relate to the process design, modeling and optimization of steam conditioning process. The thermal properties examined in this study included specific heat capacity, thermal conductivity, and thermal diffusivity. The specific heat capacity of alfalfa grind was measured by the differential scanning calorimetry with blank compensation. The specific heat capacity of alfalfa grind varied from 0.9 to 2.2 $kJ.kg^{-1}.K^{-1}$ in the temperature ranging from 10°C to 110°C and the moisture content ranging from 0.0054 (w/w, wb) to 0.32 (w/w, wb). A multiple regression model has been developed to correlate the specific heat of alfalfa grind with moisture content and temperature.

The thermal conductivity of alfalfa grind was measured by the transient hot-wire apparatus to collect temperature vs. time data that were reduced using the up-to-date maximum slope method. The thermal conductivity of alfalfa grind increased from 0.025 to 0.072 $W.m^{-1}.K^{-1}$ in the temperature ranging from 9°C to 80°C and the moisture content ranging from 0.0054 (w/w, wb) to 0.32 (w/w, wb). A response surface function has been developed to describe the relationship of the thermal conductivity of alfalfa grind vs. moisture content and temperature.

Based on the measured specific heat capacity and thermal conductivity of alfalfa grind, the thermal diffusivity of alfalfa grind was calculated. It ranged from 1.0×10^{-7} m^2/s to 1.6×10^{-7} m^2/s in the same temperature and moisture content ranges. The pattern of thermal diffusivity vs. moisture content relationship was in a concave parabola shape. The relationship of the thermal diffusivity of alfalfa grind vs. temperature and moisture content was found to be closely approximated by a response surface function developed by multiple regression.

Chapter 5

MOISTURE DIFFUSION CHARACTERISTICS OF ALFALFA GRIND

5.1 Overview

Moisture sorption and diffusion under surface condensation or evaporation is a common phenomenon occurring in many processing and handling operations such as the steam conditioning of ground forages like alfalfa grind. During steam conditioning, both condensation and diffusion of moisture occur at raised temperatures. Information on moisture sorption and diffusion characteristics of alfalfa grind under the condition of surface condensation is important to heat and mass transfer modeling and simulation.

Kinetic study is an excellent way to examine moisture sorption characteristics of alfalfa grind during steam conditioning. The kinetic data obtained enables one to determine the moisture diffusivity, a major parameter that reflects the rate of moisture sorption by alfalfa grind during steam conditioning.

Traditionally, the moisture diffusivity related to drying or rewetting of a material was determined through its kinetics measured with thin layer drying or rewetting tests. This involved solving the diffusion equations based on the second Fick's law (Becker and Sallans, 1955; Pabis and Henderson, 1961; Chu and Hustrulid, 1968; Patil, 1988). Jaros et al. (1992) proposed a general method of determining moisture diffusivity based on thin-layer drying experiments. However, one should be cautious in using the conventional thin layer drying or rewetting method in the determination of the moisture diffusivity when condensation becomes critical in a process such as the steam conditioning of alfalfa grind. This is because considerable steam condensation on the surface of the sample holder and other locations during a thin layer rewetting test would introduce error to the mass gain of the tested materials. Special consideration is needed in constructing the unit for such a test. The principle would be to reduce to minimum the area of the sample container that can collect water through condensation.

Moisture diffusivity can also be measured by applying the concept of diffusion in a semi-infinite body where a bulk particulate material is confined to, say, a long tube

with its longitudinal dimension much larger than its diameter (Bruniche-Olsen, 1962) or a thin layer with its plane dimension much larger than the thickness of the layer. In either case, one-dimensional diffusion can be approximately assumed. The analytical solution to such a diffusion problem contains the term of diffusion coefficient that can be treated as a parameter. The diffusion coefficient can be estimated by inverse method (Beck and Arnold, 1977) using the experimental data of moisture content versus time and the location along the tube or between the two surfaces of the thin layer.

5.2 Theoretical background and modeling

5.2.1 Modeling of sorption kinetics

There have basically been two approaches reportedly used to treat sorption kinetics: the lumped consideration, where mass rates are balanced as a whole without taking into account the spatial variables, and the spatial consideration, where the quantity or concentration of the sorbate in a material is a function of both time and spatial coordinates (Jayas et al., 1991). The lumped consideration resulted in the commonly used kinetic model as shown below:

$$MR = \frac{M - M_e}{M_0 - M_e} = \exp(-kt) \tag{5.1}$$

where MR is moisture ratio, M moisture content of the material, M_0 initial moisture content, M_e equilibrium moisture content, k drying or rewetting constant, and t time. This equation can also be obtained by assuming that the sorption process involves only pure diffusion phenomenon, solving analytically the differential equation governing the diffusion process, and keeping the first term of the solution in summed series with all other terms being dropped (Crank, 1975).

According to the Fick's second law, a one-dimensional diffusion process can be described by (Geankoplis, 1983):

$$\frac{\partial M}{\partial t} = -D\frac{\partial^2 M}{\partial x^2} \tag{5.2}$$

where

M the moisture content of the sample (w/w, db),

x the coordinate in the direction of diffusion from the open surface (m),

t time (s), and

D overall effective diffusion coefficient (m^2/s).

The moisture diffusivity D defined above refers to the overall effective diffusion coefficient that accounts for the liquid diffusion through the voids of the sample bulk and the pores in the individual particles as well as possible vapor diffusion through the voids of the sample bulk. It is assumed that D changes little with x and t.

Equation 5.2 applies to the case of the two different methods (i.e., the kinetic method and the "ring stack" method), which will be elaborated later, used in this study to determine moisture diffusivity under steam conditioning.

In view of the fact that steam conditioning process involves a substantial surface condensation, the surface condensation must be taken as a boundary condition (Equation 5.3) in solving Equation 5.2 by assuming that the rate of exchange on the surface was directly proportional to the difference between the actual moisture content on the surface at any time (M_s) and the equilibrium moisture content (M_e) with vapor in the environment. Crank (1975) gave the analytical solution (Equation 5.4) for the case of one-dimensional diffusion and semi-infinite body with surface condensation or evaporation:

$$-D\frac{\partial M}{\partial x} = \alpha(M_e - M_s), \qquad x = 0 \tag{5.3}$$

$$\frac{M - M_0}{M_e - M_0} = \operatorname{erfc}\frac{x}{2\sqrt{Dt}} - e^{\frac{\alpha}{D}x + \frac{\alpha^2}{D}t}\operatorname{erfc}\left(\frac{x}{2\sqrt{Dt}} + \alpha\sqrt{\frac{t}{D}}\right) \tag{5.4}$$

where

M_0 the initial moisture content of the sample (w/w, db),

M_e the equilibrium moisture content of the sample (w/w, db),

M_s the moisture content on the surface at any time (w/w, db), and

α a proportionality constant related to mass transfer between the vapor phase and the surface of the sample (m/s).

Equation 5.4 is the model based on spatial consideration for describing the kinetic relationship of a hygroscopic material at various locations in the direction of a one-dimensional diffusion under surface condensation or evaporation.

5.2.2 Determination of moisture diffusivity under surface condensation

Two different methods were used in the measurement of moisture diffusivity of alfalfa grind in the presence of steam. One method was to determine the moisture diffusivity through the measurement of the sorption kinetics of alfalfa grind. The kinetic method involved a thin layer of alfalfa grind spreading over a fine screen. The diameter of the screen was much larger than the thickness of the layer, so that the thin layer of alfalfa grind could be regarded as a semi-infinite body and the moisture diffusion in the thin layer could be taken to be one-dimensional. The second method was to determine the moisture diffusivity through a long impermeable tube that contained alfalfa grind. The longitudinal dimension of the tube was much larger than the diameter of the tube, so that it could also be regarded as a semi-infinite body and the moisture diffusion in the tube could be taken to be one-dimensional too. In either of the above two cases, Equation 5.4 applied. The moisture diffusivity, D, could be estimated by fitting Equation 5.4 to the experimental data of M vs. x at various t in the latter method and to the data of M vs. t at the central plane of the thin layer in the former method. In the latter case, M can be approximately taken as the average sample moisture content and x can be taken as one half of the thickness of the sample layer.

5.3 Materials and methods

5.3.1 Materials and preparation

Alfalfa grind was the material used in this experiment. Two types of alfalfa grind were used: dehydrated alfalfa grind and sun-cured alfalfa grind. The dehydrated alfalfa grind at the initial moisture content of 0.070 (w/w, db) was obtained from the Tisdale Dehy Ltd., as described before. The sun-cured alfalfa grind was made from the sun-cured alfalfa chops by grinding in a hammer mill (Type 10, Glenmills Inc., Clifton, NJ) using 3 mm screen. The initial moisture content of the sun-cured alfalfa grind was 0.11 (w/w, db).

Pre-treatments including tempering, drying and sieving operations were the same as described before.

The following summarizes the materials used in the experiments, number of observations, and other related information on the sample specifications:

Test Item	Material	Observation	Comments
1. Kinetics			
■ Whole grind	Dehy*	27	Loose grind
■ Fractionated	Dehy	27	Loose grind
	Sun-cured	27	Loose grind
2. Diffusivity by ring stack method			
■ Whole grind	Dehy	11	Loose grind
■ Fractionated	Dehy	7	Loose grind
3. Diffusivity under compaction by ring stack method			
	Dehy	5	Compacted grind

* Dehy - dehydrated

5.3.2 Experimental procedures

Measurement of sorption kinetics

Figure 5.1 shows a schematic of the experimental unit for the measurement of sorption kinetics of alfalfa grind. The sample holder consisted of a sample basket and a

triple-leg beam for carrying the basket. The sample basket was made of #70 metal screen that was cut into a piece of ϕ202 mm round sheet and folded up approximately 2 mm on its edge. In such a way, the basket had a diameter of about 200 mm and a depth of approximately 2 mm. The beam was made from a ϕ2 mm metal rod. The sample holder was constructed in the principle of reducing to its maximum the surface area of holder and therefore the unnecessary condensation of steam on the surface of the sample holder.

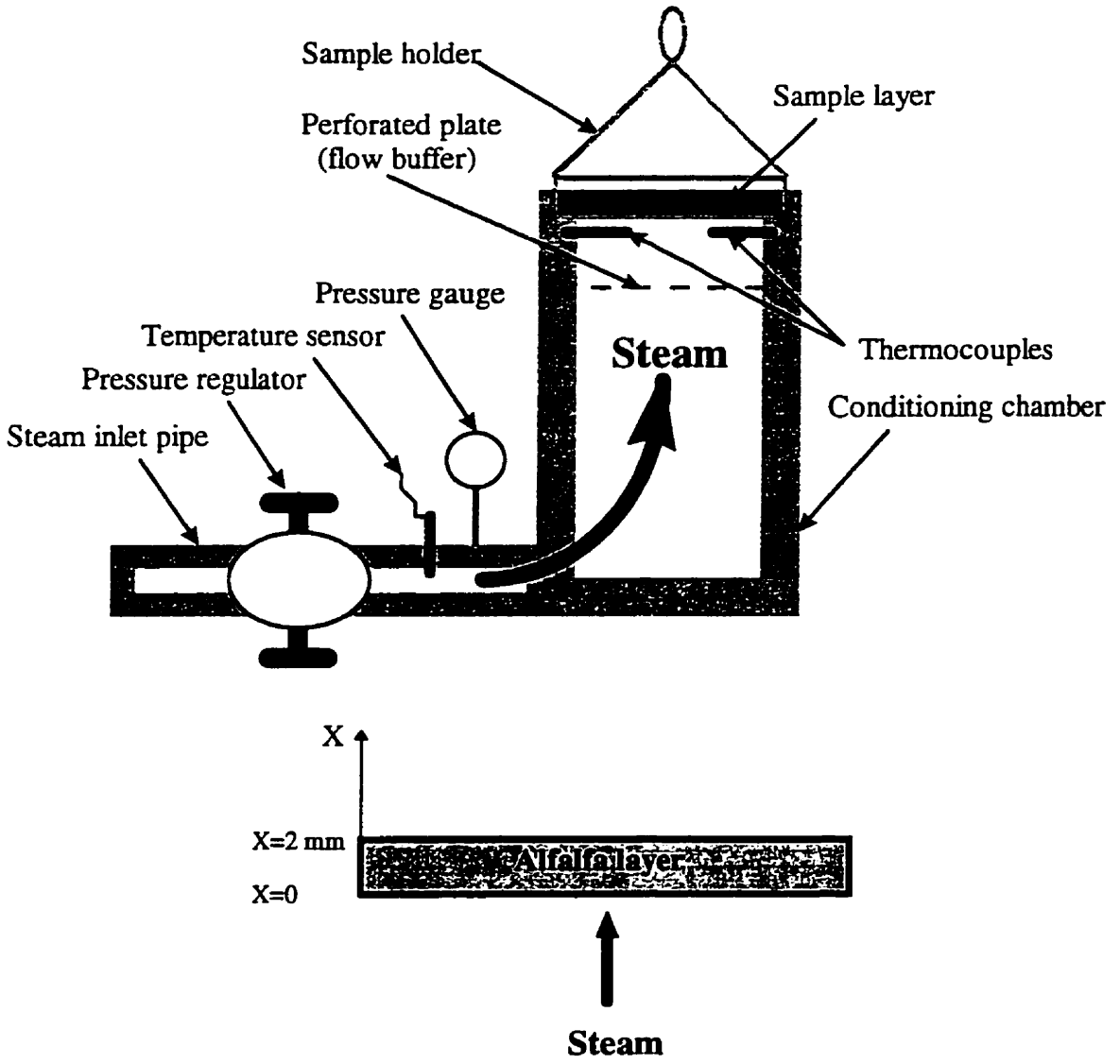

Figure 5.1: A schematic of the apparatus used to determine moisture sorption kinetics of alfalfa grind during steam conditioning and the coordinates for Equation 5.4.

Before kinetic tests, the sample holder was loaded with alfalfa grind that was deployed to become a thin layer of approximately 2 mm thick (as high as the edge of the sample basket). The sample was weighted to around 5 g by increasing or decreasing the quantity of the sample in the sample holder. The loaded sample holder was then placed on top of the conditioning chamber while time was recorded. At the end of each time interval, the sample holder was weighed (accurate to 0.001 g) and the weight gain was recorded. With the initial moisture content and the initial mass of the sample moisture content of the sample at each time interval was calculated.

Moisture diffusion tests in a semi-infinite tube

Figure 5.2 shows the experimental set-up for the moisture diffusion tests under steam conditioning. It consisted of a long tube and a steam conditioning chamber. The tube was comprised of twenty copper rings stacked one another. Each ring was 1.5 mm long and 20 mm in inner diameter. Both ends of each ring were smoothened on a fine sand paper so that they could stack together tightly. One end of the ring stack was plugged with a galvanized plug and sealed with silicone sealant, which is referred to as "Sealed end" in Figure 5.2. Three layers of scotch tapes and one final layer of duct tape were applied on the outer surface of the ring stack to hold the rings tightly together and also to partially prevent water leakage. Heat shrink rubber was then applied on top of the scotch tape and duct tape layer to prevent leakage. Silica sealant was further applied to both ends of the heat shrink rubber tube after they shrank under torch flame to further ensure that the surface of the ring stack be absolutely water-tight. Two type T thermocouples were attached to the surface of the heat shrink for sensing the temperature of the sample during steam treatment.

Alfalfa grind was filled into the stack through a funnel. The ring stack was weighed before and after each filling to know the net quantity of the sample in the tube, from which the bulk density of the sample could be calculated with respect to the volume of the ring stack. The whole stack was subjected to a steam conditioning chamber for moisture to diffuse through the sample. At the end of each test, the rings were quickly separated one after another by a thin razor blade that cut through the seam between two

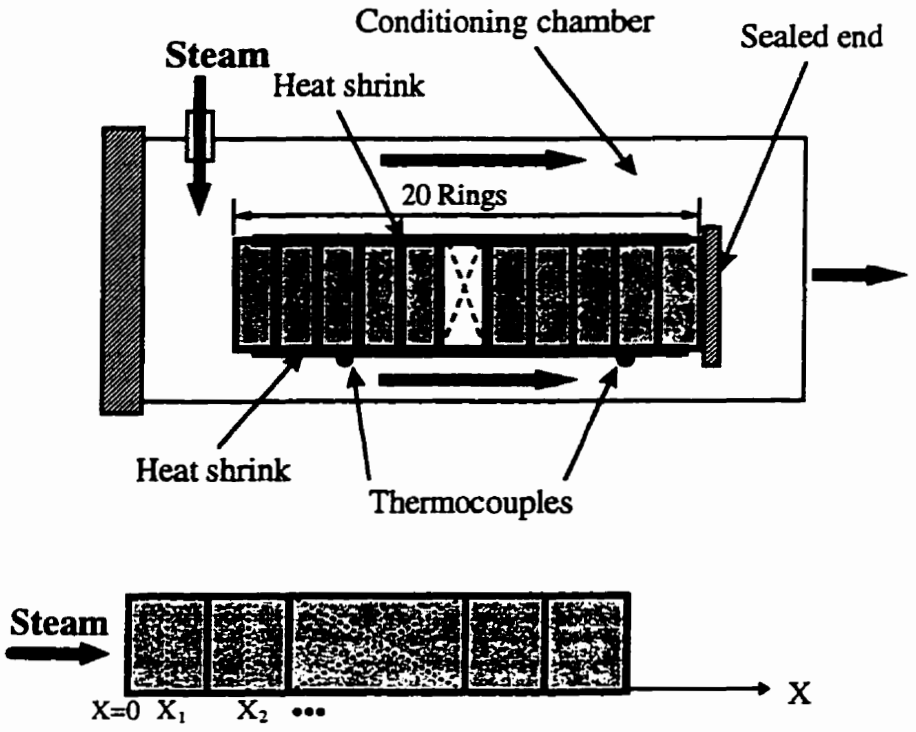

Figure 5.2: A diagram of the apparatus for moisture diffusion tests in a semi-infinite tube and the coordinates for Equation 5.4.

rings. The grind contained in each ring was carefully recovered and subjected to moisture content measurement by ASAE oven method (ASAE, 1996b). The relationship between the moisture content in each ring and the location of the rings were therefore obtained, which could be used to determine the moisture diffusivity of alfalfa grind under steam conditioning.

Determination of moisture diffusivity under steam conditioning

Moisture diffusivity of alfalfa grind under steam conditioning can, as described earlier, be determine by either kinetic method or "ring stack" method. In this study, both methods were used to determine the moisture diffusivity of alfalfa and their results were compared.

As mentioned before, the solution for either method is Equation 5.4. For the kinetic method, moisture diffusivity can be obtained using inverse method by fitting

Equation 5.4 to the data of the average moisture content of the thin-layered alfalfa sample vs. time, given x=1 mm (i.e., at the center of the thickness of the thin layer). Curve-fitting was performed in the commercial software, 'TableCurve 2D' (Jandel Scientific, 1994).

For the "ring stack" method, moisture diffusivity can be obtained by fitting Equation 5.4 to the relationship between the average moisture content of each ring and the distance of the mid-point of the ring from origin that was set at the open-end surface of the stack given a specific time.

The determination of D by the "ring stack" method necessitated a constant t in Equation 5.4. In the theoretical derivation of Equation 5.4, D was, as mentioned before, regarded as the overall effective diffusion coefficient that accounted for the liquid diffusion through the voids of the sample bulk and the pores in the individual particles as well as possible vapor diffusion through the voids of the sample bulk. Hence, D should not change with time. The effect of the length of exposure time on the magnitude of moisture diffusivity obtained from the "ring stack" method was examined in this study. This was done by subjecting the ring stack with dehydrated alfalfa grind to a steam chamber for three exposure times: 14520 s (4:02 h), 18360 s (5:06 h) and 35340 s (9:49 h), respectively. Based on the diffusivity obtained at the three times, inference and discussion could be made regarding the effect of exposure time.

Determination of moisture diffusivity at various packing densities

Measurements of the moisture diffusivity of alfalfa grind at various packing densities were carried out by the "ring stack" method. The dehy alfalfa grind was used in the tests. To achieve different packing densities, the loosely filled alfalfa grind in the ring stack was compressed in an Instron universal tester. Before filling, the 20-ring stack was extended at both ends with two pieces of copper tube at the same diameter as that of the rings. One piece of copper tube was about 100 mm long with one end hermetically sealed and water tight. This piece of tube was connected to the bottom end of the ring stack. Another piece of copper tube was about 250 mm long with both ends open. It was connected to the top end of the ring stack for filling the sample into the whole tube and

ring assembly. The whole tube and ring assembly was held together by scotch tape and duct tape. The assembly was then confined between two half-pipes (a copper pipe cut into halves along its longitudinal direction) at similar length but slightly larger diameter, and fastened using five clamps along its length. Alfalfa grind was then filled into the tube before compaction under the Instron machine. The packing density was determined by dividing the net weight of the compacted alfalfa grind over the volume of the ring stack. After the packing density reached the desired value, the compaction stopped and the tube and ring assembly was carefully dismounted. The copper tube on the top of the ring stack was then carefully removed by cutting through the seam between the tube the ring stack using a razor blade. The bottom part of the assembly was applied with a heat shrink before being subjected to the steam conditioning test. Both ends of the heat shrink was flame-melted and further sealed with silicone sealant.

Four packing densities resulted: 471.08 kg/m^3, 663.53 kg/m^3, 1163.52 kg/m^3 and 1394.65 kg/m^3, respectively. The packing density of 1394.65 kg/m^3 resembled that of a normal pellet coming out of a pelleter (ranging from 1333 to 1380 kg/m^3 depending on quality of alfalfa chops) according to Tabil (1996).

Determination of moisture diffusivity at various particle sizes

Moisture diffusivity at various particle sizes were determined by both the kinetic and the "ring stack" methods in the same procedures as described earlier.

Alfalfa grind was fractionated into the following portions by sieving using ASTM certified sieves: ASTM #14-18, #18-20, #20-30, #30-40, #40-50, #50-70, #70-100, and #100 and up. In this study, undersize was used to characterize the particle size in each sieved fraction. The particle undersize corresponding to the above-listed portions is: 1400 μm, 1000 μm, 850 μm, 595 μm, 425 μm, 297 μm, 210 μm, and 149 μm, respectively. Each fraction was used in the kinetic measurement and moisture diffusion test by ring stack. In the latter case, the fractionated alfalfa grind was loosely filled into the ring stack without any compaction.

5.4 Results and discussion

5.4.1 Moisture sorption kinetics

Moisture sorption kinetics of alfalfa grind

The moisture sorption kinetic data for both the dehydrated and the sun-cured alfalfa grinds collected in this study are presented in Appendix C. The data included the kinetics of the whole dehydrated alfalfa grind, the sieve fractionated dehydrated alfalfa grind and the sieve fractionated sun-cured alfalfa grind. The data were in the format of sample mass gain vs. exposure time.

As an example for showing the trend and magnitude of the kinetics during steam conditioning, Figure 5.3 shows the mass gain vs. exposure time data of the whole dehydrated alfalfa.

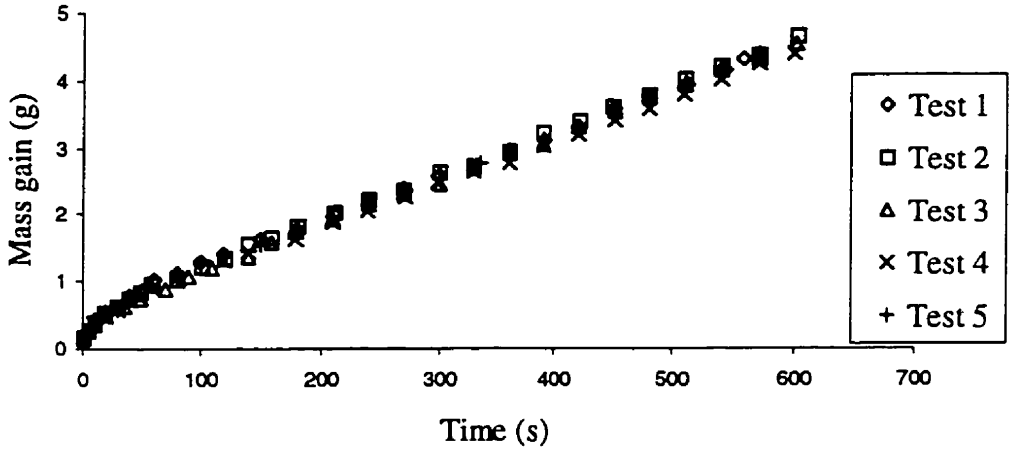

Figure 5.3: Moisture sorption kinetics of dehydrated alfalfa grind during steam conditioning at 85°C.

The data were collected in a period of about ten minutes. As can be seen, the mass gain increased from 0 to around 4.5 g in about ten minutes. This corresponded to a moisture content increase from 0.070 (w/w, db) (the initial moisture content) to 1.03 (w/w, db) in an average in this period of time.

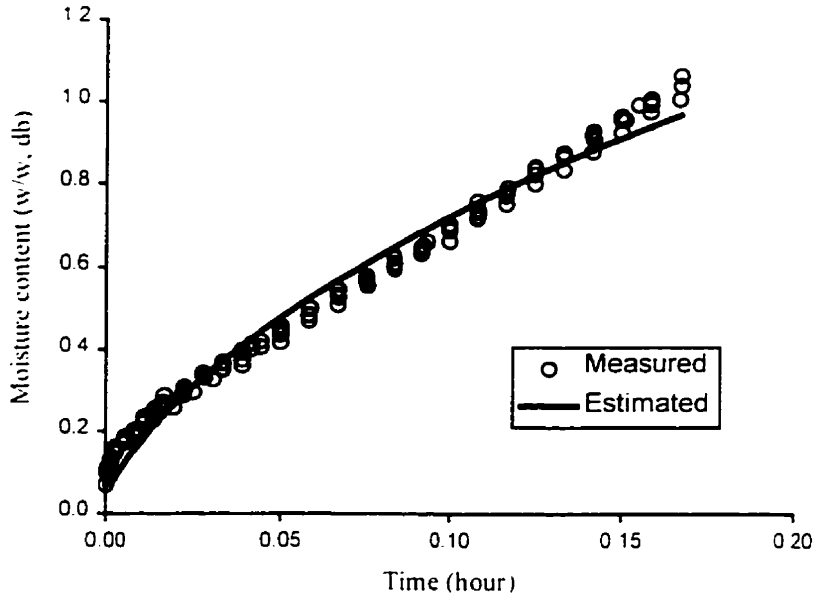

Figure 5.4: The result of curve-fitting Equation 5.4 to the kinetic data of the whole dehydrated alfalfa grind under steam conditioning at 85°C.

Applicability of the kinetic model

The kinetic model, i.e., Equation 5.4, has been fitted to the kinetic data of alfalfa grind to study the kinetic behavior of the samples and to determine the moisture diffusivity, D. Before applying the model to the kinetic data, conversion from mass gains to sample dry-basis moisture contents using the initial moisture content and the initial sample mass was made. Figure 5.4 is an example of the curve-fitting result, where the moisture content was calculated from the mass gain data in Figure 5.3 by incorporating the initial sample mass and initial moisture content. The resultant moisture diffusivity for the whole dehydrated alfalfa grind was 1.09×10^{-4} m^2/h or 3.03×10^{-8} m^2/s.

From Figure 5.4, it can be seen that at both initial and final stages of the test, Equation 5.4 underestimated the data, and in the intermediate time range it overestimated the data. The model exhibited mediocre performance towards the kinetic data. This can also be seen from the regression statistics listed in Table 5.1. The statistics include mean

Table 5.1: Curve fitting summary for both the dehydrated and the sun-cured alfalfa grinds.

ASTM Sieve #	Regression Statistics*				Moisture Diffusivity
	P (%)	R^2	Fit S.E.	F_{stat}	D (10^{-8} m^2/s)
	Whole dehydrated Alfalfa Grind				
	11.2	0.98	0.04	3440	3.0
	Fractionated dehydrated Alfalfa Grind				
18-20	6.8	0.99	0.02	2639	9.5
20-30	8.6	0.98	0.04	1176	21.9
30-40	9.9	0.98	0.04	1129	11.4
40-50	9.9	0.98	0.04	1472	4.7
50-70	10.0	0.98	0.03	1636	4.0
70-100	11.6	0.98	0.04	989	3.1
100 & up	7.9	0.99	0.03	1989	5.2
	Fractionated Sun-cured Alfalfa Grind				
14-18	9.1	0.98	0.03	1730	7.0
18-20	9.3	0.98	0.04	1119	41.1
20-30	10.3	0.98	0.04	1001	11.0
30-40	8.2	0.99	0.03	1777	5.8
40-50	8.2	0.98	0.04	940	36.6
50-70	9.8	0.98	0.04	1600	5.2
70-100	6.9	0.98	0.03	1436	24.3
100 & up	8.0	0.99	0.02	1723	7.6

* P is the mean relative percentage deviation; R^2 is the coefficient of determination; Fit S.E. is the residual standard error; F_{stat} is the F statistical value.

relative percent deviation (P%), coefficient of determination (R^2), residual standard error (Fit S.E.) and F statistic value (F_{stat}). The regression statistics in Table 5.1 showed that the P value for whole dehydrated alfalfa grind was 11.2. Generally, P values were within 10%), R^2 was 0.98 to 0.99, standard errors were 0.02-0.04, and F values were high. This indicated that the model represented the kinetic data to a certain extent, but the goodness-of-fit was still left some to be desired. The most probable reason was that during kinetic tests, the container, as pointed out in the overview section of this chapter, trapped the condensed moisture that caused the kinetic trend went somewhat higher than it should be.

The immediate consequence of this may be that higher moisture diffusivity is likely to be obtained.

Moisture diffusivity determined by kinetic measurement

Table 5.1 also shows the moisture diffusivity of the whole dehydrated alfalfa grind, the ASTM sieve fractionated dehydrated alfalfa grind, and the ASTM sieve fractionated sun-cured alfalfa grind during steam conditioning at 85°C temperature.

It was found that the moisture diffusivity of the whole dehydrated alfalfa grind was 3.0×10^{-8} m^2/s (Table 5.1). The moisture diffusivity of the fractionated dehydrated alfalfa grind ranged from 3.1×10^{-8} m^2/s to 2.2×10^{-7} m^2/s with a mean of 8.5×10^{-8} m^2/s (standard deviation 6.6×10^{-8} m^2/s). The moisture diffusivity of the fractionated sun-cured alfalfa grind ranged from 5.2×10^{-8} m^2/s to 4.1×10^{-7} m^2/s with a mean of 1.7×10^{-7} m^2/s (standard deviation 1.5×10^{-7} m^2/s).

Effect of particle size on moisture diffusivity of alfalfa grind

To show the effect of particle size on the sorption kinetics of alfalfa grind, the moisture content vs. exposure time relationships for each fraction of the sieve partitioned dehydrated alfalfa and the sun-cured alfalfa are shown in Figure 5.5 as well as Figure 5.6, respectively. It can be seen that the kinetic curves for the fractionated sun-cured alfalfa grind are quite apart from one another, especially between the curve for the undersize of 595 μm (sieve #30-40) and that for the undersize of 149 μm (sieve #100 and up). Unlike the situation for the sun-cured alfalfa grind, the kinetic curves for the dehydrated alfalfa grind vary little in lower exposure times and exhibit some marginal variation in higher exposure times. One major factor, although not excluding other causes, might have contributed to the phenomenon observed, that is, the material property changed during high temperature dehydration. It has been known that sun-cured alfalfa was dried in field by natural convective air under sunshine, while the dehydrated alfalfa was artificially dried at a fairly high temperature. Under such a high temperature, alfalfa leaves and stems are

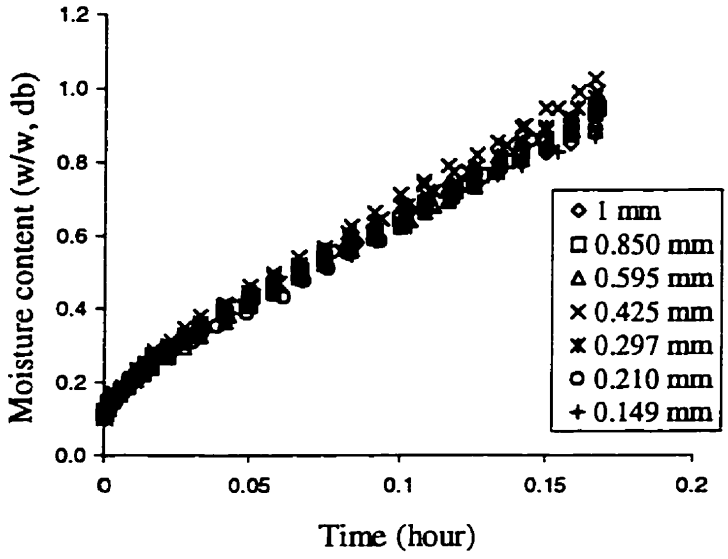

Figure 5.5: Comparison among kinetic data of the fractionated dehydrated alfalfa grind.

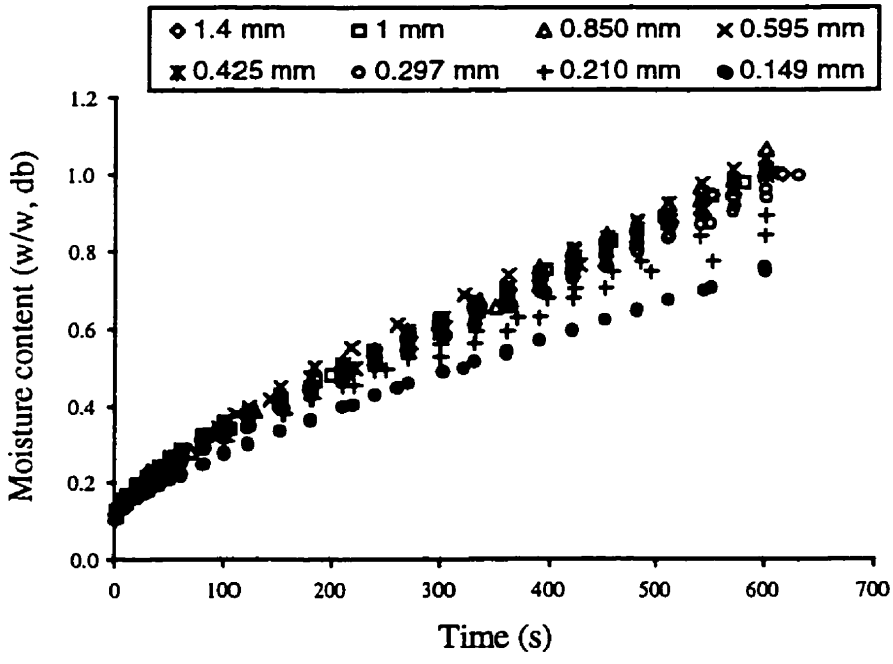

Figure 5.6: Comparison among the kinetic data of the fractionated sun-cured alfalfa grind.

expected to undergo a variety of changes in their physical property (such as increased brittleness in both leaves and stems), chemical property (such as loosened bonds between fibrils, scrambled hydrophilic and hydrophobic sites, etc.), morphological property (such as hygroscopic shrinkage) and microstructure (such as cuticular surface of the stem). The changes might have facilitated the stems to break down, during size reduction process, to fractions at a wider range of sizes, and also caused the hydrophilic and the hydrophobic sites to mingle. The result was a reduced difference in moisture sorption capacity between any two different fractions.

It was also observed that moisture diffusivity was lower on either extremity of the size fractions involved in this study (e.g., below 212 μm and above 1000 μm) and higher in between. This trend can be seen in Figure 5.7 where the moisture diffusivity for both the dehydrated and the sun-cured alfalfa fractions are plotted together in relation to particle undersize. This was probably because large particles have less surface area for steam to contact, and the tiny particles stay more compact and therefore render it rather hard for steam to penetrate. For sun-cured alfalfa, there was no obvious trend observed in the intermediate size range. For dehydrated alfalfa, a bell-shaped trend was observed, which will be further discussed later.

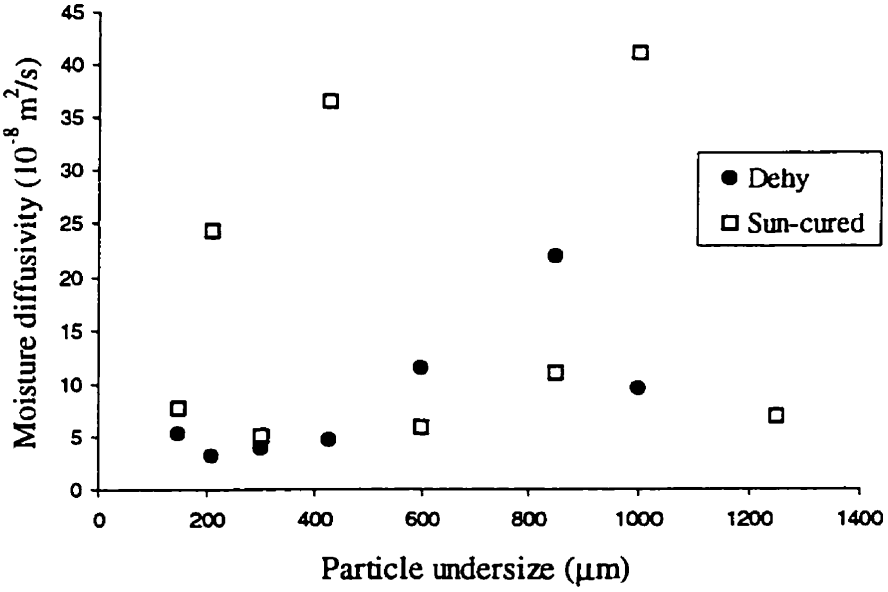

Figure 5.7: The relationship between the moisture diffusivity of alfalfa grind and its particle undersize.

Moisture diffusivity comparison between the dehydrated and the sun-cured alfalfa grinds

The mean moisture diffusivity of the dehydrated alfalfa fractions when considered as a whole was 8.5×10^{-8} m^2/s (standard deviation 6.6×10^{-8} m^2/s) and that of the sun-cured alfalfa was 1.7×10^{-7} m^2/s (standard deviation 1.5×10^{-7} m^2/s). A t-test with two unequal variances was conducted to examine whether the two means were equal. It was found that the two means were not equal at a significance level of 0.05, indicating that there was difference in moisture sorption capability between the sun-cured and the dehydrated alfalfa grinds.

5.4.2 Moisture diffusion ring tests

Experimental data by "ring stack" method

The "ring stack" method has been applied in this study to the loose dehydrated alfalfa grind which included the whole dehydrated alfalfa grind and the sieve fractionated dehydrated alfalfa grind. The measured moisture contents of the whole alfalfa grind in the rings at various locations along the direction of diffusion are listed in Appendix D. As an example to show the relationship between the ring moisture content and its location (i.e., the distance between its centroid and the surface of the open end of the ring stack), Figure 5.8 plots the experimental data (in symbols) for the whole dehydrated alfalfa grind at three tests corresponding to three lengths of exposure times: 4:02 h (14520 s), 5:06 h (18360 s) and 9:49 h (35340 s). The figure also shows the model estimated values of moisture diffusivity and residuals, which will be discussed later.

Model applicability

Performance of the model on the experimental data. Non-linear regression has been performed to fit Equation 5.4 to the data. Table 5.2 lists the resultant regression statistics and moisture diffusivity. The "Mixed Data" in Table 5.2 refers to the regression of Equation 5.4 to the mixture of the data combined from the three tests at different times.

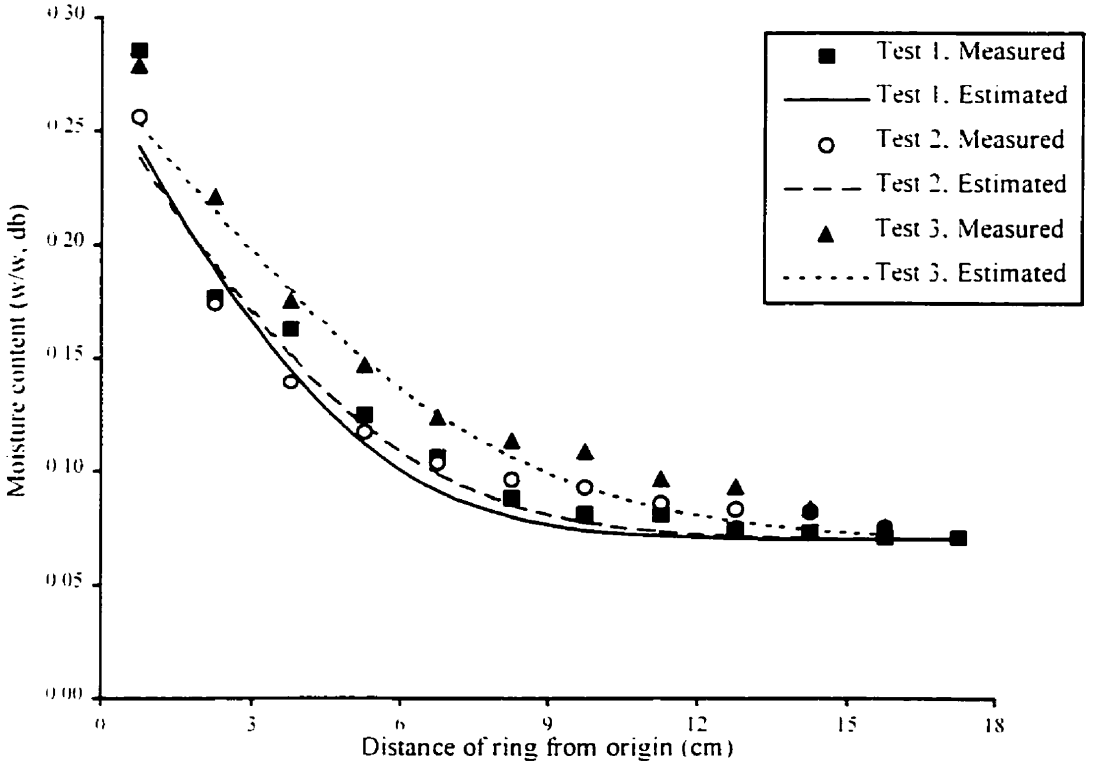

Figure 5.8: The measured and the estimated moisture contents of the dehydrated alfalfa grind in the rings.

It can be seen from Table 5.2 that average value of the relative percent deviations for the three tests was 8.58%. The coefficient of determination and the fit standard error ranged from 0.94 to 0.96 and from 0.013 to 0.017, respectively. The residuals were scattered mostly between -0.02 and 0.02. The statistical criteria obtained signified that Equation 5.4 fitted relatively well to the experimental data of alfalfa grind in a semi-infinite tube with steam condensation. This verified the applicability of the model in determining the moisture diffusivity of alfalfa grind under steam condensation.

Sensitivity of moisture diffusivity to exposure time. The overall effective moisture diffusivity of alfalfa grind under steam condensation was found to be 6.0×10^{-8}, 6.3×10^{-8} and 5.4×10^{-8} m^2/s corresponding to test 1, 2 and 3, respectively (Table 5.2). The average value was 5.9×10^{-8} m^2/s with a standard deviation of 4.7×10^{-9} m^2/s.

The three diffusivity values were obtained after the exposure times of 14520 s (4:02 h), 18360 s (5:06 h) and 35340 s (9:49 h) to steam condensation. Since the three

diffusivity values were close to one another (coefficient of variation 8%), it seemed that the exposure time had little effect on the measurement. This also seemed to verify the constant diffusivity assumption during the development of Equation 5.4.

Table 5.2: Regression statistics and model constants to show the performance of the model on the experimental data.

	Test # 1	Test # 2	Test #3	Average	Std. Dev.	Mixed Data
	$m_0 = 0.070$ (w/w, db), $m_e = 0.274$ db					<-- Same m_0 and m_e
D (m^2/s)	6.0×10^{-8}	6.3×10^{-8}	5.4×10^{-8}	5.9×10^{-8}	4.7×10^{-9}	5.6×10^{-8}
α (m/s)	46.83	6.74	26.71			18.01
R^2	0.94	0.94	0.96			0.92
P (%)	8.11	10.05	7.57	8.58	1.3	9.79
Fit S.E.	0.017	0.013	0.013	0.014	0.002	0.017
F Static	148	153	226			374
	$m_0 = 0.070$ (w/w, db) and variable m_e					<-- Same m_0 and m_e
D (m^2/s)	9.8×10^{-8}	8.9×10^{-8}	8.4×10^{-8}	9.0×10^{-8}	7.3×10^{-9}	8.6×10^{-8}
α (m/s)	0.06	0.05	0.04			0.06
m_e (db)	3.70	2.90	2.75			2.68
R^2	0.97	0.96	0.98			0.94
P (%)	4.73	8.86	5.44	6.34	2.21	8.84
Fit S.E.	0.012	0.012	0.009	0.011	0.002	0.015
F Static	166	92	253			239

Sensitivity of moisture diffusivity to the magnitude of m_e. The equilibrium moisture content, m_e, is the moisture content of alfalfa grind that is left in the steam for an infinitely long time. It is a constant in Equation 5.4. During curve-fitting processes, it can either assume the actual value of m_e or be treated as regression parameter during curve-fitting operations. There will be some difference in other resultant regression parameters (i.e., D and α) of the model, but the difference would be marginal for a drying or rewetting curve. This is because the constant-rate period of drying or rewetting predominantly determines the moisture diffusion rate, not the falling-rate period to which m_e belongs. Therefore, it would be easier to estimate the moisture diffusivity by Equation 5.4 with m_e treated as a regression parameter without suffering too much accuracy, rather than to go through the time-consuming process of measuring m_e. In this

study, the sensitivity of D to m_e was tested using the data shown in Figure 5.8. During curve-fitting, m_e was 1) approximately taken as the average of the moisture contents of the alfalfa grind in the first rings at the three tests, which was 0.274 (w/w, db), and 2) treated as a regression parameter during curve-fitting.

As can be seen in Table 5.2, the D value obtained with m_e being variable until best fit was 9.02×10^{-8} m^2/s in an average, which was as high as D could go. This was about 50% higher than the D value (5.91×10^{-8} m^2/s in an average) obtained with m_e constant at the equilibrium moisture content (i.e., 0.274 db in this case). It is noticed that in the free-changing case of m_e, the resulted m_e value as a model constant was higher than the actually equilibrium moisture content. However, the variation of m_e did not seem to substantially affect the magnitude of D. As a matter of fact, D values in both cases were in the same order and not awfully away. Thus, D could, as an approximate estimate for a problem of engineering nature, be obtained by treating m_e as a regression parameter during curve fitting in case of lacking equilibrium data.

Moisture diffusivity of alfalfa grind under steam condensation

Moisture diffusivity of the whole dehydrated alfalfa grind. Equation 5.4 was also fitted to the mixture of data combined from the three tests to determine D. The resultant D value was 5.6×10^{-8} m^2/s for the case of fixed m_0 and m_e (Table 5.2). For the case of fixed m_0 and variable m_e, the D value was 8.6×10^{-8} m^2/s. This seemed to suggest that the overall effective diffusivity could also be estimated with reasonable accuracy by applying Equation 5.4 to the mixed data of the individual diffusion tests at various exposure times. This would be more convenient than curve fitting the moisture content data by individual test.

The moisture diffusivity of the whole dehydrated alfalfa grind under steam condensation was compared with those of other agricultural products. Fasina (1994) reported that the moisture diffusivity of alfalfa pellets during absorption process ranged from 4.1×10^{-10} m^2/s to 1.3×10^{-9} m^2/s in the moisture contents from 6.5 % wb to 20 % wb at ambient temperature. For wheat kernels, the moisture diffusivity ranged approximately from 1.0×10^{-10} m^2/s to 2.4×10^{-10} m^2/s in the moisture range of about 4.8 % wb to 17 % wb

Table 5.3: Moisture diffusivity of dehydrated alfalfa grind at different particle undersize.

Particle Undersize* (μm)	ASTM Sieve Number	Moisture Diffusivity D (10^{-8} m^2/s)
150	100	3.6
212	70	1.8
300	50	1.9
425	40	1.4
600	30	2.5
850	20	5.9
1000	18	2.4
	Mean	2.8 (1.5**)

* Supplementary size R40/3 in ISO 3310-1. ** Standard deviation.

at 82°C temperature (Jaros et al., 1992). The magnitude of moisture diffusivity of the whole dehydrated alfalfa grind under steam condensation (85°C temperature) was in magnitude of 10^2 higher than those of alfalfa pellets and wheat kernels. This might be because 1) alfalfa grind had a loose structure of enormous voids in bulk, 2) its particles were porous and full of fissures and cracks inside, 3) steam condensation accelerated the rate of mass transport, and 4) temperature was higher (85°C) due to the release of the latent heat of steam.

Moisture diffusivity of the fractionated dehydrated alfalfa grind. The moisture content vs. ring location data for the fractionated dehydrated alfalfa grind are presented in Appendix E. Moisture diffusivity of the fractionated dehydrated alfalfa grind was obtained by fitting Equation 5.4 to the moisture content vs. ring location data of each fraction with variable m_e. Table 5.3 shows the resultant D values in relation to particle undersize. The moisture diffusivity of the whole dehydrated alfalfa grind was slightly higher than that of the fractionated dehydrated alfalfa grind in a general sense, but they are in the same 10^{-8} order and comparable to one another.

Effect of compaction on moisture diffusivity of alfalfa grind

The ring test data for the whole dehydrated alfalfa grind at four packing densities are presented in Appendix F. Moisture diffusivity of the compacted alfalfa grind under steam conditioning at 85°C was determined by curve-fitting Equation 5.4 to the moisture content vs. ring location data. Table 5.4 lists the resultant D values.

It was found that the magnitude of the moisture diffusivity of alfalfa grind was very sensitive to the compactness of the grind bulk. As can be seen in Table 5.4, at the packing density of 240 kg/m^3, i.e., the bulk density at no compaction, the moisture diffusivity was 8.6 x 10^{-8} m^2/s. As the packing density increased to 471 kg/m^3 which was about double its bulk density, the moisture diffusivity decreased dramatically to 3.3 x 10^{-9} m^2/s, which was about 1/18 that of loosely-contained alfalfa grind. As packing further increased to 1395 kg/m^3, there was no further decrease in moisture diffusivity observed.

The relationship between the moisture diffusivity of dehydrated alfalfa grind under steam conditioning and the packing density was found to be closely approximated by a power function:

$$D = 4062.9\ \rho^{-4.5} \qquad (5.5)$$

where D is moisture diffusivity in m^2/s and ρ is packing density in kg/m^3.

The moisture diffusivity of the compacted dehydrated alfalfa grind determined in this study was found to be slightly higher than those reported by Fasina (1994) (4.1 x 10^{-10} m^2/s to 1.3 x 10^{-9} m^2/s at ambient temperature), but they were generally comparable because they were all in the order of 10^{-10} to 10^{-9}, especially for the packing densities ranging from 664 to 1395 kg/m^3 in which the packing density of most commercial alfalfa pellets fell. The slightly higher D values in this study than those reported by Fasina (1994) were probably attributable to the fact that higher temperature (85°C) was involved in the tests during steam conditioning.

Table 5.4. Moisture diffusivity of the whole dehydrated alfalfa grind under steam conditioning at various packing densities.

Packing Density (kg/m^3)	Moisture Diffusivity (m^2/s)
240	8.6×10^{-8}
471	3.3×10^{-9}
664	2.2×10^{-9}
1164	8.8×10^{-10}
1395	9.2×10^{-10}

Effect of particle size on moisture diffusivity

The moisture diffusivity of the fractionated dehydrated alfalfa grind has been presented in Table 5.3. To compare between the D values determined by the kinetic method and the "ring stack" method, the moisture diffusivity by both methods is plotted in Figure 5.9 with respect to the particle undersize of the individual fractions. Note that the solid curves in Figure 5.10 were only for the convenience of data presentation and do not necessarily represent the trend of the D vs. particle undersize relationship.

As can be seen in Table 5.3, the moisture diffusivity measured by the "ring stack" method ranged from 1.4×10^{-8} m^2/s to 5.9×10^{-8} m^2/s, which were, as a whole, somewhat less than those obtained through kinetic measurement at each corresponding fraction, although most were more or less in the same order in all fractions except one at 850 μm undersize. One major reason was the condensation on sample holder during kinetic measurement, as mentioned earlier, which could result in higher moisture diffusivity. In this sense, the "ring-stack" method is more appropriate for measuring moisture diffusivity of powder-like materials such as alfalfa grind.

It was observed that the moisture diffusivity measured by the two different methods followed the same trend in relation to particle undersize, that is, the moisture diffusivity values were relatively low at smaller particle undersize (149 μm to 425 μm). The values started to climb as the particle undersize increased from 425 μm and peaked at a particle undersize around 850 μm. As particle undersize further increased, moisture

diffusivity decreased dramatically from its peak down to a level similar to that corresponding to the particle undersize of 149 μm to 425 μm. Although the true reasons for the phenomenon are unknown yet, there is one possible explanation that may cast some light on the peaked trend of moisture diffusivity vs. particle size. As mentioned in Chapter 3, alfalfa particles tended to stay more compacted in both lower and higher particle size ranges and less in the intermediate size range. This was because in lower size range the particles were small enough to stay closer and in higher size range the particles stay also closer due to smooth surface and less arching. The more compacted alfalfa grind is, the more difficult for moisture to penetrate and therefore the less the moisture diffusivity is likely to be, and vice versa.

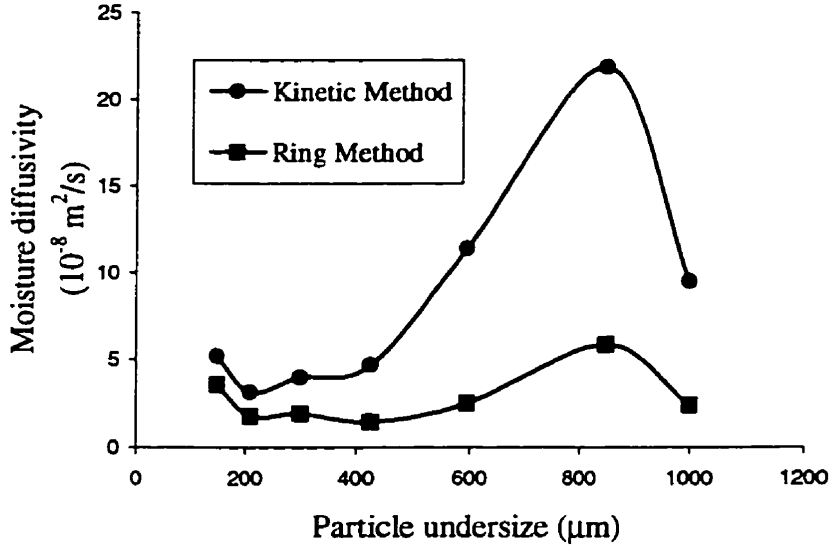

Figure 5.9: Moisture diffusivity of the whole dehydrated alfalfa grind by two different methods.

Attempts have been made to develop a relationship between the moisture diffusivity of the dehydrated alfalfa grind and its particle undersize. Ten different functions that can generate peaks, such as normal, log-normal, Lorentzian and Gaussian functions, have been curve-fitted to the data. Although many other functions were also found capable of representing such a relationship, the Gaussian function was chosen to approximate the relationship because of its simplicity relative to other functions. The Gaussian function assumes the following form:

Table 5.5: The regression constants and statistics of Equation 5.6 as applied to the D vs. particle undersize data.

Parameter	Kinetic Method	Ring Stack Method
a	4.1×10^{-8}	2.2×10^{-8}
b	2.0×10^{-7}	4.2×10^{-8}
c	784.1	791.4
d	132.9	84.4
R^2	0.99	0.80
P (%)	8.2	18.1
Fit S.E.	8.6×10^{-9}	9.5×10^{-9}
F Static	118	4

$$D = a + b\exp\left[-\frac{1}{2}\left(\frac{U-c}{d}\right)^2\right] \tag{5.6}$$

where D is moisture diffusivity in m^2/s, U is particle undersize in micrometer, and a, b, c, d are constants. Table 5.5 gives the constants (a, b, c, d) in Equation 5.6 and the regression statistics as it applied to the moisture diffusivity measured by the kinetic method and the "ring stack" method, respectively. Figure 5.10 shows the performance of Equation 5.6 to the measured D values. It can be seen from Figure 5.10 that Equation 5.6 approximated very well the data at the particle undersize above 210 μm, and the lack of fit occurred at the particle undersize below 210 μm inclusive i.e., at 210 μm and 149 μm.

5.4.3 Implications of moisture diffusivity results to steam conditioning process

The results revealed some interesting information on the relationship between moisture diffusivity and particle size. It was found that the moisture diffusivity of the dehydrated alfalfa grind collected from the industry (median size 238 μm) was in the lower part of the moisture diffusivity range as a function of particle undersize (Figure 5.9), while the highest diffusivity occurred in the particle undersize around 800 μm. There seemed to be a dilemma here. The sizes typical of commercial alfalfa grind were associated with low moisture diffusivity, but in these sizes the natural binding capacity of

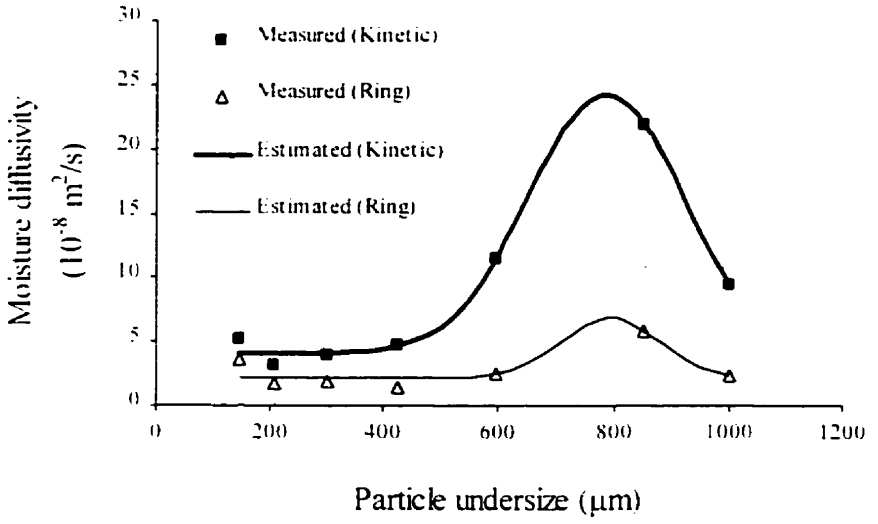

Figure 5.10: Measured and model estimated moisture diffusivity in relation to particle undersize.

alfalfa grind could be best activated and the pellets so made tended to durable even in the absence of an artificial binder. The sizes around 800 μm corresponded to the highest diffusivity, which signified that in a much shorter time alfalfa grind could be conditioned to the targeted moisture content, but alfalfa particles in these sizes are usually hard to bind. The results suggested that with the help of such an artificial binder that was capable of greatly enhancing the durability of pellets made from alfalfa particles in larger sizes, e.g., around 800 μm, the production rate could be greatly expedited by using the alfalfa grind at sizes around 800 μm. This would also facilitate or simplify the design of a hammer mill/grinder and a pelleter.

The results also showed that the moisture diffusivity of alfalfa grind was very sensitive to packing density. It decreased dramatically with the increase of packing density. This suggested that any compaction during loading of alfalfa grind to a conditioner or during conditioning would adversely affected the moisture diffusivity and therefore the production rate.

5.4.4 Comparison between dehydrated and sun-cured alfalfa grinds with regard to steam conditioning

As mentioned earlier, there was significant difference (α=0.05) in moisture sorption capability between the dehydrated and the sun-cured alfalfa grinds. The latter seemed to be in an average moisture diffusivity double that of the former (Table 5.1). From the perspective of steam conditioning itself, using sun-cured alfalfa grind would likely be more beneficial to the efficiency of steam conditioning due to the increased moisture diffusivity of sun-cured alfalfa grind as compared to using dehydrated alfalfa grind. However, this positive finding did not necessarily conclude that the sun-cured alfalfa grind was better than the dehydrated alfalfa grind as a whole. As a matter of fact, sun-cured alfalfa has also some demerits such as unstable quality due to exposure to uncontrollable weather in the field after swath, less by-pass protein available due to natural drying at lowered temperature, etc. despite the merit of higher moisture diffusivity during steam conditioning.

From the standpoint of the moisture sorption kinetics, dehydrated alfalfa grind tended to have fairly similar moisture sorption capability at each size fraction tested in this study. Sun-cured alfalfa grind behaved quite differently from dehydrated alfalfa grind. The moisture sorption capability tended to be lower for smaller size fractions of sun-cured alfalfa grind, while stayed close in larger size fractions of sun-cured alfalfa grind.

5.5 Summary

Moisture diffusion characteristics of alfalfa grind during steam conditioning were studied. Two methods, i.e., the thin-layer rewetting and the "ring stack" diffusion tests, were used to acquire the kinetic data for the dehydrated and the sun-cured alfalfa grinds. The overall diffusivity of alfalfa grind was estimated by inverse method. The effect of particle size and packing density on moisture diffusivity of alfalfa grind under steam conditioning was also studied.

From the thin-layer kinetic measurement, it was found that the moisture diffusivity of the whole dehydrated alfalfa grind was 3.0 x 10^{-8} m^2/s. The moisture diffusivity of the fractionated dehydrated alfalfa grind ranged from 3.1 x 10^{-8} m^2/s to 2.2 x 10^{-7} m^2/s with a mean of 8.5 x 10^{-8} m^2/s (standard deviation 6.6 x 10^{-8} m^2/s) in the particle undersize range of 0.149 mm to 1.4 mm. The moisture diffusivity of the fractionated sun-cured alfalfa grind ranged from 5.2 x 10^{-8} m^2/s to 4.1 x 10^{-7} m^2/s with a mean of 1.7 x 10^{-7} m^2/s (standard deviation 1.5 x 10^{-7} m^2/s) in the same particle undersize range. There was a significant difference in moisture diffusivity between the dehydrated and the sun-cured alfalfa grinds (α=0.05).

From the "ring stack" diffusion test, a mean diffusivity of 8.6 x 10^{-8} m^2/s resulted for the whole dehydrated grind. The moisture diffusivity of the fractionated dehydrated alfalfa grind ranged from 1.4 x 10^{-8} m^2/s to 5.9 x 10^{-8} m^2/s with a mean of 2.8 x 10^{-8} m^2/s (standard deviation 1.5 x 10^{-8} m^2/s) in the particle undersize range of 0.149 mm to 1.0 mm.

It was found that the moisture diffusivity of alfalfa grind under steam conditioning ranged between 9.2 x 10^{-10} m^2/s to 8.6 x 10^{-8} m^2/s in the packing density range of 240 kg/m^3 to 1395 kg/m^3, following a power relationship with packing density.

It was also found that the relationship between the moisture diffusivity of alfalfa grind and particle undersize could be best described by the Gaussian function.

Chapter 6

MOISTURE EQUILIBRIUM CHARACTERISTICS OF ALFALFA GRIND

6.1 Overview

Moisture equilibrium characteristics of a hygroscopic material generally refer to its moisture sorption isotherm or equilibrium moisture content - equilibrium relative humidity (EMC-ERH) relationship and moisture sorption hysteresis. Moisture sorption isotherm or the EMC-ERH relationship is a true reflection of the moisture sorption capacity of a hygroscopic material like alfalfa grind exposed to an environment of a certain relative humidity and temperature. The EMC-ERH relationship is also a crucial component during mathematical modeling of a drying or rewetting process. An explicit analytical expression of an isotherm for a particular material would greatly facilitate the modeling of its drying or rewetting process. Therefore, determination and modeling of an isotherm have been an important step before modeling of a drying or rewetting process becomes possible. Over 200 isotherms models, either theoretical or empirical, have so far been proposed to describe an isotherm (Yang and Cenkowski, 1993). Their capability in representing the isotherm of a particular type of material varied greatly. Sokhansanj and Yang (1995a) have newly revised the ASAE Standard D245.4 to expand the EMC-ERH data to more plant-based materials. They also included a broader number of high profile isotherm equations to this standard. Measuring the isotherms of alfalfa grind at various temperatures and finding a suitable isotherm model from the ASAE recommended isotherm equations was the primary task of this study.

Moisture sorption hysteresis refers to the phenomenon that the isotherms along an adsorption (rewetting) path generally do not overlap those along a desorption (drying) path with a gap left in between. This phenomenon has been extensively studied since it was discovered over a century ago. Several qualitative theories, such as the incomplete wetting theory (Zsigmondy, 1911), the ink bottle neck theory (McBain, 1935), the open pore theory (Cohan, 1944) and the independent-domain theory (Everett, 1967), and many interpretations (Chung and Pfost, 1967; Kapsalis, 1987; Young and Nelson, 1967) are

available to account for the origin of sorption hysteresis. Kapsalis (1981, 1987) had plausible reviews on the merits and demerits of the existing theories and interpretations. However, there has so far been a lack of quantitative description of the phenomenon. Because of this deficiency, Rizvi and Benado (1984) had the following comment: "Many theories concerning the origin of hysteresis can be found in the literature, several of which can be proven to have an effect on isotherms in a qualitative way. ... To date, however, no model has been found to quantitatively describe the hysteresis loop of foods, and there will probably be no final solution to this problem for a long time to come."

Close examination of the existing theories reveals that most theories emphasize the initial and final equilibrium states of a material and neglect the intermediate process that occurs between the initial and final equilibrium states. In the intermediate process, a material undergoes a series of physical, thermal and structural changes. It has been proved by many researchers (Pierce and Benner, 1986; Tao et al., 1992a; Tao et al., 1992b; Simonson et al., 1993) that phase change mass transfer is coupled with heat transfer during a sorption process, while the resultant heat transfer can alter the local temperature of the material significantly. The intermediate process that connects any two equilibrium states might play so important a role in the occurrence of sorption hysteresis that it should not have been overlooked.

Therefore, the primary purposes of this chapter were to 1) determine and model the EMC-ERH relationship of alfalfa grind at various temperatures, and 2) develop a mathematical model to quantify sorption hysteresis loop and verify the applicability of the developed model to the hysteresis data of alfalfa grind collected in this study.

6.2 Theoretical background and modeling

6.2.1 Mathematical models for describing the EMC-ERH relationship

In the newly revised ASAE Standard D245.5 (ASAE, 1996a), five isotherms equations, as shown below, have been recommended for describing the EMC-ERH relationship of plant-based agricultural products. These five equations were selected as ASAE standard isotherm equations based on their excellent performance in describing the

EMC-ERH relationships of plant-based agricultural products (Sokhansanj and Yang, 1995a). The five equations are:

1) Modified Henderson equation

$$RH = 1 - \exp\left[-A(T + C)M^{B}\right] \tag{6.1}$$

2) Modified Chung-Pfost equation

$$RH = \exp\left[-\frac{A}{T+C}\exp(-B*M)\right] \tag{6.2}$$

3) Modified Halsey equation

$$RH = \left[-\frac{\exp(A + B*T)}{M^{C}}\right] \tag{6.3}$$

4) Modified Oswin equation

$$RH = \left[\left(\frac{A + B*T}{M}\right)^{C} + 1\right]^{-1} \tag{6.4}$$

5) Guggenheim-Anderson-de Boer (GAB) equation

$$M = \frac{A*B*C*RH}{(1 - B*RH)(1 - B*RH + B*C*RH)} \tag{6.5}$$

where RH is the relative humidity in fraction, T is temperature in °C, M is moisture content in fraction dry basis, and A, B, C are constants.

Among the five equations, the Modified Henderson and the Modified Chung-Pfost equations generally describe better the isotherms of starchy and fibrous materials (Chen and Morey, 1989). The Modified Halsey and the Modified Oswin equations tend to approximate better the oil-rich materials (Chen and Morey, 1989; Yang and Cenkowski,

1993), although some exceptions exist. The GAB equation has been reported to approximate well the isotherms of most agricultural and food materials (Sokhansanj and Yang, 1995b).

There are basically two methods involved in the development of a mathematical model for describing the EMC-ERH relationship: the theoretical method and the empirical approach. In early dates when isotherm models were deficient, a lot of efforts were made by many researchers to derive an isotherm equation based on the principle of equilibrium thermodynamics. The five ASAE standardized isotherm equations were some of the many theoretical isotherm models that resulted from the efforts. As more and more theoretical isotherm models were available for selection, empirical approach prevailed in which search of the best-fit model from the existing isotherm models by means of statistical regression became the prime process. In this study, empirical approach was also used to develop mathematical model(s) for expressing the EMC-ERH relationship of alfalfa grind. The statistical regression was also done in the commercial computer software for curve-fitting, "TableCurve 2D".

6.2.2 Development of a new hysteresis model

Prior to the derivation of the model for hysteresis quantification, some facts, hypotheses, and assumptions about a sorption material and a sorption process are presented. The facts are: 1) a sorption process involves not only mass transfer, but also heat transfer (exothermic for adsorption and endothermic for desorption in most cases); and 2) phase change mass transfer is coupled with heat transfer during a sorption process, and the resultant heat transfer can alter the local temperature of the material significantly (Pierce and Benner, 1986; Tao et al., 1992a; Tao et al., 1992b; Simonson et al., 1993). The hypotheses are: 1) owing to the thermal nature of a sorption process, there existed internal instantaneous generation (in adsorption) or evacuation (in desorption) of heat that caused change in the temperature of sorption sites (i.e., local temperature); 2) temperature gradient between a sorption site and the environment was built up due to altered local temperatures; 3) the temperature gradient in turn gave rise to sorbate mass redistribution

within sorption sites and in the regions between a sorption site and the outer surface of the material; 4) sorbate redistribution within the sorption sites involved giving up some of the sorbate molecules that were absorbed into the material during adsorption or gaining back some of the sorbate molecules that evaporated from the materials during desorption, while sorbate redistribution in the rest of the material included inducing the evaporation of existing sorbate in this region to the environment (in adsorption) or condensing gaseous sorbate molecules in the environment to the material (in desorption); and 5) after the adjustment of sorbate mass, local temperatures of the material restored to that of the environment. The assumptions are: 1) evaporation and condensation were the major means of sorbate mass transfer, and other ways of mass transfer are not considered for the time being; 2) conduction was the predominant mode of heat transfer inside the material; 3) during an adsorption process, the sorbate molecules that were absorbed into the material could be regarded as a continuously distributed spherical energy source with a radius r_o that instantaneously released a pulse of energy $g_o(r_o,t_o)$ at time t_o; 4) the material could be taken as an infinite body in relation to the dimension of the spherical surface source; 5) the transient heat conduction in the material could be regarded as radial flow in a spherical system, in other words, temperature was only a function of time and the radius, and independent of polar angles in spherical coordinates; and 6) in desorption, the assumptions were similar to those considered in adsorption, except that the instantaneous source had an energy equal to $-g_o(r_o,t_o)$.

The instantaneously generated or evacuated heat would conduct through the material as governed by Equation 6.6 in a spherical coordinate system (Carslaw and Jaeger, 1959):

$$\frac{1}{r}\frac{\partial^2 (rT)}{\partial r^2} + \frac{g(r,t)}{k} = \frac{1}{\alpha}\frac{\partial T}{\partial t} \qquad (6.6)$$

where k is thermal conductivity of the material in $W.m^{-1}.K^{-1}$, α its thermal diffusivity that equals $k/(\rho c)$ where ρ is the density of the material in kg/m^3 and c its specific heat in $kJ.kg^{-1}.K^{-1}$, and $g(r,t) = \delta(t-t_o)\delta(r-r_o)g(r_o,t_o)/(4\pi r_o^2)$ where δ is the Dirac delta function.

The initial condition is $T(r,0)=T_O$. The temperature on the surface of the material ($r \rightarrow \infty$) is assumed to be T_O.

The solution to Equation 6.6 in terms of Green's Functions is (Beck et al., 1992):

$$T(r,t) = T_i(r,t) + T_g(r,t) + T_{b,c}(r,t) \tag{6.7}$$

where $T_i(r,t)$ accounts for the contribution of initial condition to $T(r,t)$. It is written as:

$$T_i(r,t) = \int_o^{\infty} 4\pi GF(r,t|r_o,t_o)T(r_o,0)r'^2\,dr' \tag{6.8}$$

where r' is a dummy variable.

$T_g(r,t)$ is associated with internal generation and can be expressed as:

$$T_g(r,t) = \int_{\tau=o}^{t}\int_{r'=o}^{\infty} \frac{4\pi\alpha}{k} GF(r,t|r_o,t_o)g(r_o,t_o)r'^2\,dr'\,d\tau \tag{6.9}$$

where τ is a dummy variable.

$T_{b,c}(r,t)$ is the contribution of boundary conditions, which is found to be zero in this case.

The Green's function for radial flow of heat in an infinite body in spherical coordinates can be written as (Beck et al., 1992):

$$GF(r,t|r_o,t_o) = \frac{1}{8\pi\, r\, r_o \sqrt{\pi\alpha(t-t_o)}}\left\{\exp\left[-\frac{(r-r_o)^2}{4\alpha(t-t_o)}\right] - \exp\left[-\frac{(r+r_o)^2}{4\alpha(t-t_o)}\right]\right\} \tag{6.10}$$

Integration of Equation 6.8 and Equation 6.9 incorporating Equation 6.10 yields

$$T_i(r,t) = T_O$$

and

$$T_g(r,t)=\frac{g_o(r_o,t_o)}{\rho c}\frac{1}{8\pi r r_o\sqrt{\pi\alpha(t-t_o)}}\left\{\exp\left[-\frac{(r-r_o)^2}{4\alpha(t-t_o)}\right]-\exp\left[-\frac{(r+r_o)^2}{4\alpha(t-t_o)}\right]\right\} \quad (6.11)$$

Thus,

$$T(r,t)=T_o+\frac{g_o(r_o,t_o)}{\rho c}\frac{1}{8\pi r r_o\sqrt{\pi\alpha(t-t_o)}}\left\{\exp\left[-\frac{(r-r_o)^2}{4\alpha(t-t_o)}\right]-\exp\left[-\frac{(r+r_o)^2}{4\alpha(t-t_o)}\right]\right\} \quad (6.12)$$

As hypothesized earlier, sorbate mass redistribution would take place within a sorption site (or rather, spherical source) and the rest of the material. Separate approaches were taken to deal with the sorbate mass transfer in these two regions.

Sorbate redistribution within the spherical source

The mean temperature change, T_{ave}, of the spherical source due to instantaneous heat generation or evacuation can be calculated as:

$$T_{ave}=\frac{\int_o^{r_o} r\,T(r,t)dr}{\int_o^{r_o} r dr} \quad (6.13)$$

Integrating Equation 6.13 incorporating Equation 6.12 yields

$$T_{ave}=T_o+\frac{g_o(r_o,t_o)}{4\pi r_o^{\,3}\rho_w c_w}\left\{2\,\mathrm{erf}\left[\frac{r_o}{\sqrt{4\alpha_w(t-t_o)}}\right]-\mathrm{erf}\left[\frac{2r_o}{\sqrt{4\alpha_w(t-t_o)}}\right]\right\} \quad (6.14)$$

where ρ_w is the density of sorbate in liquid state, c_w its specific heat, and α_w its thermal diffusivity.

To offset the effect of local temperature alteration, a quantity of sorbate, h_i, that carried away from the spherical source an amount of energy equal to $m_o c_w(T_{ave}-T_o)$, where m_o is the mass of the spherical source, would be responsively desorbed (in adsorption) or resorbed (in desorption) by means of evaporation or condensation, as assumed earlier. Accordingly, the following relationship holds:

$$h_i L_{T_{ave}} = m_o c_w (T_{ave} - T_o) \tag{6.15}$$

where h_i is the amount of redistributed sorbate within the spherical source in either adsorption or desorption, and L_{Tave} the latent heat of vaporization or condensation at T_{ave}. Rearranging Equation 6.15 after inclusion of Equation 6.14 comes to

$$h_i = \frac{m_o g_o(r_o, t_o)}{4\pi r_o^3 \rho_w L_{T_{ave}}} \left\{ 2\,\mathrm{erf}\left[\frac{r_o}{\sqrt{4\alpha_w (t - t_o)}} \right] - \mathrm{erf}\left[\frac{2r_o}{\sqrt{4\alpha_w (t - t_o)}} \right] \right\} \tag{6.16}$$

Equation 6.16 is a general form accountable for the hysteresis either in adsorption or desorption. The overall hysteresis within the spherical source, H_i, is the sum of h_i in both adsorption and desorption, as expressed in Equation 6.17.

$$H_i = \left[\frac{m_o g_{o,a}(r_o, t_o)}{L_{a,T_{ave}}} + \frac{m_o \left| g_{o,d}(r_o, t_o) \right|}{L_{d,T_{ave}}} \right] \frac{1}{4\pi \rho_w r_o^3} * \left\{ 2\,\mathrm{erf}\left[\frac{r_o}{\sqrt{4\alpha_w (t - t_o)}} \right] - \mathrm{erf}\left[\frac{2r_o}{\sqrt{4\alpha_w (t - t_o)}} \right] \right\} \tag{6.17}$$

where $g_{o,a}(r_o,t_o)$ and $g_{o,d}(r_o,t_o)$ are the amount of heat generated (in adsorption) and evacuated (in desorption), respectively, and $L_{a,Tave}$ and $L_{d,Tave}$ are used to differentiate the latent heat of condensation (in adsorption) and the latent heat of vaporization (in desorption) of sorbate, respectively.

Recall that the instantaneous heat evacuation during a desorption process was assumed to be equal to the heat generation in adsorption in value but negative in sign, i.e., $|g_{o,d}(r_o,t_o)|=g_{o,a}(r_o,t_o)=g_o(r_o,t_o)$. Also, $L_{a,Tave}$ and $L_{d,Tave}$ are the same in most cases, namely, $L_{a,Tave}=L_{d,Tave}= L_{Tave}$. Equation 6.17 is simplified as:

$$H_i = \frac{2m_o\, g_o(r_o,t_o)}{L_{T_{ave}}} \frac{1}{4\pi \rho_w r_o^3} \left\{ 2\,\mathrm{erf}\left[\frac{r_o}{\sqrt{4\alpha_w (t-t_o)}} \right] - \mathrm{erf}\left[\frac{2r_o}{\sqrt{4\alpha_w (t-t_o)}} \right] \right\} \quad (6.18)$$

Sorbate redistribution outside the spherical source

In the region outside the spherical source, a spherical shell of infinitely small thickness dr is taken at a radius r. The volume of this thin shell is $4\pi r^2 dr$. Assuming that the specific heat and the density of the material contained in it are c_S and ρ_S, respectively, the mass of the material in the thin shell is $4\pi\rho_S r^2 dr$. Similar to the treatment inside spherical source, a quantity of sorbate, dh_r, would be responsively evaporated (in adsorption) or condensed (in desorption) due to the variation in temperature at the radius r, i.e., $T(r,t|r_o,t_o) - T_o$. The following relationship exists:

$$dh_r L_T = 4\pi\rho_S c_S [T(r,t|r_o,t_o)-T_o] r^2 dr$$

or,

$$dh_r\, L_T = \frac{4\pi\rho_s\, c_s\, g_o(r_o,t_o)}{8\pi\, r\, r_o\, \rho_s\, c_s \sqrt{\pi\alpha_s (t-t_o)}} \left\{ \exp\left[-\frac{(r-r_o)^2}{4\alpha_s (t-t_o)} \right] - \exp\left[-\frac{(r+r_o)^2}{4\alpha_s (t-t_o)} \right] \right\} r^2 dr \quad (6.19)$$

where L_T is the latent heat of either vaporization or condensation of sorbate at the temperature T corresponding to the radius r and α_s the thermal diffusivity of the material. Integration of Equation 6.19 with h_r varying from 0 to $h\theta$ (the amount of redistributed mass that is equal to the hysteresis amount in this region either in adsorption or desorption) and r from r_o to ∞ gives

$$h_\theta = \int_{r_o}^{\infty} \frac{g_o(r_o,t_o)}{2r_o L_T \sqrt{\pi\alpha_s(t-t_o)}} \left\{ \exp\left[-\frac{(r-r_o)^2}{4\alpha_s(t-t_o)} \right] - \exp\left[-\frac{(r+r_o)^2}{4\alpha_s(t-t_o)} \right] \right\} rdr \qquad (6.20)$$

Using the intermediate-value theorem of integration, Equation 6.20 becomes

$$h_\theta = \frac{g_o(r_o,t_o)}{2r_o L_\Gamma \sqrt{\pi\alpha_s(t-t_o)}} \int_{r_o}^{\infty} \left\{ \exp\left[-\frac{(r-r_o)^2}{4\alpha_s(t-t_o)} \right] - \exp\left[-\frac{(r+r_o)^2}{4\alpha_s(t-t_o)} \right] \right\} rdr \qquad (6.21)$$

where L_Γ is the latent heat of vaporization or condensation of sorbate at an intermediate temperature Γ, corresponding to the radius r_Γ ($r_o < r_\Gamma < \infty$). Further integration of Equation 6.21 yields

$$h_\theta = \frac{g_o(r_o,t_o)\sqrt{\alpha_s(t-t_o)}}{2\sqrt{\pi}\, r_o L_\Gamma} \left\{ 1 - \exp\left[-\frac{r_o^2}{\alpha_s(t-t_o)} \right] + \frac{2r_o\, \mathrm{erfc}(r_o)}{\sqrt{\alpha_s(t-t_o)}} \right\} \qquad (6.22)$$

where $\mathrm{erfc}(r_o)$ is the complementary error function. Similarly, $h\theta$ accounts for the hysteresis in the region outside the spherical source in either adsorption or desorption. The total hysteresis in this region, H_θ, is

$$H_\theta = \frac{2g_o(r_o,t_o)}{L_\Gamma} \frac{\sqrt{\alpha_s(t-t_o)}}{2\sqrt{\pi}\, r_o} \left\{ 1 - \exp\left[-\frac{r_o^2}{\alpha_s(t-t_o)} \right] + \frac{2r_o\, \mathrm{erfc}(r_o)}{\sqrt{\alpha_s(t-t_o)}} \right\} \qquad (6.23)$$

The total hysteresis in the entire material, H, can be calculated by addition of H_i and H_θ, i.e.,

$$H = \frac{m_o g_o(r_o,t_o)}{L_{T_{wc}}} \frac{1}{2\pi \rho_w r_o^3} \left\{ 2\,\mathrm{erf}\left[\frac{r_o}{\sqrt{4\alpha_w (t-t_o)}} \right] - \mathrm{erf}\left[\frac{2r_o}{\sqrt{4\alpha_w (t-t_o)}} \right] \right\} +$$

$$\frac{g_o(r_o,t_o)}{L_T} \frac{\sqrt{\alpha_s (t-t_o)}}{\sqrt{\pi}\, r_o} \left\{ 1 - \exp\left[-\frac{r_o^2}{\alpha_s (t-t_o)} \right] + \frac{2r_o\, \mathrm{erfc}(r_o)}{\sqrt{\alpha_s (t-t_o)}} \right\} \qquad (6.24)$$

During an isothermal sorption process, a material equilibrates with a sorbate at a constant environmental temperature for a time long enough for equilibrium between the material and the sorbate to be reached. This can be approximately regarded as the situation when $(t-t_0) \rightarrow \infty$. This situation deserves special attention due to the fact that all the published isotherms were obtained by equilibrating a sorbent with a sorbate in a temperature controlling environment for a sufficiently long time. In the case of $(t-t_0) \rightarrow \infty$, Equation 6.24 becomes

$$H = \frac{2g_o(r_o, t_o)}{\sqrt{\pi}\, L_T} \mathrm{erfc}(r_o) \qquad (6.25)$$

In adsorption, sorbate molecules in gaseous phase are liquefied onto and spread over the surface of the material before they further diffuse inwards. In desorption, sorbate molecules in liquid state evaporate and recede from the surface of the material. For the convenience of mathematical treatment, a sorption process is perceived as the case of liquid spreading over or contracting from a solid surface, and a relationship between r_O

and the relative pressure of sorbate that is similar to the Kelvin's equation is assumably applied. Hence, we have

$$RT\ln\left(\frac{p}{p_o}\right) = -\frac{2\sigma V\cos\theta}{r_o} \tag{6.26}$$

or

$$r_o = -\frac{2\sigma V\cos\theta}{RT\ln(p/p_o)} \tag{6.27}$$

where p/p_O is the relative pressure of sorbate at temperature T, σ the surface tension, V the molar volume of the sorbate, θ the angle of contact, and R the universal gas constant.

Since g_O is the heat generation or evacuation during adsorption or desorption, its magnitude is equal to $m_O*\Delta E$ by energy balance, where ΔE is the net enthalpy change in adsorption or desorption. Replacing $g_O(r_O,t_O)$ with $m_O*\Delta E$ and substituting r_O in Equation 6.25 with Equation 6.27, we have

$$H = \frac{2m_o\,\Delta E}{\sqrt{\pi}\,L_\Gamma}\,\mathrm{erfc}\left[-\frac{2\sigma V\cos\theta}{RT\ln(p/p_o)}\right] \tag{6.28}$$

or,

$$H = A'm_o\,\mathrm{erfc}\left[-B\ln^{-1}\left(\frac{p}{p_o}\right)\right] \tag{6.29}$$

where A' and B equal to $\frac{2\Delta E}{\sqrt{\pi}\,L_\Gamma}$ and $\frac{2\sigma V\cos\theta}{RT}$, respectively.

As defined earlier, r_O is the radius of a spherical source. The spherical source can theoretically be considered as a collection of sorbate all over a material, although the sorbate might become sorbed in the material at different locations. Therefore, r_O should accordingly be regarded as an equivalent radius of the collection of sorbate contained in the material. When there was no sorption, r_O=0. At low relative pressures, r_O was small

due to limited sorption. As sorption increased with relative pressure, r_o also increased until at extremely high relative pressure when it approached the dimension of the material (infinite body), i.e., $r_o \rightarrow \infty$. Therefore, r_o actually related to different regions of an isotherm and could be expressed with respect to relative pressure by a certain function such as Equation 6.27.

Since m_o is the mass of the spherical source, it would eventually contribute to equilibrium mass of a sorbate in a material as a sorption process proceeds. As mentioned earlier, r_o could be related to relative pressure of sorbate in different regions of an isotherm, so m_o could also be expressed in relation to relative pressure. Relationships similar to the ASAE standardized isotherm models could be used in this regard.

6.3 Material and methods

6.3.1 Material and preparation

The same dehydrated alfalfa grind as described before was used in this experiment. The dehydrated alfalfa grind had an initial moisture content of 0.070 (w/w, db). Pre-treatments including tempering the alfalfa grind to a moisture content higher than the initial moisture content or drying it to a moisture content lower than the initial moisture content followed the same procedures as described before. The materials used in the experiments, number of observations, and other related information are summarized as follows:

Test Item	Material	Observation*		Comments**
		Isotherm	Hysteresis	
• 9°C	Dehydrated	12	6	Ads. and des.
• 25°C	Dehydrated	16	8	Ads. and des.
• 50°C	Dehydrated	12	16	Ads. and des.

* Triplicate samples were tested at each observation.
**Ads – adsorption; des – desorption.

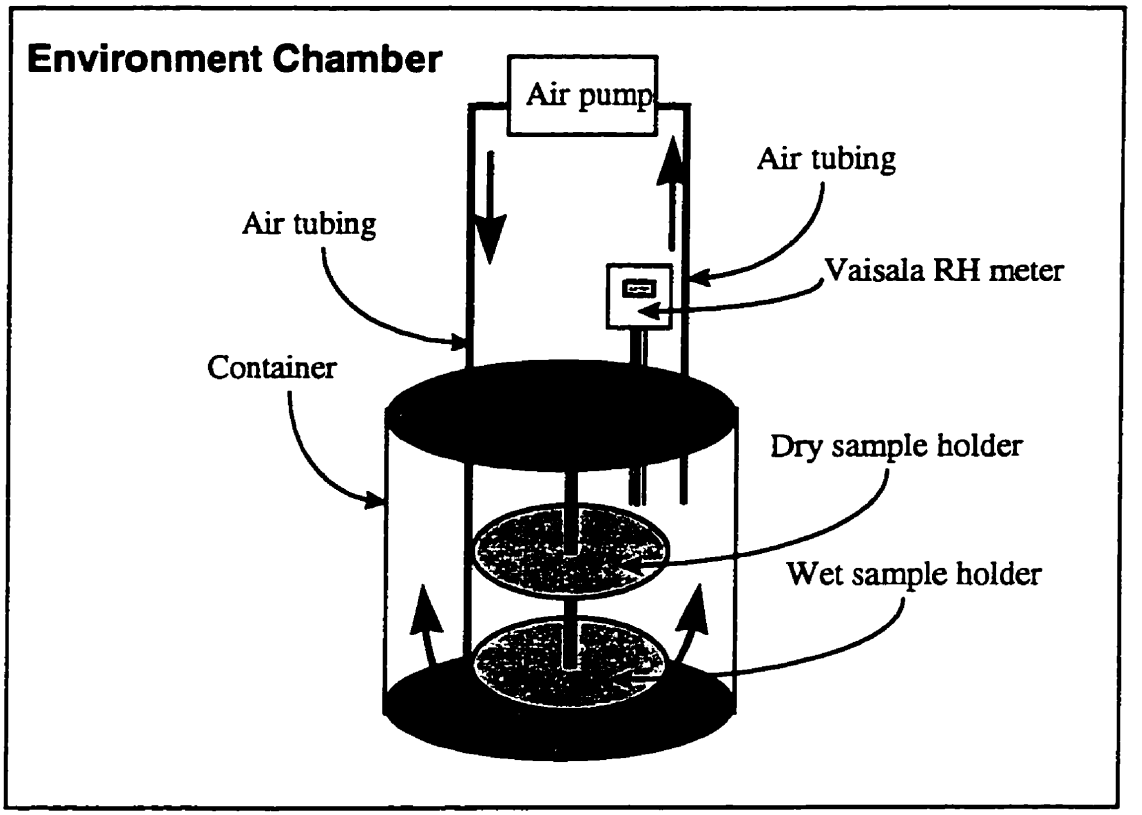

Figure 6.1: A schematic of the experimental set-up for measuring moisture sorption isotherms.

6.3.2 Measurement of moisture sorption isotherm and hysteresis loop

Moisture sorption isotherms of alfalfa grind were measured by a dynamic method. This method involved bringing a dry and a wet layer of alfalfa grind together in an air-tight and air-circulated container for equilibrium to reach between both layers and the headspace. The container was placed in an environment-controlled chamber that was capable of adjusting to various temperatures for equilibration. The experimental unit used in the isotherm measurement is shown in Figure 6.1. It consisted of a cylindrical container of 190 mm in diameter and 205 mm in height, two sample holders made from No. 100 screen, an air pump and tubing for circulating air in a closed loop, and a relative humidity sensor. The container was made of plexi glass of about 5 mm thick. Measurements were conducted at three temperatures: 9°C, 25°C and 50°C. The wet and dry layer of alfalfa

grind was loaded at various wet-to-dry combination ratios to aim at different final equilibrium relative humidity (Yang and Cenkowski, 1993). The equilibration period lasted from about 48 hours to about 170 hours depending on the temperatures and wet-to-dry ratios. Relative humidity in the headspace was checked every hour using the Vaisala HM 34 relative humidity and temperature meter (Vaisala, Finland) after equilibration at a specific temperature for 24 hours. The criteria for judging whether the sample reached equilibrium was that the relative humidity readings changed not more than 0.1% for three consecutive hours. At the end, the relative humidity of the headspace was recorded. The equilibrated dry and wet samples were unloaded respectively and subjected to moisture measurement in triplicates following the ASAE oven method (ASAE, 1996b).

6.4 Results and discussion

6.4.1 Experimental data of the isotherms and hysteresis of alfalfa grind

Figure 6.2 shows the measured isotherms of alfalfa grind at the temperatures of 9°C, 25°C and 50°C. The isotherms of alfalfa grind exhibited a sigmoid-shape that is typical of most biological materials (e.g., sugar isotherm is not). At 9°C, the moisture sorption isotherms of alfalfa grind were measured in the relative humidity ranging from 0.123 to 0.925, and the corresponding equilibrium moisture content ranged from 0.035 (w/w, db) to 0.39 (w/w, db) for adsorption path and from 0.063 (w/w, db) to 0.44 (w/w, db) for desorption path. At 25°C, the moisture sorption isotherms were measured in the relative humidity ranging from 0.154 to 0.909, and the corresponding equilibrium moisture content ranged from 0.039 (w/w, db) to 0.32 (w/w, db) for adsorption path and from 0.052 (w/w, db) to 0.35 (w/w, db) for desorption path. At 50°C, the moisture sorption isotherms of alfalfa grind were measured in the relative humidity ranging from 0.163 to 0.998, and the corresponding equilibrium moisture content ranged from 0.031 (w/w, db) to 0.33 (w/w, db) for adsorption path and from 0.044 db to 0.33 (w/w, db) for desorption path. As shown in Figure 6.2, the isotherms decreased as temperature increased.

By subtracting the equilibrium moisture content on the adsorption path from that on the desorption path at the same relative humidity at the temperature of 9°C, 25°C and 50°C, the magnitude of the hysteresis was obtained and plotted in Figure 6.3, Figure 6.4

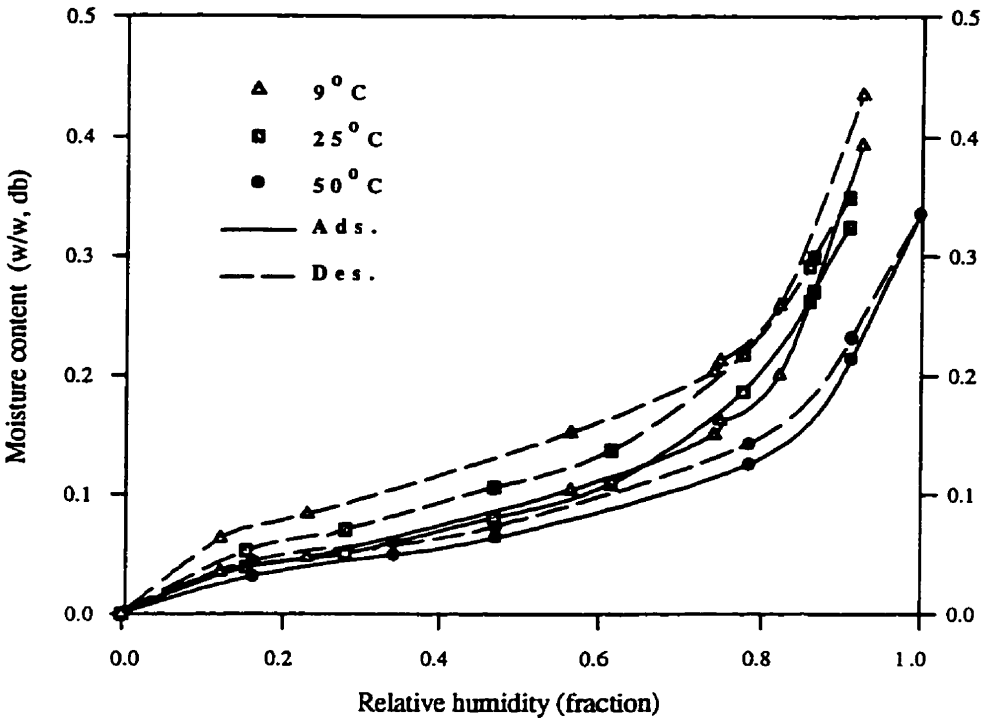

Figure 6.2: Moisture sorption isotherms of alfalfa grind at three temperatures.

and Figure 6.5, respectively. The magnitude of the hysteresis of alfalfa grind ranged from 0.028 (w/w, db) to 0.058 (w/w, db) at 9°C, from 0.014 (w/w, db) to 0.031 (w/w, db) at 25°C, and from 0 to 0.018 (w/w, db) at 50°C in the relative humidity ranges described earlier, exhibiting an ever-narrowing hysteresis span as temperature increased. For instance, the maximum hysteresis value at 9°C was about 0.058 (w/w, db) at about 0.8 relative humidity. It dropped to about 0.018 (w/w, db) at 50°C. It was noticed that the hysteresis peaked in the 0.7 - 0.9 relative humidity range, indicating the third type of peak orientation, i.e., towards the capillary condensation region.

6.4.2 The mathematical models for describing the isotherms of alfalfa grind

The capability of the five ASAE recommended isotherm equations for describing the isotherm of alfalfa grind has been examined in this study by non-linear regression of these equations to both the adsorption and desorption isotherms of alfalfa grind. Similarly, the curve-fitting was done in "TableCurve 2D". During curve-fitting, moisture

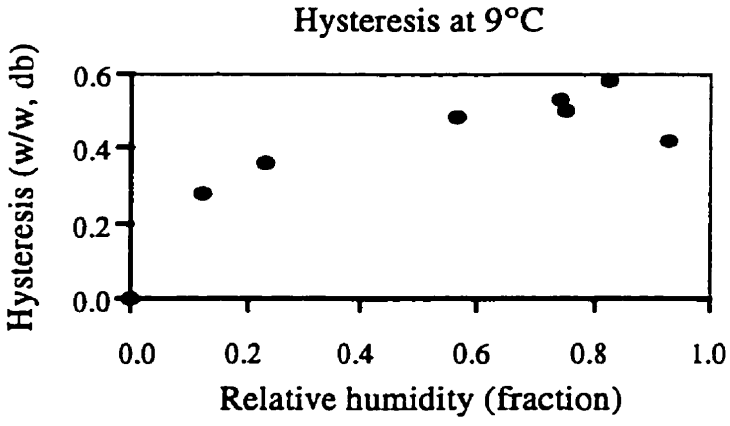

Figure 6.3: Moisture sorption hysteresis of alfalfa grind at 9°C.

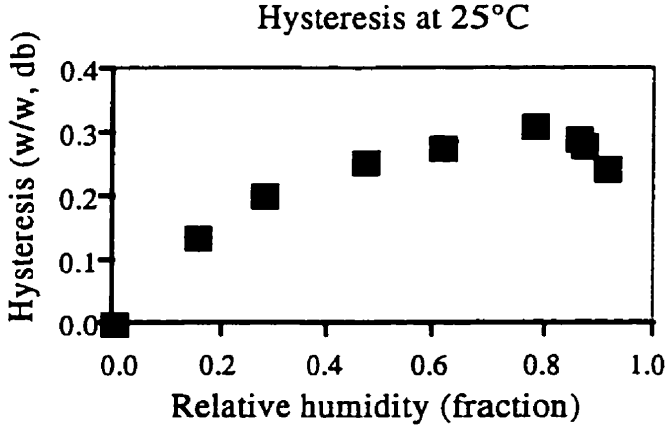

Figure 6.4: Moisture sorption hysteresis of alfalfa grind at 25°C.

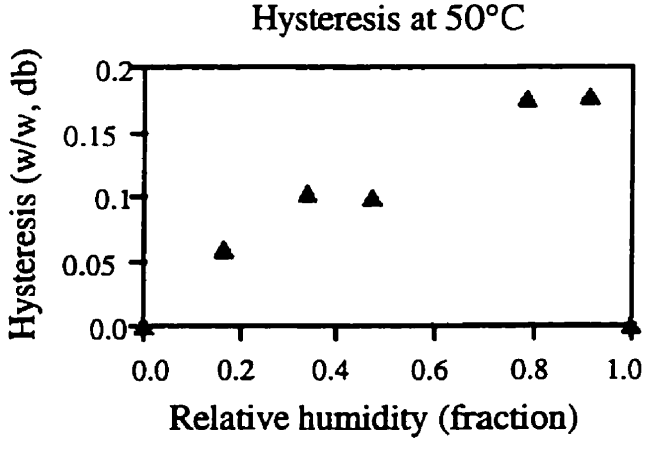

Figure 6.5: Moisture sorption hysteresis of alfalfa grind at 50°C.

content was in fraction dry basis, relatively humidity was in fraction, and temperature was in °C. Table 6.1 summarizes the curve-fitting results which include the model constants (A, B, and C) and the statistical criteria for judging the goodness-of-fit. The statistical criteria were the same as used in Chapter 5, that is, mean relative percentage deviation (P%), coefficient of determination (R^2), curve-fitting standard error (Fit S.E.), and F statistical value (F_{stat}).

It was noted that although their goodness-of-fit varied from one another as denoted by the values of P(%), R^2, Fit S.E. and F_{stat} in Table 6.1, these five ASAE isotherm models were all capable of describing the EMC-ERH relationship of alfalfa grind.

Table 6.1: Regression results and statistical criteria for the five ASAE standardized isotherm equations as applied to the isotherms of alfalfa grind on both adsorption and desorption paths.

Regression Parameters	Modified Henderson	Modified Chung-Pfost	Modified Halsey	Modifed Oswin	GAB	Modified Henderson	Modified Chung-Pfost	Modified Halsey	Modifed Oswin	GAB
	9°C - Adsorption path					9°C - Desorption path				
A	0.3948	7.1689	-13.8718	-4.4468	0.04586	0.4400	19.5032	-2.5702	-4.2818	0.06674
B	1.3229	15.2816	1.1413	0.5040	0.9556	1.7485	13.0814	-0.1557	0.4909	0.9147
C	30.3127	-6.7286	1.2950	1.882	15.1827	38.337	-4.6313	1.7594	2.5206	103.1199
P(%)	5.9	6.6	3.5	2.0	3.4	8.2	6.0	2.2	3.2	2.7
R^2	0.992	0.987	0.998	0.999	0.998	0.987	0.990	0.999	0.998	0.998
Fit S.E.	0.037	0.048	0.021	0.012	0.0065	0.047	0.041	0.009	0.018	0.0064
F_{stat}	310	189	1010	3147	1296	197	251	4926	1350	1570
	25°C - Adsorption path					25°C - Desorption path				
A	0.1550	-643.99	-1.9551	-0.2005	0.0592	0.162	67.9631	26.1913	-0.7827	0.07034
B	1.1068	13.0723	-0.06586	0.00578	0.9099	1.2799	11.6998	-1.1952	0.03591	0.8898
C	35.5892	-276.9196	1.2999	1.7599	5.4245	38.3710	-2.1698	1.4997	2.0421	10.6888
P(%)	8.57	10.3	1.6	4.2	4.1	8.3	8.0	3.4	2.8	2.2
R^2	0.987	0.967	0.999	0.997	0.998	0.988	0.979	0.998	0.998	0.998
Fit S.E.	0.044	0.071	0.013	0.02	0.0062	0.043	0.056	0.017	0.017	0.0063
F_{stat}	230	88	2606	1082	1405	246	142	1548	1650	1592
	50°C - Adsorption path					50°C - Desorption path				
A	0.1771	118.1024	-1.3167	-25.0003	0.04321	0.1909	123.3328	-2.9941	-25.0204	0.05059
B	1.3625	21.6269	-0.06582	0.5014	0.8752	1.5099	19.9511	-0.04046	0.5020	0.8534
C	92.0339	-13.8594	1.5416	2.1272	9.1066	99.6044	16.8392	1.8060	2.4091	14.3900
P(%)	4.9	5.2	5.9	0.8	1.6	8.2	8.0	1.9	4.8	3.1
R^2	0.997	0.992	0.994	0.999	0.999	0.991	0.990	0.997	0.997	0.999
Fit S.E.	0.031	0.042	0.036	0.016	0.0042	0.045	0.048	0.024	0.027	0.0053
F_{stat}	457	248	329	1751	2464	213	193	746	599	1492

The Modified Oswin, the GAB and the Modified Halsey models (P% mostly within 5, R^2 over 0.99, Fit S.E. from 0.0042 to 0.036, and F_{stat} mostly over 1000) was found to generally fit the isotherms of alfalfa grind better than the Modified Henderson and the Modified Chung-Pfost models (P% mostly above 5, R^2 0.99 or below, Fit S.E. basically over 0.036, and F_{stat} under 1000). The performance of the Modified Oswin, the GAB and the Modified Halsey equations was similar to one another, so any one of the three models could therefore be used to represent the isotherms of alfalfa grind to use in the drying or conditioning modeling of alfalfa grind.

The GAB equation is taken as an example to show the goodness-of-fit of the models towards the isotherms of alfalfa grind. Figure 6.6 depicts the measured and the GAB model estimated isotherms at the temperature of 9°C, 25°C and 50°C. As can be seen, the GAB model predicted very well both the magnitude and shape of the isotherms of the alfalfa grind in both the adsorption and the desorption paths.

In the first four of the five ASAE standardized isotherm equations listed earlier, temperature has been incorporated as a variable. There is no temperature term in the GAB equation. Sokhansanj and Yang (1995b) addressed the need to study the temperature dependency of the GAB equation due to its plausible performance on a wide range of agricultural and food products as reported by many researchers. Attempt has been made to examine the temperature dependency of the model constants obtained as GAB equation applied to the isotherm of alfalfa grind. It was found that for alfalfa grind constants A and B in the GAB equation changed little with temperature, and constant C varied considerably with temperature in the 9°C to 50°C range (Table 6.1). Figure 6.7 shows the variation of constant C with temperature at both adsorption and desorption paths. Note that the solid lines that connect data points in Figure 6.7 do not necessarily indicate the trend of the constant C vs. temperature relationship. The results suggested that constant C was where a temperature term could be incorporated into the GAB equation to enhance its versatility in predicting temperature effect on isotherms. Mathematical relationship was developed to correlate constant C to temperature as shown in Equation 6.30 and Equation 6.31.

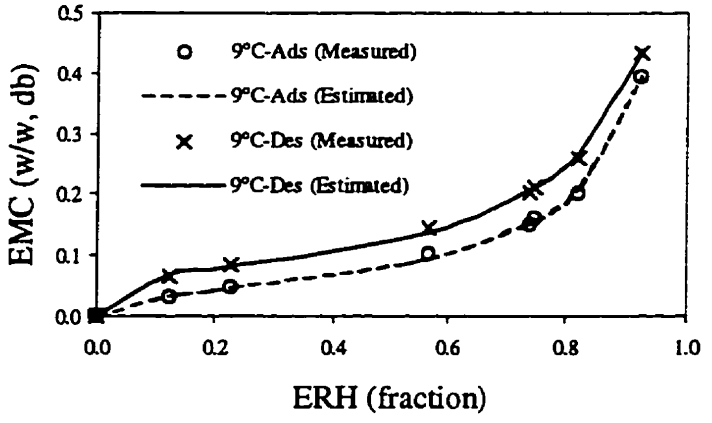

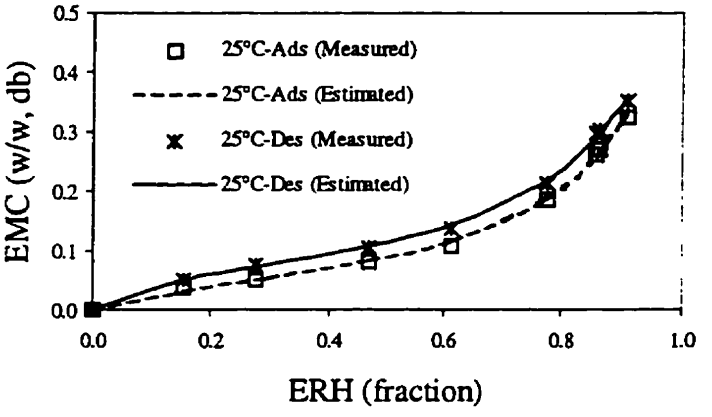

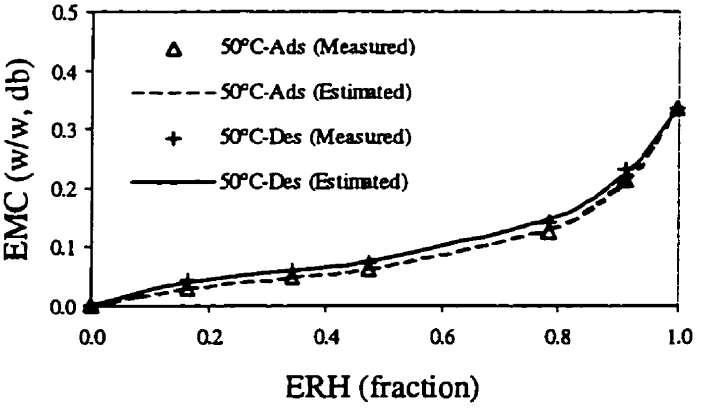

Figure 6.6: Comparison between the measured and the GAB model estimated isotherms of alfalfa grind at the temperature of (A) 9°C, (B) 25°C and (C) 50°C.

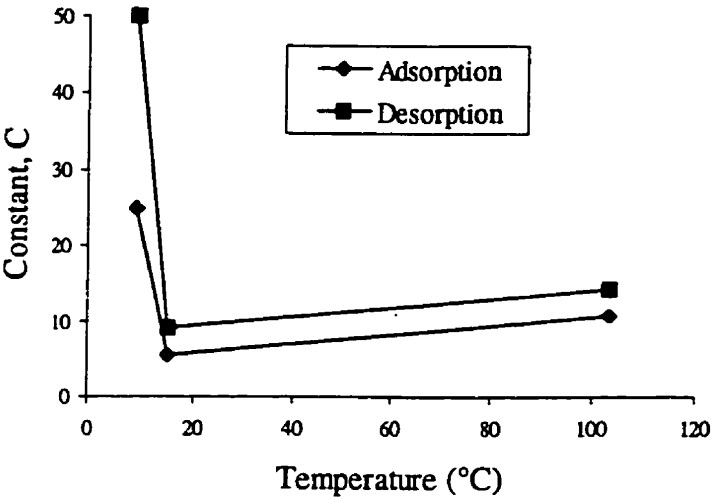

Figure 6.7: Dependency of constant C in the GAB equation on temperature.

Adsorption path: $C = 7.2655 + 6.4153 \times 10^{4} \exp(-T)$ (R^2=0.87, n=3) (6.30)

Desorption path: $C = 12.5394 + 7.3398 \times 10^{5} \exp(-T)$ (R^2=0.99, n=3) (6.31)

However, it should be pointed out that Equations 6.30 and 6.31 were preliminary and approximate due to only three data points available in this study. The relationship needs further verification.

6.4.3 Verification of the applicability of the hysteresis model to alfalfa grind

Equation 6.29 was a general model to account for the sorption hysteresis of most substances. Its capability has been verified using a wider range of materials of organic and inorganic nature (Yang et al., 1995a; Yang et al., 1996b). The hysteresis data of alfalfa grind at three temperatures obtained in this study were also used to test the capability of the theoretical hysteresis model developed in this study. It was done through inverse method, as mentioned before, by means of the TableCurve 2D.

After plugging the five ASAE isotherm equations into Equation 6.29, five hysteresis models resulted as listed in Table 6.2. Before combining into Equation 6.29, the first four of the five equations were transformed to the format with moisture content

being the dependent variable. For convenience, temperature dependency was not considered in the hysteresis models for the time being, and the temperature terms in the first four ASAE isotherm equations were therefore treated as constants. The statistical criteria, i.e., the mean relative percent deviation (P%), the coefficient of determination (R^2), the curve-fitting standard error (Fit S.E.) and the F statistical values (F_{stat}) were used to evaluate the performance of the five hysteresis models towards. The best fit model should possess the highest R^2, largest F_{stat}, and least Fit S.E. among the models tested.

Table 6.3 gives the regression information (R^2, Fit S.E., P%, model constants, and equilibration temperature) of the five hysteresis models. As can be seen from the statistics listed in Table 6.4, most hysteresis models (#1, #3, #4 and #5) fitted very well the hysteresis data of alfalfa at the three temperatures except for #2 model that originated

Table 6.2: Hysteresis models based on Equation 6.29 and the five ASAE standardized isotherm equations

1. $H = A\left[-\frac{\ln(1-a_w)}{C}\right]^{\frac{1}{D}} \text{erfc}\left[-\frac{B}{\ln(a_w)}\right]$ (Combined with the Henderson equation)

2. $H = \left\{A - C\ln\left[-\ln(a_w)\right]\right\}\text{erfc}\left[-\frac{B}{\ln(a_w)}\right]$ (Combined with the Chung – Pfost equation)

3. $H = A\left[-\frac{C}{\ln(a_w)}\right]^{\frac{1}{D}} \text{erfc}\left[-\frac{B}{\ln(a_w)}\right]$ (Combined with the Halsey equation)

4. $H = A\left(\frac{1-a_w}{a_w}\right)^{-\frac{1}{C}} \text{erfc}\left[-\frac{B}{\ln(a_w)}\right]$ (Combined with the Oswin equation)

5. $H = \frac{A\,C\,D\,a_w}{(1-C\,a_w)(1-C\,a_w+C\,D\,a_w)}\text{erfc}\left[-\frac{B}{\ln(a_w)}\right]$ (Combined with the GAB equation)

Where H is the magnitude of hysteresis, a_w is water activity and A, B, C and D are constants.

from plugging the Chung-Pfost isotherm equation into Equation 6.29. The #2 hysteresis model predicted well both the magnitude and shape of the hysteresis loops in higher relative humidity range, but overestimated those at lower relative humidity (Figure 6.8B, 6.9B and 6.10B). It was noticed that R^2 values for the #1, #3, #4 and #5 hysteresis

Table 6.3: Model constants and regression statistics for the five hysteresis models listed in Table 6.2 as applied to the hysteresis data of alfalfa grind.

Hysteresis Model	Regression Parameter	Statistical Values		
		9°C	25°C	50°C
#1 (Associated with the Henderson equation)	A	0.05531	0.03039	0.01075
	B	0.03134	0.04433	0.02403
	C	1.0111	0.8651	0.5420
	D	3.1375	2.3610	1.7836
	R^2	0.991	0.997	0.988
	P (%)	2.5	2.3	4.6
	Fit S.E.	0.0026	0.00076	0.0011
	F_{stat}	181	701	85
#2 (Associated with the Chung-Pfost equation)	A	0.04347	0.023549	0.01068
	B	0.02819	0.02755	0.003528
	C	0.01142	0.006266	0.003033
	D	/	/	/
	R^2	0.973	0.956	0.931
	P (%)	5.9	7.8	13.0
	Fit S.E.	0.0042	0.0028	0.0024
	F_{stat}	106	76	26
#3 (Associated with the Halsey equation)	A	0.06180	0.03345	0.01195
	B	0.05239	0.06867	0.05427
	C	0.3639	0.4555	0.7076
	D	2.2924	2.0022	1.5762
	R^2	0.976	0.977	0.989
	P (%)	3.5	5.2	4.6
	Fit S.E.	0.0043	0.0022	0.0011
	F_{stat}	68	85	89
#4 (Associated with the Oswin equation)	A	0.04850	0.02756	0.01235
	B	0.04034	0.05576	0.04105
	C	3.9947	3.1366	2.3432
	D	/	/	/
	R^2	0.992	0.994	0.991
	P (%)	2.7	3.3	4.1
	Fit S.E.	0.0022	0.0011	0.00087
	F_{stat}	384	552	212
#5 (Associated with the GAB equation)	A	0.03585	0.02765	0.007664
	B	0.03255	0.03625	0.03563
	C	0.5829	0.43756	0.8242
	D	41.0350	13.0315	16.1055
	R^2	0.992	0.998	0.992
	P (%)	4.31	1.3	4.2
	Fit S.E.	0.0025	0.00054	0.00095
	F_{stat}	200	1409	117

models were 0.98 and up, P (%) values ranged from 1.3 to 5.2, and Fit S.E. values were quite small. This signifies that Equation 6.29, when incorporated with any one of the following ASAE isotherm models: the Modified Henderson, the Modified Halsey, the Modified Oswin and the GAB equations, reduced considerably the sum of squared residuals to result in a remarkable fit to the hysteresis data of alfalfa grind. Among these four hysteresis models, #4 model would be most recommended due to the fact that it has smaller number of constants in the model (refer to Table 6.2), and #3 model least recommended because of its tendency to overestimate the hysteresis magnitude in lower relative humidity range, which will be discussed later.

Although #1, #3, #4, and #5 hysteresis models all fitted well to the hysteresis data of alfalfa grind based on the resultant regression statistics, they seemed to differ slightly to one another in their behavior of predicting the magnitude and shape of the hysteresis loops. Figure 6.8, Figure 6.9 and Figure 6.10 depict the trend of the regression curves by the five hysteresis models in contrast to the magnitude and shape of the measured hysteresis loops at temperatures of 9°C, 25°C and 50°C, respectively. As can be seen, #5 model predicted most realistically the magnitude and shape of the hysteresis loop, and #1 and #3 models were next to #5 model in terms of performance. Both the #2 and #3 models had similar behavior of overshooting the hysteresis values in 0-0.25 relative humidity range.

It is evident from the results obtained that Equation 6.29 represented very well both the magnitude and shape of the hysteresis loop of alfalfa grind. The goodness-of-fit of the hysteresis model developed in this study to the hysteresis data of alfalfa grind further suggested that the model and its supporting hypotheses were capable of describing sorption hysteresis phenomenon. A good agreement between Equation 6.29 and the experimental data seemed to support the hypothesis proposed in this study to explain the fundamental causes for sorption hysteresis. However, further observations and experiments using Equation 6.29 are desired before a profound conclusion can be made on the capability of Equation 6.29 in expressing sorption hysteresis as a general model.

6.5 Summary

Moisture equilibrium characteristics of alfalfa grind, which included moisture sorption isotherms and hysteresis behavior, were studied. The moisture sorption isotherms of alfalfa grind were measured by a dynamic method. The isotherms of alfalfa grind exhibited a sigmoid shape. Measured simultaneously on both the adsorption and desorption paths, the EMC values of alfalfa grind ranged from 0.035 (w/w, db) to 0.44 (w/w, db) in the relative humidity ranging from 0.123 to 0.925 at 9°C, ranged from 0.039 (w/w, db) to 0.35 (w/w, db) in the relative humidity ranging from 0.154 to 0.909 at 25°C, and ranged from 0.031 (w/w, db) to 0.33 (w/w, db) in the relative humidity ranging from 0.163 to 0.998 at 50°C. The magnitude of the isotherm decreased as temperature increased.

Empirical method was used in this study to develop mathematical model for describing the EMC-ERH relationship of alfalfa grind. The five ASAE standardized isotherm equations were found to be all capable of describing the EMC-ERH relationship of alfalfa grind in a fairly wide range of relative humidity, but the Modified Oswin, the GAB and the Modified Halsey equations performed better than the Modified Henderson and the Modified Chung-Pfost equations.

The moisture sorption hysteresis of alfalfa grind exhibited the 3rd-type peak orientation in the capillary condensation region. The magnitude of the hysteresis of alfalfa grind ranged from 0.028 (w/w, db) to 0.058 (w/w, db) at 9°C, from 0.014 (w/w, db) to 0.031 (w/w, db) at 25°C, and from 0 to 0.018 (w/w, db) at 50°C in the relative humidity range of 0.123 to 0.998. The span of the hysteresis loops decreased as temperature increased.

A theory was proposed to account for the origin of sorption hysteresis. Based on the theory a mathematical model was developed to quantify the magnitude of hysteresis loops. The applicability of the developed model has been verified by the hysteresis data of alfalfa grind.

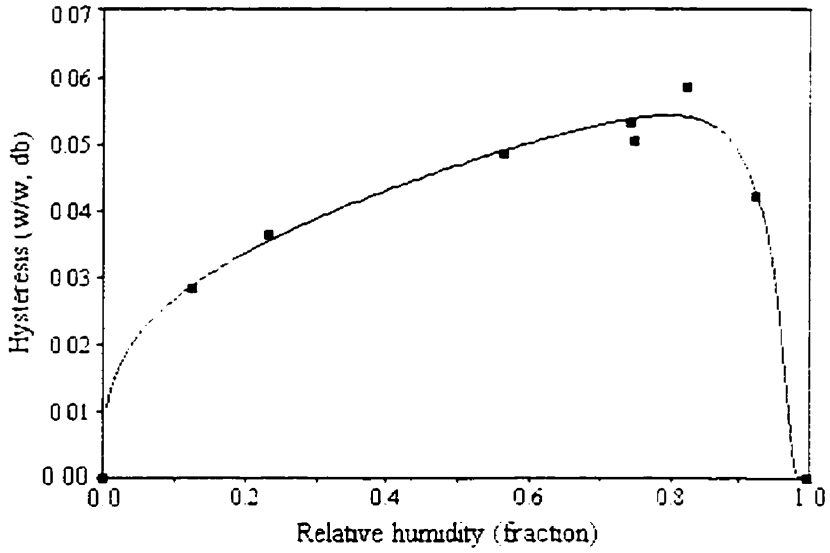

Figure 6.8A: #1 hysteresis model

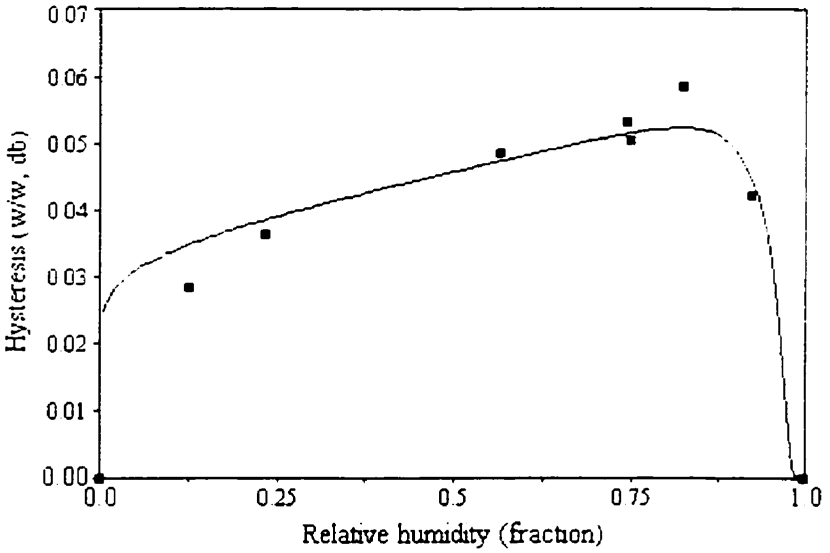

Figure 6.8B: #2 hysteresis model

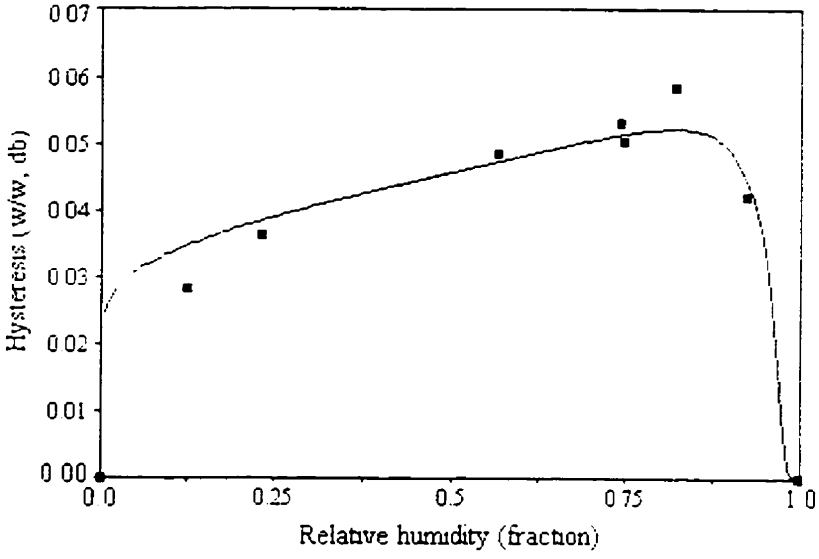

Figure 6.8C: #3 hysteresis model

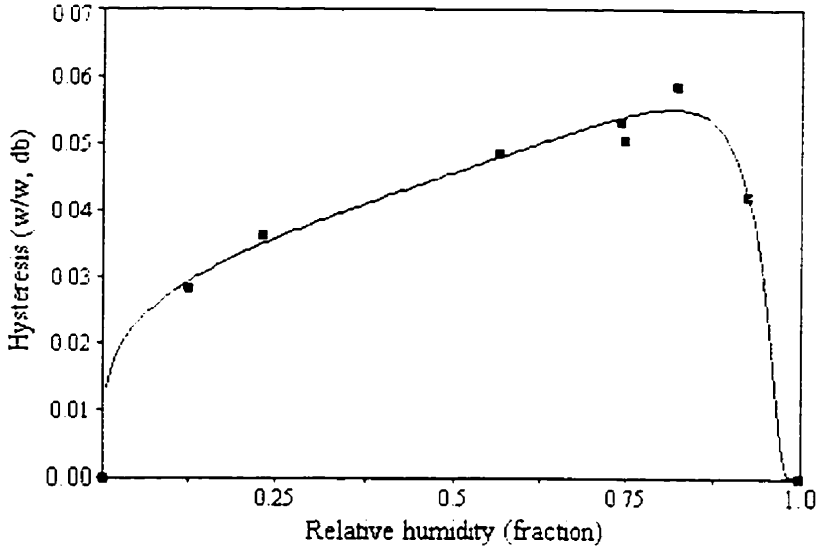

Figure 6.8D: #4 hysteresis model

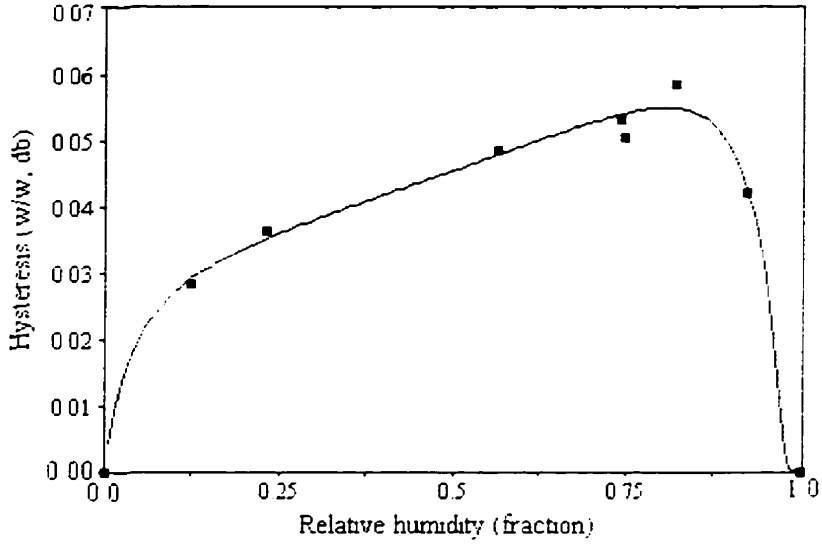

Figure 6.8E: #5 hysteresis model

Figure 6.8: Performance comparison among the five hysteresis models for the hysteresis data of alfalfa grind at 9°C. In figures 6.8A, B, C, D and E, solid squares denote the measured data and solid curves denote the estimated values.

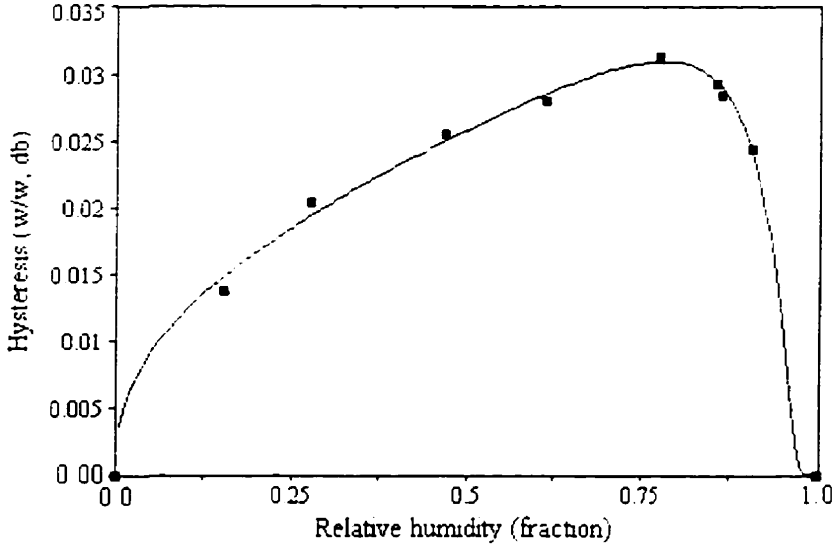

Figure 6.9A: #1 hysteresis model

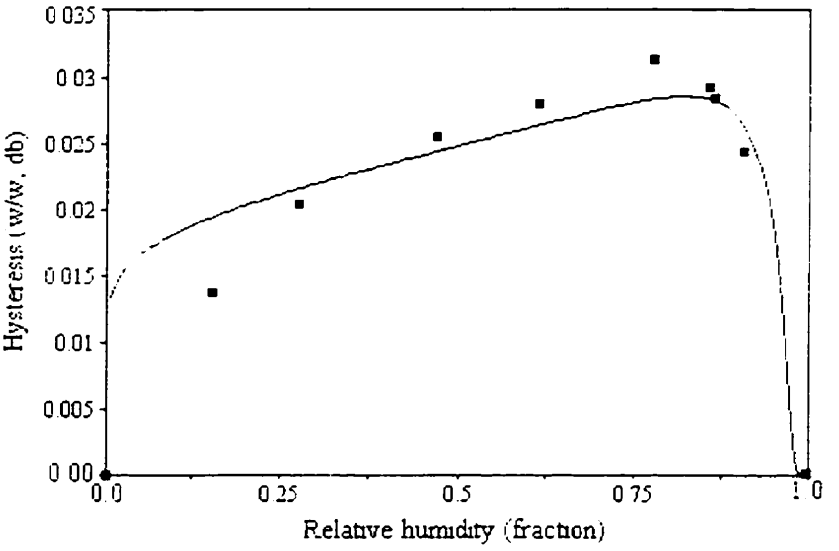

Figure 6.9B: #2 hysteresis model

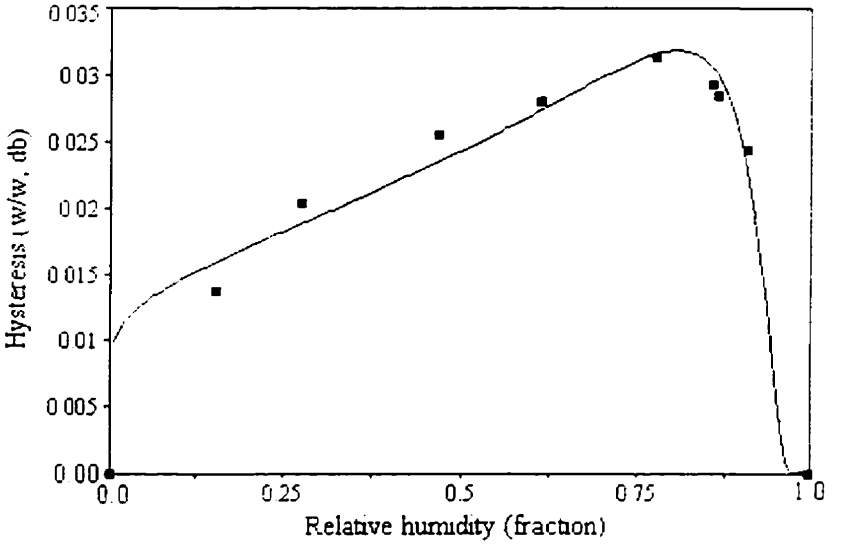

Figure 6.9C: #3 hysteresis model

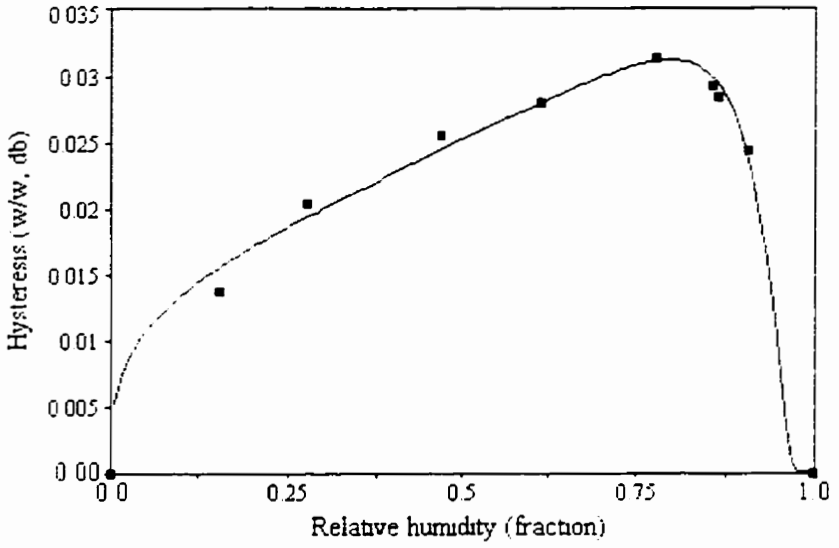

Figure 6.9D: #4 hysteresis model

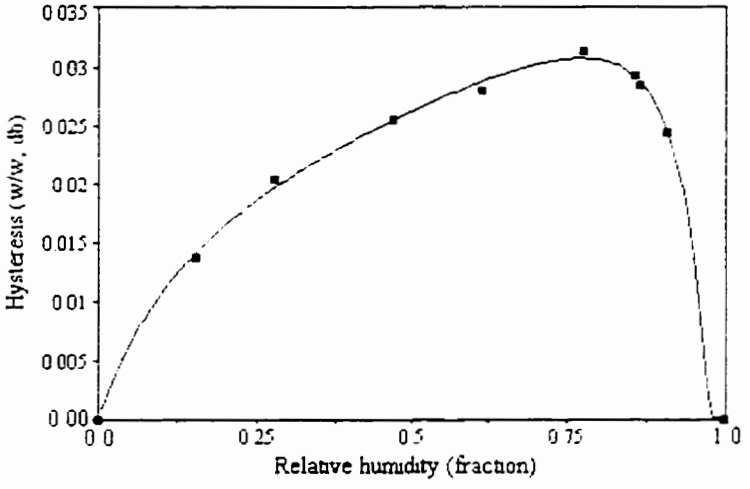

Figure 6.9E: #5 hysteresis model

Figure 6.9: Performance comparison among the five hysteresis models for the hysteresis data of alfalfa grind at 25°C. In figures 6.9A, B, C, D and E, solid squares denote the measured data and solid curves denote the estimated values.

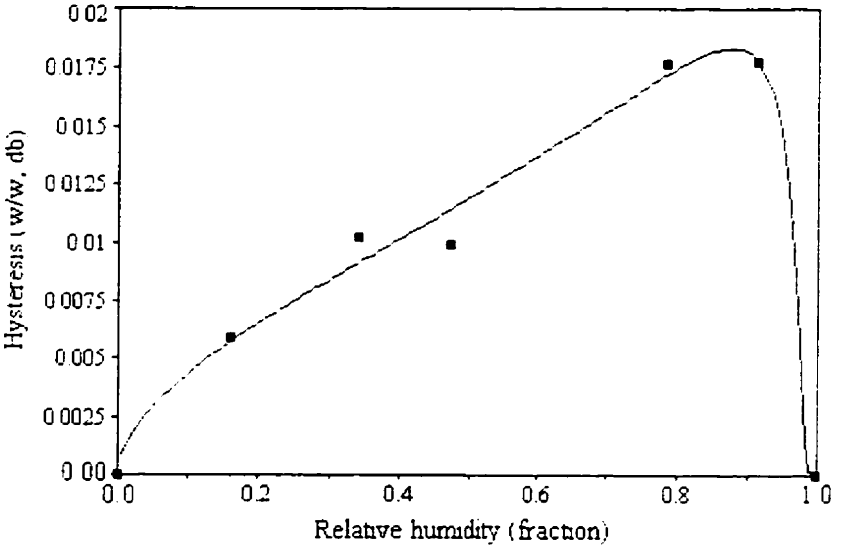

Figure 6.10A: #1 hysteresis model

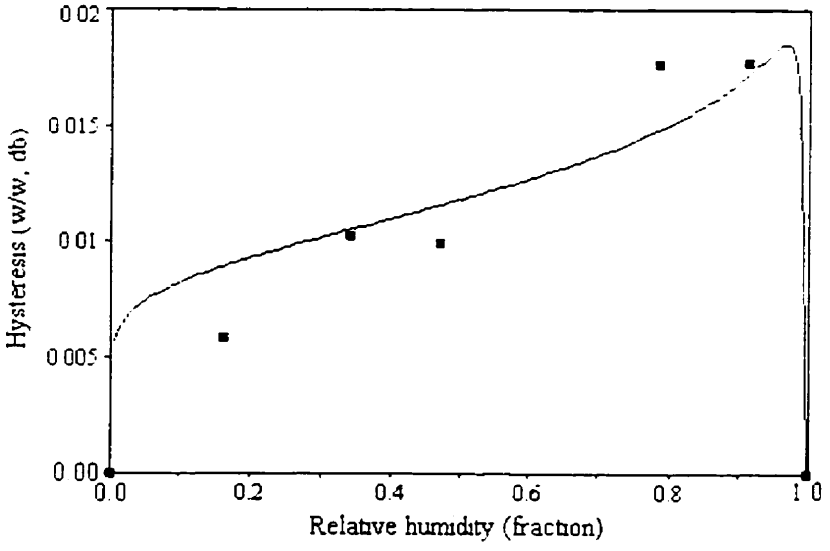

Figure 6.10B: #2 hysteresis model

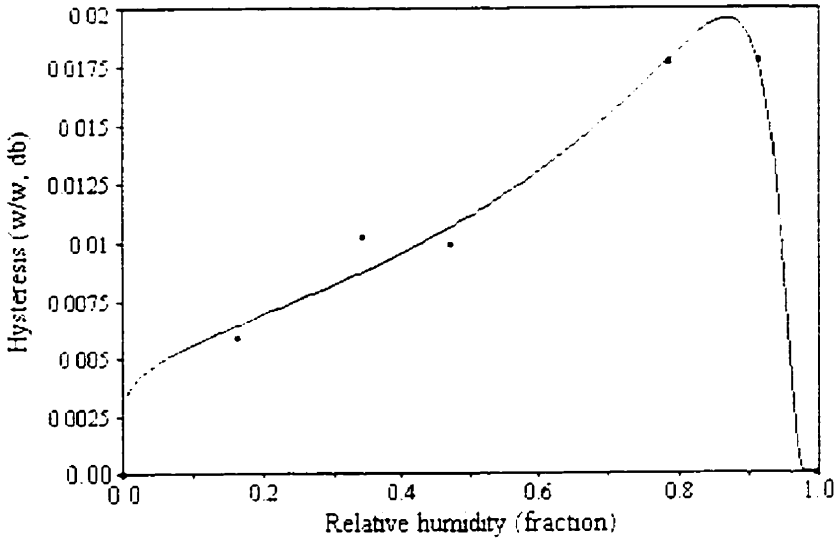

Figure 6.10C: #3 hysteresis model

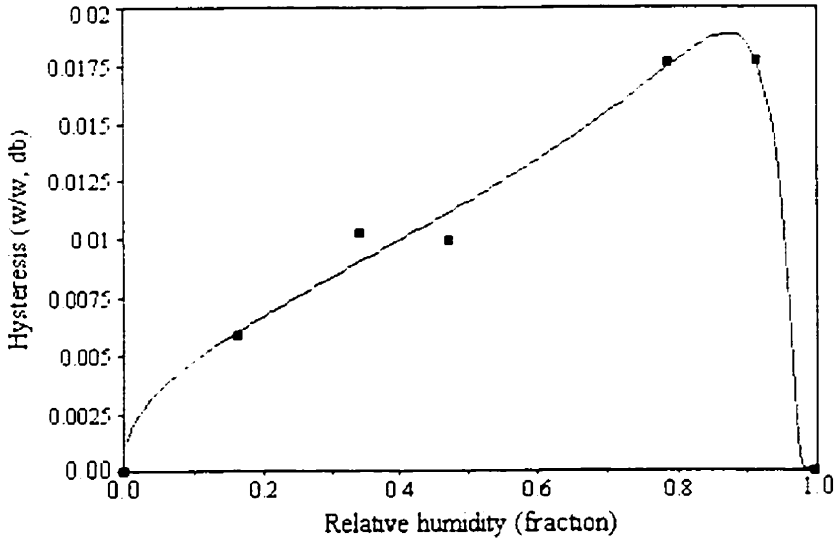

Figure 6.10D: #4 hysteresis model

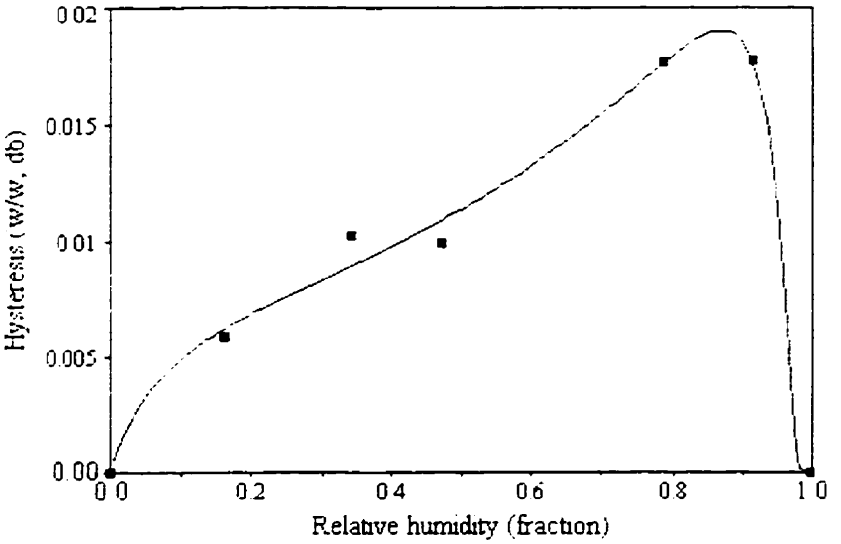

Figure 6.10E: #5 hysteresis model

Figure 6.10: Performance comparison among the five hysteresis models for the hysteresis data of alfalfa grind at 50°C. In figures 6.10A, B, C, D and E, solid squares denote the measured data and solid curves denote the estimated values.

Chapter 7

MATHEMATICAL MODELING OF STEAM CONDITIONING PROCESS

7.1 Overview

In the previous chapters, steam conditioning of alfalfa grind was discussed based on the experimental results in a laboratory scale. In this chapter, the steam conditioning process is modeled mathematically and verified with the pilot-scale test results.

As mentioned in Chapter 1 the steam conditioning in alfalfa processing is more an art than a science at the present time. There are some reports on the effect of conditioning parameters on the quality of pellets (Dobie, 1959; Smith, 1959; Bartikoski, 1962; Hill and Pulkinen, 1988; Sokhansanj and Wood, 1990; Tabil and Sokhansanj, 1992, 1993). There was no information available on heat and mass transfer modeling of the steam conditioning process of alfalfa grind. Attempts have been made in this study to develop mathematical models to predict meal temperature and moisture content of alfalfa grind in a steam conditioner.

As mentioned in Chapter 5, two approaches were often used in model development: the lumped and the spatial (or distributed) considerations. In this study, the model development of steam conditioning process followed the lumped consideration, because the pilot-scale tests on the steam conditioning process conducted in this study showed that the meal inside a steam conditioner could be regarded as well mixed. This was mainly because the meal inside the conditioner was constantly stirred by a propeller (or paddle) that ran at a fairly high revolution (typically 500 - 1200 rpm).

It was observed that both meal temperature and moisture content of alfalfa grind at various locations of the conditioner chamber equalized very quickly after the injection of steam. Figure 7.1 shows the experimental evidence that meal temperature inside the steam conditioner changed little along the conditioner when the meal flow and steam contact were fully developed (Average temperature on flat portion of the curve 93±1.5°C). Figure 7.2 shows the meal moisture content data at three locations of the

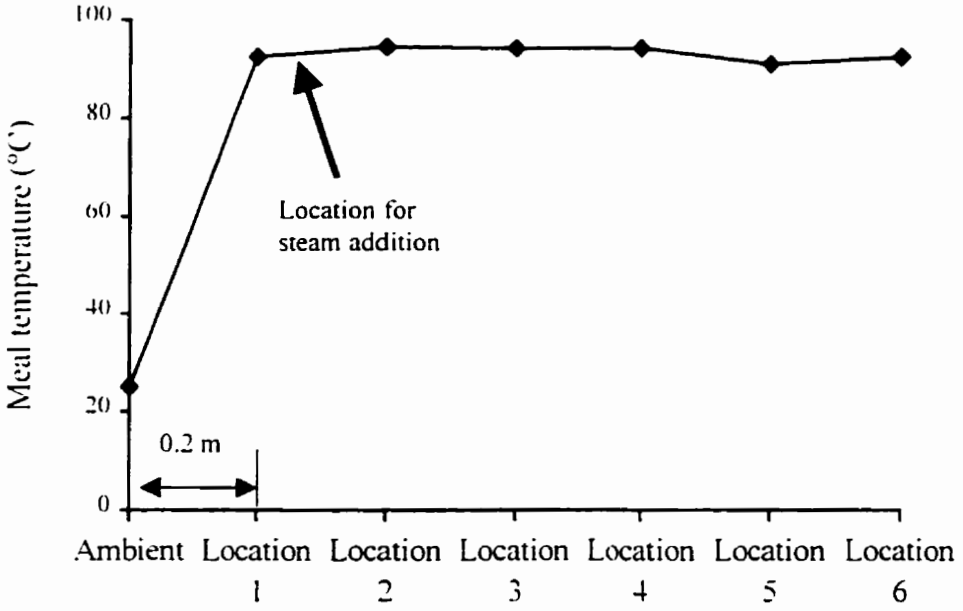

Figure 7.1: Temperature of alfalfa meal at 6 locations of both experimental steam conditioner chambers in relation to conditioning time.

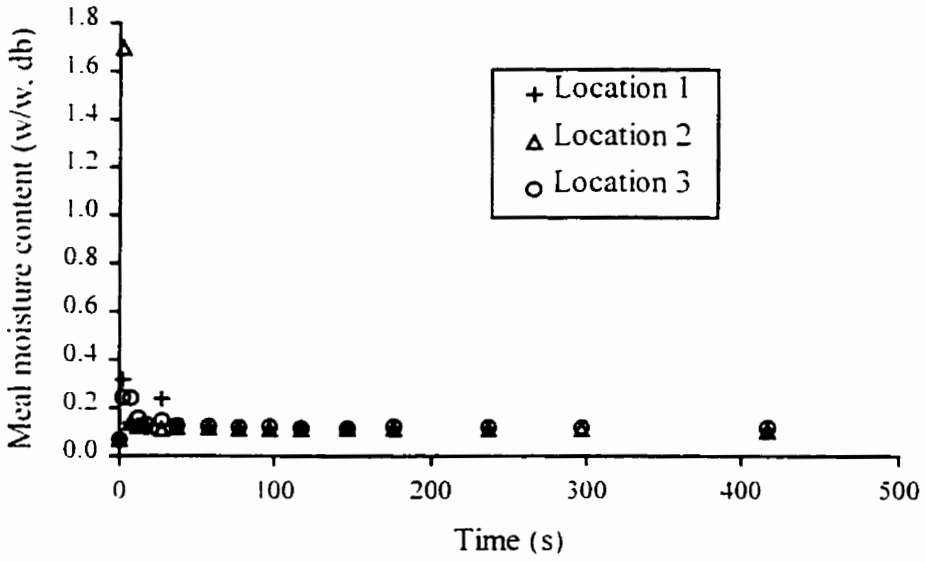

Figure 7.2: Moisture content of alfalfa meal at three locations of the top steam conditioner in relation to conditioning time. Operational conditions: intake meal flow rate 2.7 kg/hr, inlet steam pressure 3.45 kPa (0.5 psi gauge) and propeller rotational speed approximately 840 rpm.

conditioner, which exhibited stability over time following a fairly short transition period after the injection of steam. In Figures 7.1 and 7.2, locations 1 to 3 were inside the top

conditioner chamber and locations 4 to 6 inside the bottom conditioner chamber (refer to Figure 7.5 and section 7.3.2 for details). Alfalfa grind was introduced into the conditioner at about 25°C. As can be seen in Figure 7.1, the temperature of alfalfa meal remained basically unchanged after the grind passed the sampling location 1 around which steam was injected into the conditioner. Figure 7.2 shows the moisture content of alfalfa meal at locations 1 to 3 of the top conditioner chamber. It is evident that meal moisture content at these three locations stayed close to one another regardless of the longitudinal geometry of the conditioner after the peaked transitional period.

7.2 Model development

Heat and mass transfer models were developed based on the assumption that the grind was well mixed in a steam conditioner, as mentioned earlier. Figure 7.3 depicts the

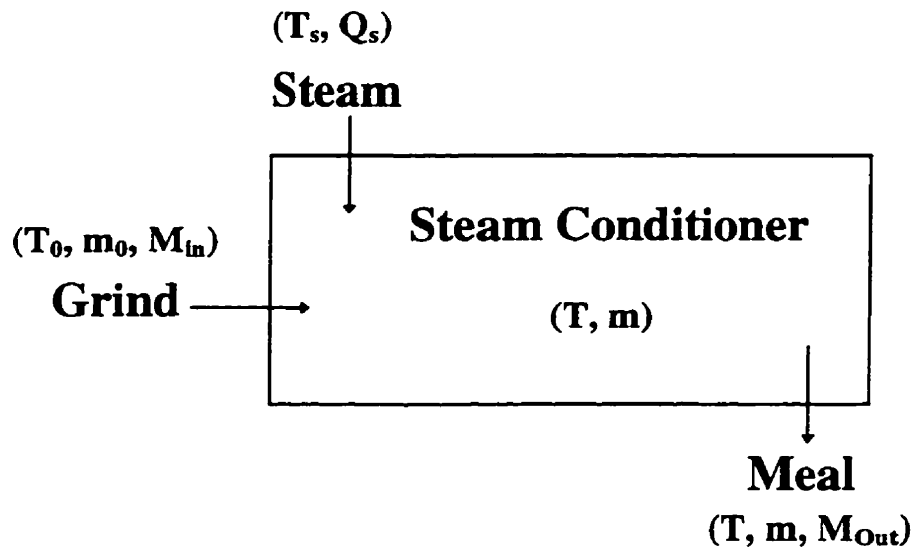

Figure 7.3: Diagram showing the incoming and outgoing masses and energy in a steam conditioner.

incoming and outgoing temperatures, mass and moisture in a steam conditioner under the above assumption. The grind enters the conditioner at the moisture content of m_0, temperature T_0 and mass flow rate M_{in}. It mixes with super-heated steam (temperature T_s and flow rate Q_s,) and exits in the form of moist hot grind hereinafter called meal

(temperature T and moisture content m). The overall mass and energy balances for a steam conditioner as defined in Figure 7.3 are:

$$M_{in}\frac{m_0}{1+m_0}+Q_s-M_{in}\frac{m}{1+m_0}=\rho_d V\frac{dm}{dt} \tag{7.1}$$

$$c_d\frac{M_{in}}{1+m_0}T_0+c_w m_0\frac{M_{in}}{1+m_0}T_0+c_s(T_s-100)Q_s+Q_s h_{fg}+Q_s c_w 100$$
$$-Q_s c_w T-c_d\frac{M_{in}}{1+m_0}T-c_w m\frac{M_{in}}{1+m_0}T=c_p\rho V\frac{dT}{dt} \tag{7.2}$$

where

m_0	initial moisture content of alfalfa grind (0.0701) (w/w, db)
M_{in}	mass flow rate of alfalfa grind at intake (kg/s)
Q_s	mass flow rate of the steam that condensed on alfalfa grind (kg/s)
m	moisture content of conditioned alfalfa grind (w/w, db)
ρ	mean bulk density of alfalfa grind in the conditioner (kg/m^3)
ρ_d	mean bulk density for the dry matter of alfalfa grind (kg/m^3)
V	Effective volume of conditioner for steam conditioning (m^3)
c_d	specific heat capacity of dry matter ($kJ.kg^{-1}.K^{-1}$)
c_w	specific heat capacity of water ($kJ.kg^{-1}.K^{-1}$)
c_s	specific heat capacity of super-heated steam (kJ/kg.K)
c_p	mean specific heat capacity of alfalfa grind (kJ/kg.K)
T_0	initial temperature of alfalfa grind (°C)
T_s	temperature of super-heated steam (°C)
T	temperature of conditioned alfalfa grind (°C)
h_{fg}	latent heat of vaporization of water at 100°C and atmospheric pressure (kJ/kg)

Equations 7.1 and 7.2 are correlated heat and mass transfer models, since Equation 7.2 contains both m and T that are the two variables in question. Integrating Equation 7.1 gives

$$\ln\left[m_0+\frac{Q_s(1+m_0)}{M_{in}}-m\right]=-\frac{M_{in}}{\rho_d V(1+m_0)}t+C \tag{7.3}$$

where C is an integration constant and can be found by initial condition of meal moisture

content.

$$C = \ln\left[\frac{Q_s(1+m_0)}{M_{in}}\right] \qquad (m|_{t=0} = m_0) \tag{7.4}$$

$$m = m_0 + \frac{Q_s(1+m_0)}{M_{in}}\left(1 - e^{-\frac{M_{in}}{\rho_d V(1+m_0)}t}\right) \tag{7.5}$$

During the development of Equation 7.5, Q_s, the amount of steam condensation, was assumed to be invariant. In a real situation Q_s would change with time due to the fact that Q_s is a function of the temperature difference between the steam and the grind. At the onset of steam conditioning, alfalfa grind was at ambient temperature that was much lower than the temperature of steam, and steam condensation was therefore severely high. As the meal and the conditioner chamber were heated up as time passed, the temperature difference diminished. So did Q_s before it reached steady state eventually. However, experimental observation in meal moisture content and temperature trends suggested that change of Q_s over time took place mostly in the initial stage of steam injection. After 5 to 10 seconds, Q_s approached a constant level and remained almost unchanged with time. Such a behavior of steam condensation could be best represented by an inverted logarithmic power series, that is,

$$Q_s = K\left\{1 + \frac{1}{\ln(t)} + \frac{1}{[\ln(t)]^2} + \frac{1}{[\ln(t)]^3} + \bullet\bullet\bullet\right\} \qquad (t>0,\ t\neq 1) \tag{7.6}$$

where K is a constant accounting for the quantity of steam condensation, kg/s. Figure 7.4 shows the trend of Equation 7.6 as approximated by the first four terms, where K is assumed to be 1 kg/s for demonstration purpose. Increasing or decreasing the terms in

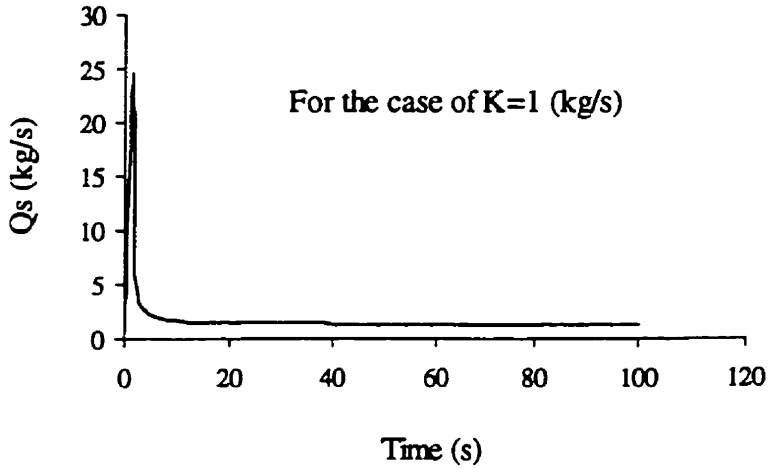

Figure 7.4: A plot showing the trend of Equation 7.6 in relation to time.

Equation 7.6 only increases or decreases, respectively, the magnitude of the dependent variable in the vicinity of t=1 at which Equation 7.6 should not be applied, but does not change the shape of the curve at all. To simplify the solution to m, all higher-order components except for the first two terms in Equation 7.6 are phased out. Equation 7.6 thus becomes

$$Q_s = K\left[1+\frac{1}{\ln(t)}\right] \tag{7.7}$$

Inserting Equation 7.7 into Equation 7.5, we have

$$m = m_0 + \frac{K\left[1+\frac{1}{\ln(t)}\right](1+m_0)}{M_{in}}\left(1-e^{-\frac{M_{in}}{\rho_a V(1+m_0)}t}\right) \tag{7.8}$$

or

$$m = m_0 + \frac{K\left[1+\frac{1}{\ln(t)}\right](1+m_0)}{M_{in}}\left(1-e^{-At}\right) \tag{7.9}$$

where A is a constant that is equal to $\frac{M_{in}}{\rho_d V(1+m_0)}$.

To solve Equation 7.2, Q_s and m need to be replaced by Equation 7.7 and Equation 7.9 respectively. However, the replacement made Equation 7.2 too complicated to be solved analytically due to the hindrance of the two integrals: $\int e^{e^t} dt$ and $\int \frac{1}{\ln(t)} dt$. Either numerical or semi-empirical approach is required to solve Equation 7.2. In this study, the semi-empirical approach was adopted to come up with the solution for T. As discussed earlier, Q_s and m varied little with time after a short transition period of time (Figure 7.2 and Figure 7.4), Q_s and m could be reasonably taken as invariant in Equation 7.2. The analytical solution to Equation 7.2 based on the above-mentioned treatment is

$$T = \frac{D}{E} + \left(T_0 - \frac{D}{E}\right) e^{-Et} \tag{7.10}$$

where D and E assume the following forms:

$$D = \frac{(c_d + c_w m_0)\frac{M_{in}}{1+m_0} T_0 + \left[c_s (T_s - 100) + h_{fg} + 100 c_w\right] Q_s}{c_p \rho V} \tag{7.11}$$

$$E = \frac{Q_s c_w + c_d \frac{M_{in}}{1+m_0} + c_w \frac{M_{in}}{1+m_0} m}{c_p \rho V} \tag{7.12}$$

The parameters D and E can be revised empirically to take into account the variation of m and Q_s with time. This can be done by incorporating Equation 7.7 and Equation 7.9 into both Equation 7.11 and Equation 7.12, which leads to

$$D = \frac{(c_d + c_w m_0)\frac{M_{in}}{1+m_0}T_0 + \left[c_s(T_s - 100) + h_{fg} + 100c_w\right]K\left[1 + \frac{1}{\ln(t)}\right]}{c_p \rho V} \tag{7.13}$$

$$E = \frac{K\left[1 + \frac{1}{\ln(t)}\right]c_w + c_d\frac{M_{in}}{1+m_0} + c_w\frac{M_{in}}{1+m_0}\left\{m_0 + \frac{K\left[1 + \frac{1}{\ln(t)}\right](1+m_0)}{M_{in}}\left(1 - e^{-At}\right)\right\}}{c_p \rho V} \tag{7.14}$$

The parameter E in exp(-Et) was roughly treated as a constant for simplicity consideration. Such a treatment seemed to be reasonable due to the fact that in Equation 7.12 both Q_s and m approached steady state very swiftly after a short transition period of time (refer to Figure 7.2 and Figure 7.4) to result in a basically invariant E. Equations 7.9, 7.10, 7.13 and 7.14 are the models developed semi-empirically in this study to describe the relationship of meal temperature and moisture content versus time. Their capability of predicting the trends of meal temperature and moisture content will be tested using the pilot-scale experimental data.

Table 7.1: Summary of the tests conducted on the pilot steam conditioner.

Tests	**Observation**	**Comments**
1. Meal temp. distribution	2704 per location	Six locations
2. Meal moisture distribution	19 per location	3 locations
3. Outgoing meal m.c. vs. t	17 per run	3 runs, duplicate samples
4. Intake grind flow rate	8 flow rates	3 replicates at each flow rate
5. Propeller revolution	3 times	Mean of 3 readings
6. Inlet steam pressure	7 times	Check once per test

7.3 Material and methods

7.3.1 Material and preparation

The material used in the pilot-scale steam conditioning tests was the non-fractionated dehydrated alfalfa grind as used in other experiments reported in previous

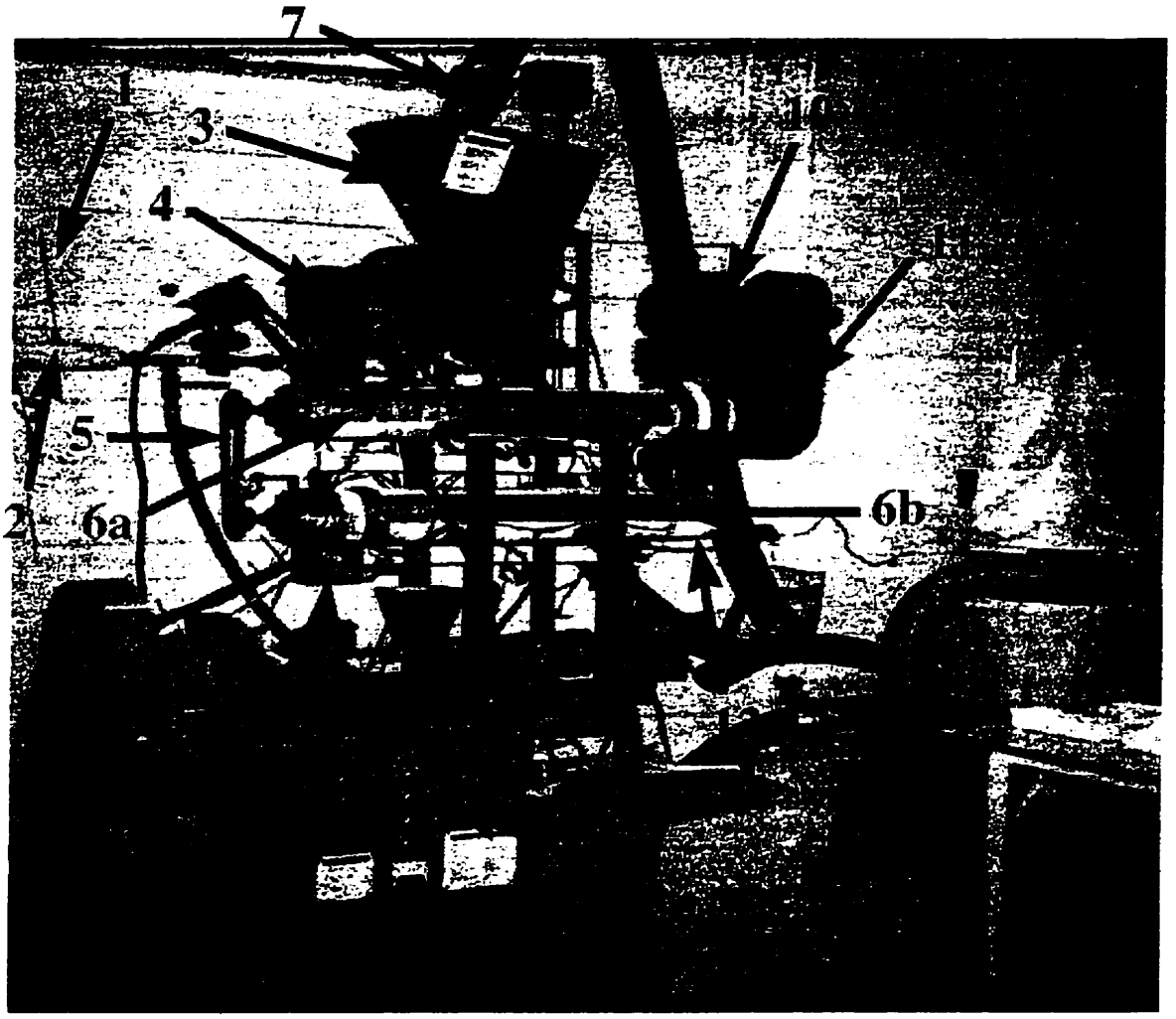

1 Steam line temperature probe
2 - Steam line
3 - Vibratory feeder
4 - Feed intake duct
5 - Chain drive
6a - Upper conditioner
6b - Lower conditioner
7 - Dust collector
8 - Steam intake
9 - Sampling and thermocouple hole (For other holes see Figure 7.5b)
10 – Motor
11 - Pulley case
12 - Upper conditioner outlet
13 - Lower conditioner outlet
14 - Feeder speed knob
15 - Control panel

Figure 7.5a: The pilot-scale pellet mill used in this study.

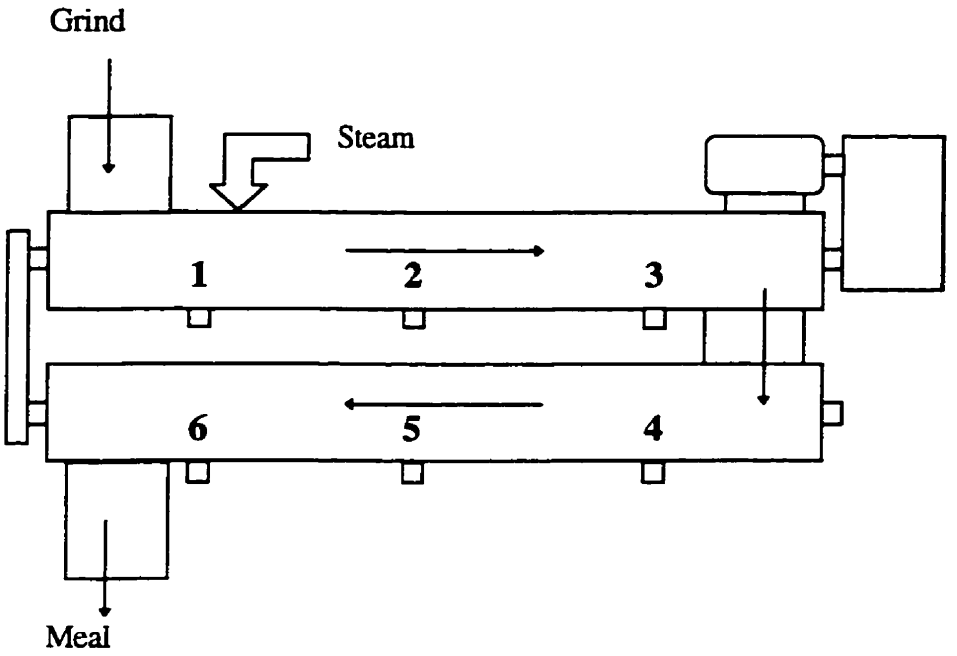

Figure 7.5b: Relative locations of the steam orifice and the six holes for sampling and thermocouple placement.

chapters. The initial moisture content of the dehydrated alfalfa grind was 0.0701 db. Table 7.1 summarizes the tested items, the materials used in the experiments, number of observations, and other related information on the sample specifications.

7.3.2 The pilot-scale steam conditioner

Figure 7.5a shows the CPM pilot-scale pellet mill (California Pellet Mill, California) used in this study. It consists of three major parts: a feeder, a steam conditioner and a pelleter. The steam conditioner and the feeder are the major parts of the mill for this study.

Principal components of the mill that related to this study are listed below the figure. Alfalfa grind was manually loaded to the vibratory feeder (3), maintaining 2/3 of the holding capacity of the hopper. The flow rate of alfalfa grind from the feeder was frequency controlled, which was done by rotating the feeder speed knob (14) on the control panel (15) to increase or decrease the vibration frequency of the feeder chute. The grind flowed through the feed intake duct (4) into steam conditioner (6a) where it

was stirred and carried forward by a propeller (or paddle) towards the center of the conditioner. Steam was injected into the conditioner through the steam intake orifice (8) where it was mixed with the grind and also diffused to other part of the conditioner chamber. At the end of the upper conditioner (6a), alfalfa meal dropped to the lower conditioner (6b) to continue with the conditioning process until it reached the end of the lower conditioner where it was discharged to a screw feeder and conveyed to the pelleter for pellet making. There was a sampling hole (about 10 cm x 25 cm) in the transition duct between the upper and the lower conditioner chambers. Meal dropping from the top chamber could be sampled from this hole. During steam conditioning, meal temperature was monitored by thermocouples located in the sampling holes (9). Meal samples were taken from the sampling holes (9) as well as the conditioner outlets (12, 13) for moisture content measurement.

7.3.3 Experimental procedures

Alfalfa grind temperature

Alfalfa grind temperature was measured by type T thermocouples mounted in the cork plugs in the sampling holes. The thermocouples were mounted through the center of a cork plug and soldered to a piece of copper that was tightly embedded onto the surface of the cork. The cork plugs snapped into the sampling holes in such a way that the copper pieces could maintain contact with the meal in the conditioner but kept a clearance to the tips of the paddles. Temperature data were collected through a data acquisition system consisting of a data logger and a personal computer (not shown in Figure 7.5a). There were three sampling holes in either conditioner chamber, located at 0.20 m, 0.44 m, and 0.75 m from the left end of the conditioner. In Figure 7.5a, only the first sampling hole was indicated and the rest were not marked due to congestion of the figure. They were shown in Figure 7.5b instead. The first sampling hole was located between the material intake and the steam inlet. The second sampling hole was in the middle portion of the conditioner. The third sampling hole was close to the transition duct between the upper and the lower conditioner chambers.

Alfalfa grind moisture content

The meal moisture content vs. time relationship was measured by taking samples from the sampling holes at different time intervals. When the cork plugs were removed, meal could drop out of the conditioner chamber from the holes while the paddle rotated. Containers were held under the sampling holes to collect the meal. A scoop with long handle was used to sample the meal from the sampling hole in the transition between the top and the bottom chambers. The interval between two consecutive samplings was 5s, 10s, 20s, 30s, and 60s at different stages of conditioning, shorter at early stage and longer at later stage. At each sampling, the receiving time was 4 s. The actual time was set at the median of the starting and ending times of that sampling. ASAE oven method (ASAE, 1996b) was used to measure the moisture content of alfalfa meal when the quantity of the meal collected satisfied the specified mass in the standard. In cases of smaller-sized samples at the samplings during early stage of steam conditioning, moisture content measurement followed the temperature and time specifications of the ASAE standard but with less mass at each measurement to compromise for the smaller sizes.

Alfalfa grind flow rate, steam pressure, steam temperature and paddle revolution

The flow rate of alfalfa grind at the intake of the conditioner was measured by collecting and weighing the grind dropped from the feeder chute for a length of time. The flow rate was controlled through the current control knob on the control panel of the mill. Meal flow rates were measured at the knob locations of 24, 30, 40, 60, 70, 80, 90 and 100 mA. The test results are presented in Table 7.2. Steam pressure was taken from the pressure gauge in the steam pipe (not seen in Figure 7.5, on the back of the mill) that branched to the steam conditioner. Steam temperature was measured with a type K thermocouple mounted in the same pipe as for the pressure gauge. Steam temperature data were collected through the same data acquisition system used for meal temperature monitoring. The rotational speed of the paddle was measured at the end of the shaft where the paddles were attached using a tachometer.

Table 7.2: The flow rates of alfalfa grind from the vibratory feeder into the steam conditioner.

Current (mA)		Test 1	Test 2	Test 3	Test 4	Test 5	Mean (g/s)	Stdev	Rate (kg/h)
24	Mass (g)	59.1	40.2	31.6	34.0	36.9			
24	Time (s)	120.0	120.1	119.9	120.0	120.3			
24	Flow rate (g/s)	0.5	0.3	0.3	0.3	0.3	0.3	0.03	1.1
30	Mass (g)	166.9	163.2	171.5					
30	Time (s)	122.9	123.2	125.1					
30	Flow rate (g/s)	1.4	1.3	1.4			1.4	0.02	4.9
40	Mass (g)	257.3	266.4	240.0					
40	Time (s)	119.9	120.0	120.0					
40	Flow rate (g/s)	2.1	2.2	2.0			2.1	0.1	7.6
60	Mass (g)	263.6	288.0	271.0					
60	Time (s)	119.8	120.0	120.0					
60	Flow rate (g/s)	2.2	2.4	2.3			2.3	0.1	8.2
70	Mass (g)	286.3	284.1	336.4					
70	Time (s)	120.1	120.1	130.1					
70	Flow rate (g/s)	2.4	2.4	2.6			2.4	0.1	8.8
80	Mass (g)	294.7	282.9	323.0					
80	Time (s)	120.0	119.8	120.2					
80	Flow rate (g/s)	2.5	2.4	2.7			2.5	0.2	9.0
90	Mass (g)	339.5	310.8	310.8					
90	Time (s)	120.3	119.9	120.0					
90	Flow rate (g/s)	2.8	2.6	2.6			2.7	0.1	9.6
100	Mass (g)	394.1	368.6	349.1					
100	Time (s)	132.3	119.6	120.1					
100	Flow rate (g/s)	3.0	3.1	2.9			3.0	0.1	10.8

7.4 Results and discussion

7.4.1 Experimental data of meal temperature and moisture content

The measured data of meal moisture content are presented in Figure 7.2, Figure 7.6, Figure 7.7 and Figure 7.8. The data in Figure 7.2 were collected at three locations of the top steam conditioner at the intake meal flow rate of 2.7 kg/h, the inlet steam pressure of 3.4 kPa and the propeller rotational speed of approximately 840 rpm. The data in Figures 7.6, 7.7 and 7.8 were collected at the top conditioner discharge in the following conditions: intake mass flow rate 10.8, 9.6 and 7.6 kg/h, respectively; inlet steam pressure 34.5 kPa; propeller revolution about 840 rpm. The meal moisture content trend exhibited such a characteristic that it peaked during the initial few seconds following the injection of the steam. It then decreased from the peak and leveled off subsequently. The data in Figure 7.2, Figure 7.6, Figure 7.7 and Figure 7.8 were used to test the applicability of the model developed for predicting meal moisture trend.

Table 7.3 presents the experimental data of meal temperature at 6 locations of the steam conditioner. The behavior of meal temperature trend was unlike that of meal moisture content trend. It increased steadily with time without an abrupt peak in the early stage of the temperature course before it started to remain constant throughout the experiment after a certain period of time (see Figure 7.10). The data in Table 7.3 were used to test the applicability of the model developed for predicting meal temperature trend.

7.4.2 Model verification

Model for meal moisture content

Equation 7.9 was applied to meal moisture content data as shown in Figure 7.2, Figure 7.6, Figure 7.7, and Figure 7.8. The inverse method described in previous chapters was also used to examine the performance of Equation 7.9 towards the measured meal moisture content data. Model constants and regression statistics were recorded. Before curve-fitting, m_o and M_{in} in Equation 7.9 were replaced by 0.0701

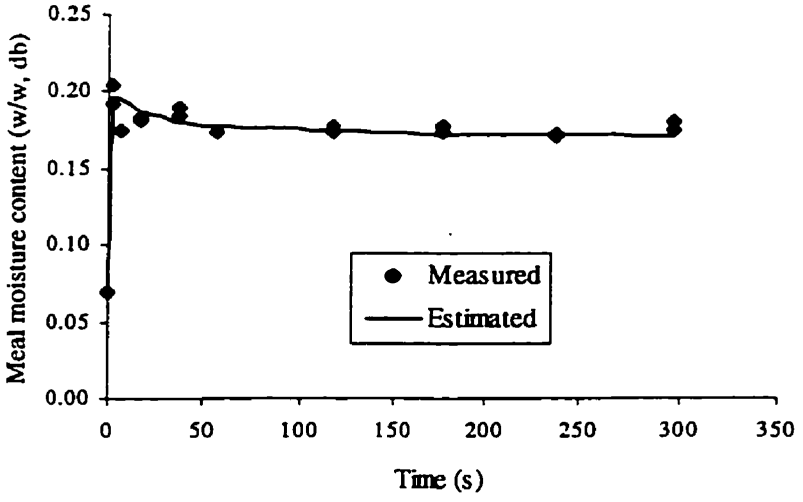

Figure 7.6: Comparison between the model estimated and the measured meal moisture contents at top conditioner discharge at an intake mass flow rate of 10.8 kg/h, inlet steam pressure of 34.5 kPa and propeller revolution of about 840 rpm.

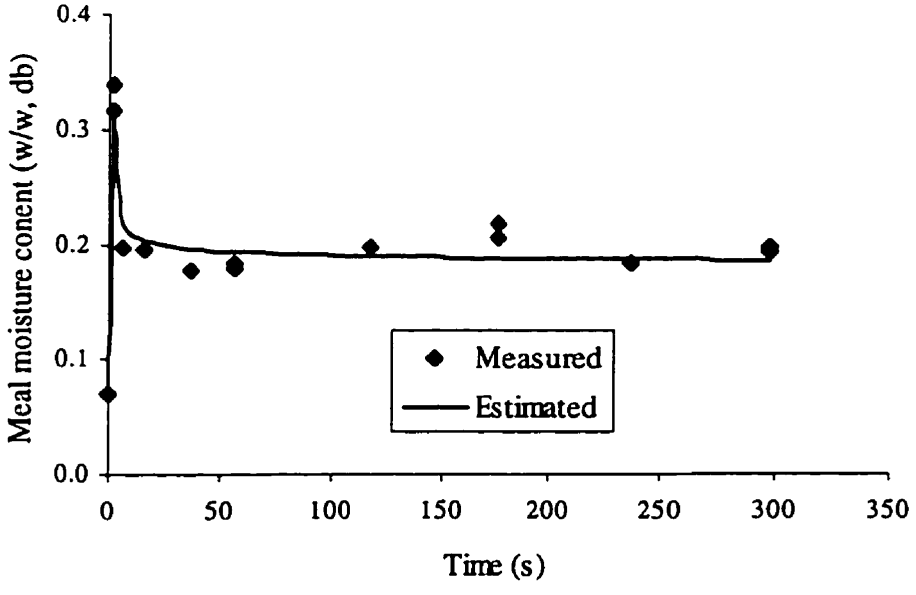

Figure 7.7: Comparison between the model estimated and the measured meal moisture contents at top conditioner discharge at an intake mass flow rate of 9.6 kg/h, inlet steam pressure of 34.5 kPa and propeller revolution of about 840 rpm.

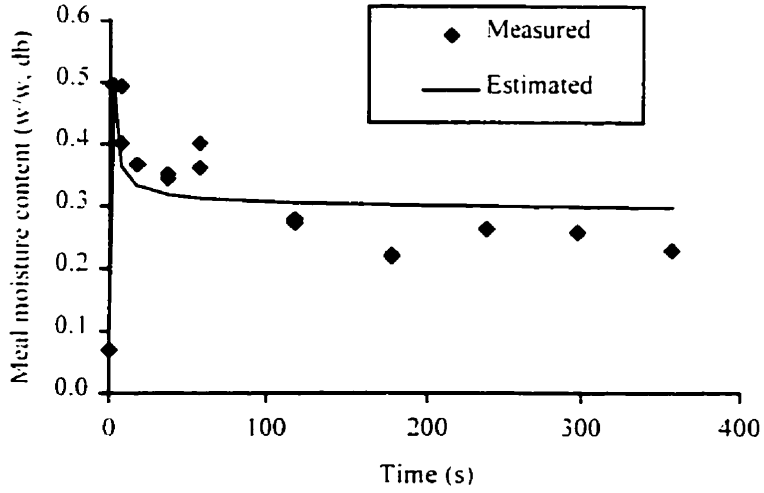

Figure 7.8: Comparison between the model estimated and the measured meal moisture contents at top conditioner discharge at an intake mass flow rate of 7.6 kg/h, inlet steam pressure of 34.5 kPa and propeller revolution of about 840 rpm.

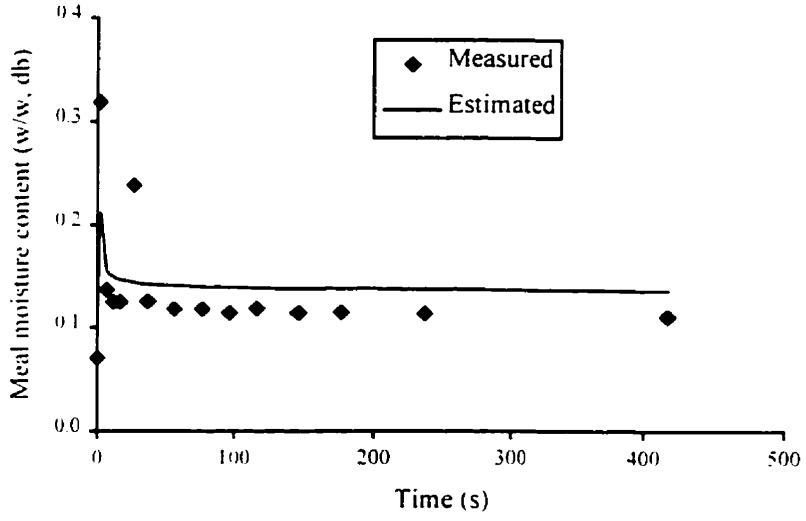

Figure 7.9a: Comparison of the model estimation with the experimental data of meal moisture content at location 1 of the top conditioner at the following conditions: 2.7 kg/h intake meal flow rate, 3.45 kPa inlet steam pressure and approximately 840 rpm paddle revolution.

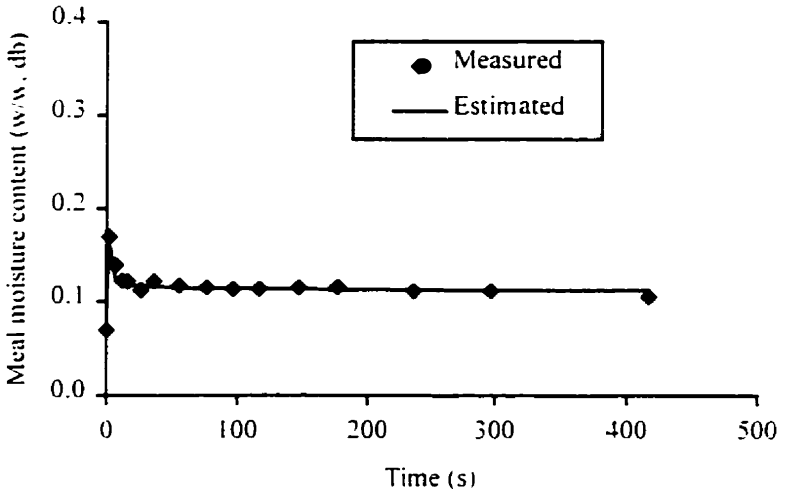

Figure 7.9b: Comparison of the model estimation with the experimental data of meal moisture content at location 2 of the top conditioner at the following conditions: 2.7 kg/h intake meal flow rate, 3.45 kPa inlet steam pressure and approximately 840 rpm paddle revolution.

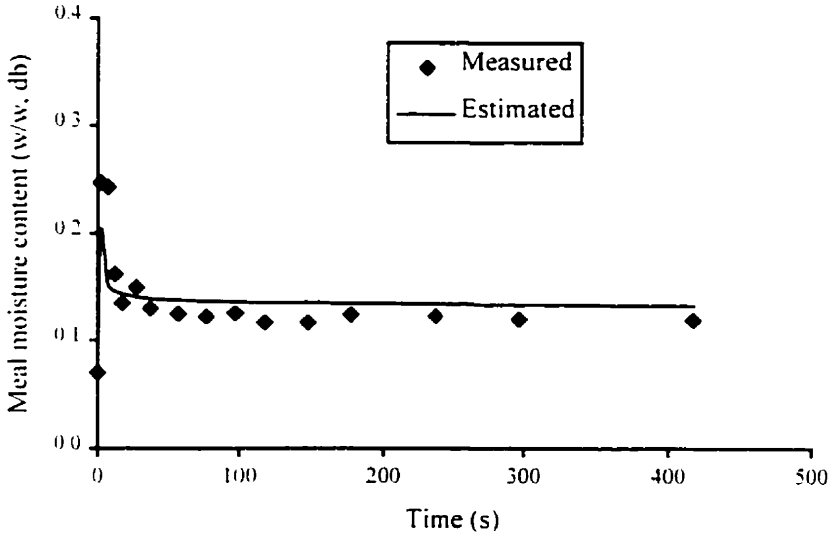

Figure 7.9c: Comparison of the model estimation with the experimental data of meal moisture content at location 3 of the top conditioner at the following conditions: 2.7 kg/h intake meal flow rate, 3.45 kPa inlet steam pressure and approximately 840 rpm paddle revolution.

Table 7.3: Meal temperature data at 6 locations of the pilot-scale conditioner.

Elapsed Time (s)	Meal Temperature (°C)					
	Top Conditioner Thermocouples			Bottom Conditioner Thermocouples		
	#1	#2	#3	#4	#5	#6
0	25.0	25.0	25.0	25.0	25.0	25.0
37	41.9	31.0	29.6	28.4	29.7	29.9
63	51.2	40.4	36.2	31.1	34.7	36.1
98	55.7	47.6	41.9	34.0	38.5	40.7
124	57.5	51.6	45.7	36.1	41.0	43.5
151	59.8	55.2	49.5	38.5	43.9	47.1
186	61.7	58.8	53.0	41.4	46.8	50.5
213	64.1	61.2	55.5	43.4	48.9	52.5
248	66.8	64.9	59.3	46.9	52.4	56.7
276	66.8	66.8	62.0	49.6	54.8	59.2
304	67.6	68.9	64.4	52.0	56.9	61.5
331	68.0	70.3	66.2	54.4	59.0	63.3
368	69.8	72.3	68.7	57.7	61.7	66.0
397	70.7	73.2	69.9	59.9	63.2	67.3
424	71.7	74.2	71.1	61.8	64.7	68.7
452	72.6	75.3	72.4	63.7	66.1	70.0
481	73.6	76.4	73.8	65.6	67.6	71.5
518	74.1	77.2	74.7	67.8	69.2	72.9
546	77.0	78.5	76.2	69.2	70.2	74.0
574	78.4	79.8	77.7	71.1	72.0	75.6
602	79.8	81.4	79.6	73.0	73.6	77.1
631	80.7	82.2	80.6	74.7	75.1	78.6
668	81.9	83.6	82.3	77.1	77.1	80.5
696	82.8	84.7	83.5	78.8	78.5	81.8
725	83.7	85.5	84.5	80.5	79.8	83.1
753	84.6	86.7	85.8	82.0	81.1	84.3
781	85.6	87.7	87.0	83.6	82.5	85.8
818	86.6	89.0	88.3	85.6	84.2	87.3
847	87.2	89.7	89.2	87.0	85.5	88.6
875	87.8	90.4	89.9	88.3	86.5	89.5
903	88.3	90.9	90.6	89.6	87.4	90.4
932	88.3	91.1	90.6	90.3	87.7	90.7
969	89.1	92.0	91.7	91.5	88.9	91.8
998	89.7	92.6	92.3	92.5	89.6	92.5
1026	90.2	93.0	92.8	93.2	90.3	93.1
1054	90.7	93.5	93.3	93.9	90.8	93.7
1083	91.0	93.7	93.4	94.3	90.7	93.4
1111	93.1	94.9	95.1	94.7	91.3	93.2
1148	94.2	95.1	95.1	94.6	90.1	92.3
1177	94.5	95.6	95.7	94.9	90.9	92.2
1205	94.7	95.8	95.8	94.9	91.5	92.0

Table 7.4: Model constants and regression parameters as Equation 7.9 was fitted to the measured meal moisture content data.

		Meal moisture content data in		
Parameters	**Figure 7.2**	**Figure 7.8**	**Figure 7.7**	**Figure 7.6**
Flow rate (kg/h)	2.7	7.6	9.6	10.8
Steam Pressure (kPa)	3.4	34.5	34.5	34.5
Revolution (rpm)	840	840	840	840
Statistics		**Figure 7.8**	**Figure 7.7**	**Figure 7.6**
K (kg/hr)		1.3861	0.8855	0.8678
A		1.1432	21.3401	0.4596
R^2		0.69	0.78	0.94
Std Err		0.060	0.029	0.0073
F_{stat}		35.7	48.9	226.4
P%		15.79	5.77	2.71
		Moisture content data in Figure 7.2		
		Location 1	**Location 2**	**Location 3**
K (kg/hr)		0.1430	0.0902	0.1362
A		27.1894	66.5752	313.2361
R^2		0.47	0.41	0.59
Std Err		0.044	0.304	0.030
F_{stat}		12.6	10.4	20.4
P%		20.2	7.8	11.6

(initial moisture content of alfalfa grind in dry basis) and the corresponding meal flow rates in kg/h, respectively. The resultant regression statistics are presented in Table 7.4, and the estimated meal moisture content values are plotted in Figure 7.6, Figure 7.7 and Figure 7.8 as well as in Figure 7.9a, b and c, respectively. The model estimations in Figure 7.9a, b and c resulted from curve-fitting Equation 7.9 to the meal moisture content data at each of the three locations of the top conditioner as shown in Figure 7.2. Curve-

fitting results showed Equation 7.9 described relatively well both the magnitude and shape of meal moisture content vs. time trends as a whole except for Figures 7.8 and 7.9a where the residuals were somewhat higher than in other cases. This is evident from the P% values in Table 7.4. The relatively low R^2 values mainly resulted from the variation in meal moisture data that caused the least squared sum to be in a high magnitude. The relatively large variation in Figures 7.8 and 7.9a could be attributed to the one major factor although not excluding other possible factors, that is, errors in sampling from the pilot scale steam conditioner and in moisture content measurement that could cause the meal moisture content data to scatter.

It was also noticed that Equation 7.9 described better the asymptotic portion of the meal moisture content vs. time relationship in terms of both magnitude and trend, but more often than not underestimated the trend immediately following the onset of steam injection (i.e., the sharp peak), as exemplified in Figure 7.8 and Figure 7.9c.

Application to meal temperature data

Similarly, inverse method was used to verify Equation 7.10 for describing the relation of meal temperature versus time. There existed two distinguished cases: invariant D and E (Equation 7.10) and variable D and E (Equation 7.13 and Equation 7.14). Equation 7.10 was fitted to the meal temperature data as presented in Table 7.2 (see Figure 7.10). The conditions under which the meal temperature data in Table 7.2 were obtained are given in Table 7.5. After inserting the parameters in Table 7.5 into Equation 7.13 and Equation 7.14, Equation 7.13 and Equation 7.14 become

$$D = 41.0869 + 481.5884K\left[1 + \frac{1}{\ln(t)}\right] \tag{7.15}$$

$$E = 1.6435 + 0.6933K\left[1 + \frac{1}{\ln(t)}\right]\left(2 - e^{-0.0006045t}\right) \tag{7.16}$$

Note that in Equations 7.15 and 7.16 the time t is in seconds and K in kg/h.

Table 7.5: Parameters used in the verification of meal temperature model.

m_0	initial moisture content of alfalfa grind (w/w, db)	0.0701
M_{in}	mass flow rate of alfalfa grind at intake (kg/h)	8.2
ρ	Mean bulk density of alfalfa grind (kg/m^3)	240
V	Effective volume of conditioner to hold meal (Conditioner chamber diameter 0.2m, 50% filled)	0.0157
c_d	specific heat capacity of dry matter (kJ/kg.K)	1
T_0	initial temperature of alfalfa grind (°C)	25
c_w	specific heat capacity of water (kJ/kg.K)	4.18
c_s	specific heat capacity of super-heated steam ($kJ.kg^{-1}.K^{-1}$)	2.09
c_p	mean specific heat capacity of alfalfa grind ($kJ.kg^{-1}.K^{-1}$)	1.6
T_s	temperature of super-heated steam (°C)	160
h_{fg}	latent heat of vaporization of water (kJ/kg)	2360

Table 7.6 lists the resultant regression statistics including the constants D, E and K, coefficient of determination (R^2), curve-fitting standard error (Std Err), F statistical value (F_{stat}) and the average relative percentage deviation (P%). Curve-fitting results showed that Equation 7.10 was capable of describing the T-t relationship of the alfalfa meal in the steam conditioner (Table 7.6), equally in both constant D and E case and variable D and E case. As an example of showing the applicability of Equation 7.10 to the experimental data at both cases of invariant and variable D and E, Figure 7.10A and B depicts the model estimated meal temperature in contrast to the experimental data at location 6 as presented in Table 7.2. In Table 7.6, most R^2 values are over 0.99, and most P% values are below 5%. This signifies that Equation 7.10, with D and E either constant or variable with time, could approximate very well the meal temperature trend in the time range involved. However, Equation 7.10 with D and E constant would be recommended due to its simplicity.

7.5 Summary

Heat and mass transfer models were developed in a semi-empirical way in this study to describe the meal temperature and moisture content of alfalfa grind in a steam

A.

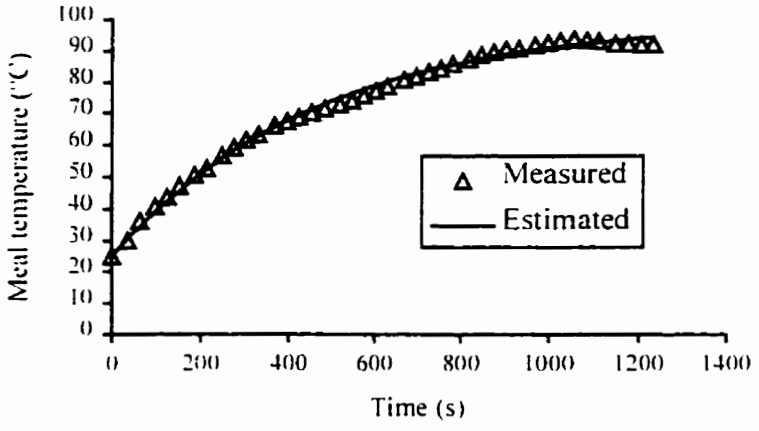

B.

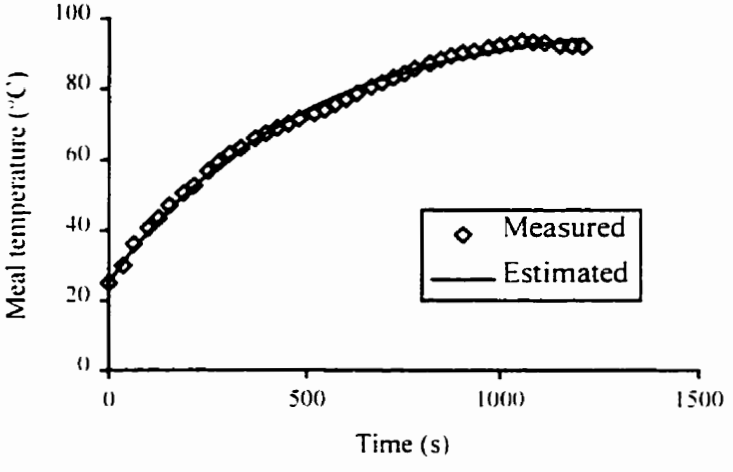

Figure 7.10: Goodness-of-fit of Equation 7.10 to meal temperature data at location 6 of the steam conditioner in the cases of (A) constant D and E and (B) variable D and E.

conditioner. Pilot-scale steam conditioning tests were conducted to collect the meal temperature and moisture content data for verifying the models by means of the inverse method. Regression statistics showed that both the models for meal temperature and moisture content prediction were capable of describing the temperature-time and moisture content-time relationships of alfalfa grind in a steam conditioner.

Table 7.6: Regression statistics as Equation 7.10 is fitted to the meal temperature data.

Location	D, E Status	D or K*	E	R^2	Std Err	F_{stat}	P %
1	Constant	0.3327	0.003689	0.910	4.69	404	5.27
1	Variable	0.2443	0.003158	0.908	4.73	385	5.32
2	Constant	0.2924	0.003079	0.984	2.29	2509	2.75
2	Variable	0.2685	0.002643	0.984	2.32	2396	2.80
3	Constant	0.2331	0.002356	0.996	0.99	1.29	1.63
3	Variable	0.2948	0.001992	0.996	1.27	9379	1.61
4	Constant	0.1360	0.001091	0.996	1.46	9445	1.71
4	Variable	0.5389	0.000766	0.996	1.43	9452	1.76
5	Constant	0.1763	0.001725	0.997	1.03	14524	1.29
5	Variable	0.3246	0.001414	0.998	0.96	16229	1.23
6	Constant	0.2114	0.002119	0.995	1.37	8286	1.72
6	Variable	0.3040	0.001765	0.996	1.28	9254	1.63

*D for constant D and E case and K for variable D and E case.

Chapter 8

CONCLUSIONS

The following conclusions are made based on the experiments and analysis conducted in this research:

1. Physical and morphological characteristics of alfalfa grind

Alfalfa grind was composed of such particles for which the sizes distributed log-normally around a median size of 238 μm at a log-normal standard deviation of 0.65. The 2D projection parameters of alfalfa particles approximately followed a linear relationship with the sieve nominal openings. This information was useful in animal ration, nutrition, and metabolism studies where approximate geometric dimensions of alfalfa particles in a certain size groups can be estimated by the known size of other groups without actually measuring them under a microscope. It was revealed in this study that the traditional BET nitrogen sorption method for surface area measurement of particulate materials was not suitable for alfalfa grind due to its porous nature that resulted in the total area of all exposed surfaces rather than the outer surface of the particles. Because of this, the roundness of alfalfa grind that was calculated from projection parameters obtained by a SEM might be a better criterion to indicate its sphericity.

The results also showed that the bulk density and the solid density of alfalfa grind all varied with moisture content (0.0057 to 0.52 w/w, db) and particle size (150 to 1000 μm) within certain ranges. For a problem that requires analytical solution, the formulas developed in this study to correlate the bulk density and the solid density to moisture content or particle undersize could be readily used. However, for an approximate calculation, the bulk density and the solid density of alfalfa grind could be taken as 229 kg/m^3 (standard deviation 20 kg/m^3) and 1293 kg/m^3 (standard deviation 49 kg/m^3), respectively.

2. Heat transfer characteristics of alfalfa grind

The specific heat capacity of alfalfa grind varied from 0.9 to 2.2 $kJ.kg^{-1}.K^{-1}$ in the temperature ranging from 10°C to 110°C and the moisture content ranging from 0.0054 (w/w, wb) to 0.32 (w/w, wb). This specific heat capacity was in a magnitude similar to those of most grains and oilseeds in the same moisture and temperature ranges. The thermal conductivity of alfalfa grind was much smaller than those of grains and oilseeds in the same moisture and temperature ranges (approximately 1/6 - ½ that of grains and oilseeds). The thermal diffusivity, as well as those of baled alfalfa and alfalfa cubes, was close to that of water.

3. Moisture diffusion characteristics of alfalfa grind

It was found from kinetic measurement that the moisture diffusivity of the whole dehy alfalfa grind was 3.0×10^{-8} m^2/s. The moisture diffusivity of the fractionated dehy alfalfa grind ranged from 3.1×10^{-8} m^2/s to 2.2×10^{-7} m^2/s with a mean of 8.5×10^{-8} m^2/s (standard deviation 6.6×10^{-8} m^2/s) in the particle undersize range of 0.149 mm to 1.4 mm. The moisture diffusivity of the fractionated sun-cured alfalfa grind ranged from 5.2×10^{-8} m^2/s to 4.1×10^{-7} m^2/s with a mean of 1.7×10^{-7} m^2/s (standard deviation 1.5×10^{-7} m^2/s) in the same particle undersize range. There was a significant difference in moisture diffusivity between the dehy and the sun-cured alfalfa grinds (α=0.05).

The "ring stack" diffusion test resulted in a mean diffusivity of 8.6×10^{-8} m^2/s for the whole dehy grind. The moisture diffusivity of the fractionated dehy alfalfa grind ranged from 1.4×10^{-8} m^2/s to 5.9×10^{-8} m^2/s with a mean of 2.8×10^{-8} m^2/s (standard deviation 1.5×10^{-8} m^2/s) in the particle undersize range of 0.149 mm to 1.0 mm.

The moisture diffusivity of alfalfa grind under steam conditioning ranged between 9.2×10^{-10} m^2/s to 8.6×10^{-8} m^2/s in the packing density range of 240 kg/m^3 to 1395

kg/m^3. It decreased dramatically with the increase of packing density following a power relationship.

It was also found that the relationship between the moisture diffusivity of alfalfa grind and particle undersize could be best described by the Gaussian function.

The overall moisture diffusivity of alfalfa grind during steam conditioning was much higher than that of grains and oilseeds (in magnitude of 10^2 higher). For the whole dehy alfalfa grind, the overall moisture diffusivity could be approximately taken as 8.6×10^{-8} m^2/s. For the sun-cured alfalfa grind, the overall moisture diffusivity could be roughly taken as 17.3×10^{-8} m^2/s.

4. Moisture equilibrium characteristics of alfalfa grind

Like many other agricultural products, the isotherms of alfalfa grind exhibited a sigmoid shape. The isotherm relationships could be expressed by the five standard ASAE EMC-ERH equations with the Modified Oswin, the GAB and the Modified Halsey equations better than the other. Therefore, any one of these three equations could be used for describing the isotherms of alfalfa grind in a heat and mass transfer modeling. Alfalfa grind exhibited a medium-sized type C (Kapsalis, 1981) hysteresis. The hysteresis model developed in this study was capable of describing the magnitude and the shape of the hysteresis loops of alfalfa grind.

5. Mathematical modeling for the steam conditioning process

Semi-empirical models were developed in this study to describe the trends of the meal temperature and moisture content of alfalfa grind in a steam conditioner. Meal temperature and moisture content data were collected in pilot-scale steam conditioning tests. The models were verified by these data to be capable of describing the temperature-time and moisture content-time relationships of alfalfa grind in a steam conditioner.

RECOMMENDATONS AND FUTURE WORK

Mathematical models were developed in this study through a semi-empirical method. Numerical method is also desired to solve Equation 7.2 and verify it with the pilot-scale test data.

During specific heat measurement, an interesting phenomenon was, as mentioned in Chapter 2, that specific heat values digressed from its main course at a certain temperatures before they came back again. Any further investigation of this phenomenon can lead to a better understanding of the DSC procedure.

Although the "ring-stack" method was developed in this study for alfalfa grind, it was intended to become a general method for moisture diffusivity measurement of powder-like materials. It is desired to apply this method to other powders to examine its applicability and the places that can be improved to make it a better method for moisture diffusivity measurement of powder materials.

Some work has been done in this research to study the temperature dependency of the constants in the GAB isotherm equation. Verification of the C vs. T relationship with isotherms of alfalfa grind at broader temperatures is desired.

The moisture sorption hysteresis model developed in this study has been proven capable of predicting the magnitude and shape of a number of inorganic, organic, agricultural, food and biological materials. Verification of this model to a broader range of materials is also expected.

REFERENCES

ASAE. 1996a. ASAE Standard D245.5: Moisture Relationships of Plant-Based Agricultural Products. St. Joseph, MI: ASAE.

ASAE. 1996b. ASAE Standard S358.2: Moisture Measurement - Forages. St. Joseph, MI: ASAE.

ASAE. 1996c. ASAE Standards S319.2: Methods of Determining and Expressing Fineness of Feed Materials by Sieving. St. Joseph, MI: ASAE.

ASAE. 1996d. ASAE Standards. D243.3: Thermal Properties of Grain and Grain Products. St. Joseph, MI: ASAE.

Asher, G.B., E.D. Sloan and M.S. Graboski. 1986. A computer-controlled transient needle-probe thermal conductivity instruments for liquids. International Journal of Thermophysics 7:285.

Bartikoski, R. 1962. The effect of steam on pellet durability. In: Cost Reductions Through In-Plant Production Controls. pp42-47. Kansas City, KS: Feed Production School.

Beck, J.V. and K.J. Arnold. 1977. Parameter Estimation in Engineering and Science. New York: John Willey and Sons.

Beck, J.V., K.D. Cole, A. Haji-sheikh and B. Litkouhi. 1992. *Heat Conduction Using Green's Functions*. Washington, DC: Hemisphere Publishing Corp.

Becker, H.A. and H.R. Sallans. 1955. A study of internal moisture movement in the drying of wheat kernel. Cereal Chemistry 32:212-226.

Brunauer, S., P.H. Emmett and E. Teller. 1938. Adsorption of gases in multimolecular layers. Journal of American Chemical Society 60:309-319.

Bruniche-Olsen, H. 1962. Solid-Liquid Extraction. Copenhagen: Nyt Nordisk Forlag, Arnold Busck.

BSI. 1989. BS 1796: Part 1: 1989 - Methods using test sieves of woven wire cloth and perforated metal plate. pp1-16. London: British Standards Institution.

Carslaw, H.S. and J.C. Jaeger. 1959. *Conduction of Heat in Solids*, 2nd Edn. London: Oxford University Press.

Chakrabarti, S.M. and W.H. Johnson. 1972. Specific Heat of flue-cured tobacco by differential scanning calorimetry. Transactions of the ASAE 15(5):928-931.

Chen, C. and R.V. Morey. 1989. Comparison of four EMC/ERH equations. Transactions of the ASAE 32(3):983-990.

Chu, S.T. and A. Hustrulid. 1968. General characteristics of variable diffusivity process and the dynamic equilibrium moisture content. Transactions of the ASAE 11(5):709-710,715.

Chung, D.S. and H.B. Pfost. 1967. Adsorption and desorption of water vapor by cereal grains and their products. Part III: A hypothesis for explaining the hysteresis effect. Transactions of the ASAE 10:556-557.

Cohan, L.H. 1944. Hysteresis and the vapor pressure of concave surfaces. Journal of American Chemical Society 66:98.

Crank, J. 1975. *The Mathematics of Diffusion*. Oxford, England: Clarendon Press.

Dobie, J.B. 1959. Engineering appraisal of hay pelleting. Agricultural Engineering 40(2):76-77,92.

Dutta, S.K., V.K. Nema and R.K Bhardwaj. 1988. Thermal properties of gram. Journal of Agricultural Engineering Research 39:269-275.

Dynes, J.J. and P.M. Huang. 1995. Influence of citrate on selenite sorption-desorption on short-range ordered aluminum hydroxides. In: Environmental Impact of Soil Component Interactions. Metals, Other Inorganics, and Microbial Activities. Vol. 2. (eds.) P.M. Huang, J. Berthelin, J.-M. Bollag, W.B. McGill and A.L. Page. Boca Raton, FL: CRC Press, Inc. pp47-61.

Everett, D.H. 1967. Adsorption hysteresis. In *The Solid-Gas Interface*, ed. E.A. Flood, 1055. New York, NY: Marcel Dekker, Inc.

Fasina, O.O. 1994. Cooling Characteristics of Alfalfa Pellets. Unpublished Ph.D. dissertation, Department of Agricultural, University of Saskatchewan, Saskatoon, SK, Canada.

Geankoplis, C.J. 1983. *Transport Processes and Unit Operations*. Boston: Allyn and Bacon, Inc.

Hill, B. and D.A. Pulkinen. 1988. A study of factors affecting pellet durability and pelleting efficiency in the production of dehydrated alfalfa pellets. A special report. Tisdale, SK: Saskatchewan Dehydrators Association.

Hooper, F.C. and F.R. Lepper. 1950. Transient heat flow apparatus for determination of thermal conductivity. Transactions of ASHVE 56:309-322.

ISO. 1988. ISO 2591-1: 1988. Test Sieving - Part 1: Methods using test sieves of woven wire cloth and perforated metal plate. Geneva: International Organization for Standardization. pp1-19.

ISO. 1990. ISO 9276-1: 1990 Representation of results of particle size analysis - Part 1: Graphical representation. Geneva: International Organization for Standardization.

Jandel Scientific. 1994. TableCurve 2.02 User's Manual. Los Angeles: Jandel Corp.

Jaros, M., S. Cenkowski, D.S. Jayas and S. Pabis. 1992. A method of determination of the diffusion coefficient based on kernel moisture content and its temperature. Drying Technology 10(1):213-222.

Jayas, D.S., S. Cenkoswki, S. Pabis and W.E. Muir. 1991. Review of thin-layer drying and wetting equations. Drying Technology 9(3):551-558.

Jiang, S., J.C. Jofriet adn G.S. Mittal. 1986. Thermal properties of haylage. Transactions of the ASAE 29:601-606.

Kapsalis, J.G. 1981. Moisture sorption hysteresis. In *Water Activity: Influences on Food Quality*, eds. L.B. Rockland and G.F. Stewart, 143-177. New York, NY: Academic Press.

Kapsalis, J.G. 1987. Influence of hysteresis and temperature on moisture sorption isotherms. In *Water Activity: Theory and Applications to Food*, eds. L.B. Rockland and L.R. Beuchat, 173-213. New York, NY: Marcel Dekker, Inc.

Kazarian, E.A. and C.W. Hall. 1965. The thermal properties of grain. Transactions of the ASAE 8(1): 33-37, 40.

Khoshtaghaza, M.H., S. Sokhansanj and R.J. Ford. 1995. Thermal diffusivity and thermal conductivity of alfalfa cube. Canadian Agricultural Engineering 37(4):321-325.

Koch, P. 1969. Specific heat of oven dry spruce, pine wood and bark. Wood Science 1(4): 203-314.

Luginbuhl, J.M., K.R. Pond, J.C. Burns and J.C. Russ. 1989. Eating and ruminating behavior of steers fed Coastal bermudagrass hay at four levels. Journal of Animal Science 67:3410-3418.

Maier, D.E. and J. Gardecki. 1993. Evaluation of pellet conditioning: understanding steam. Feed Management 44(7):15-18.

McBain, J.W. 1935. An explanation of hysteresis in the hydration and dehydration of gels. Journal of American Chemical Society 57:699.

McMillin, C.W. 1969. Specific heat of oven dry loblolly pine wood. Wood Science 2(2):107-111.

Mettler Instrumente AG. 1984. Operating Instructions. TA3000 System. A system for measurement and evaluation of DSC, TMA and TG. 52-55. Switzerland: Mettler Instrumente AG.

Mohsenin, N.N. 1980. *Thermal Properties of Foods and Agricultural Materials*. 83-121. New York, NY: Gordon and Breach.

Murakami, E.G. and M.R. Okos. 1988. Measurement and prediction of thermal properties of foods. In: *Food Properties and Computer-aided Engineering of Food Processing Systems*. eds. P.R. Singh and A.G. Medina. 3. Boston, MA: Kluwer Academic.

Murata, S., A. Tagawa and S. Ishibashi. 1987. The effect of moisture content and temperature on specific heat of cereal grains measured by DSC. Journal of the Japanese Society of Agricultural Machinery 46(6): 547-554.

Neter, J., W. Wasserman and M.H. Kutner. 1985. *Applied Linear Statistical Models*. 289. Homewood, IL: Richard D. Irwin, Inc.

Ott, L.E. and L.W. Hurbut. 1964. Thermal diffusivity of compressed alfalfa hay. ASAE Paper No. 64-817. St. Joseph, MI: American Society of Agricultural Engineers.

Pabis, S. and S.M. Henderson. 1961. Grain drying theory. A critical analysis of the drying curve for shelled maize. Journal of Agricultural Engineering Research 6(4):272-277.

Patil, N.D. 1988. Evaluation of diffusion equation for simulating moisture movement within an individual kernel. Drying Technology 6(1):21-42.

Patil, R. 1995. Kinetics of Dehydration and Quality Changes of Alfalfa. Unpublished Ph.D. dissertation, Department of Agricultural Engineering, University of Saskatchewan, Saskatoon, SK, Canada.

Patil, R. and S. Sokhansanj. 1992. Particle size characterization in alfalfa cubes using machine vision and NIR. ASAE Paper No. 92-6541. St. Joseph, MI: American Society of Agricultural Engineers.

Pfost, H. and V. Headley. 1976. Methods of determining and expressing particle size. In: *Feed Manufacturing Technology*. eds. H.B. Pfost and D. Pickering. 512-517. Arlington, Virginia: American Feed Manufacturers Association, Inc.

Pierce, D.A. and Benner, S.M. 1986. Thermally induced hygroscopic mass transfer in a fibrous medium. International Journal of Heat and Mass Transfer 29:1683-1694.

Polley, S.L., O.P. Synder, and F. Kotnour. 1980. A compilation of thermal properties of foods. Food Technology 34(11):76-80, 82-84, 86-88, 90-92, 94.

Pulkinen, D.A. 1994. 1993 statistical process control study on alfalfa dehydration. Presented in the KSL Quality Management and Processing Technology Seminar sponsored by the KAPT-AL Services, Tisdale, SK, Canada, March 10 and 11, 1994.

Rizvi, S.S.H. and A.L. Benado. 1984. Thermodynamic properties of dehydrated foods. Food Technology 38:83-92.

SAS. 1985. SAS User's Guide: Statistics. 5th Edition. 433-506. Cary, NC: SAS Institute Inc.

Simonson, C.J., Y.-X Tao, and R.W. Besant. 1993. Thermal hysteresis in fibrous insulation. International Journal of Heat and Mass Transfer 36:4433-4441.

Singh, R.P. and D.R. Heldman. 1993. Introduction to Food Engineering. 2nd ed. 140. San Diego, CA: Academic Press, Inc.

Skoch, E.R., K.C. Behnke, C.W. Deyoe and S.F. Binder. 1981. The effect of steam-conditioning rate on the pelleting process. Animal Feed Science and Technology 6:83-90.

Smith, O.B. 1959. Factors in conditioning pellets mash. In: Pelleting and Related Subjects. pp40-50. Kansas City, KS: Feed Production School.

Sokhansanj, S. and H.C. Wood. 1990. Engineering aspects of forage processing for pellets, cubes, chops and dense bales. CSAE Paper No. 90-207. Saskatoon, SK: Canadian Society of Agricultural Engineering.

Sokhansanj, S. L. Tabil, R. Ford and O. Fasina. 1992. Grinding of dried alfalfa chops for pelleting. Presented in the KSL Quality Management and Processing Technology Seminar sponsored by the KAPT-AL Services, Tisdale, SK, Canada, March 1992.

Sokhansanj, S. and W. Yang. 1995a. Revision of ASAE D245.4: Moisture Relationships of Grains. Transactions of the ASAE 39(2):639-642.

Sokhansanj, S. and W. Yang. 1995b. Enhancing ASAE D245.4: Moisture Relationships of Grains. ASAE Paper No. 956103. St. Joseph, MI: American Society of Agricultural Engineers.

Sokhansanj, S. and W. Yang. 1996. Revision of ASAE Standard: S319.2: Method of Determining and Expressing Fineness of Feed Materials by Sieving. ASAE Paper No. 966002. St. Joseph, MI: American Society of Agricultural Engineers.

Suter , D.A., K.K. Agrawal and B.L. Clary. 1975. Thermal properties of peanut pods, hulls and kernels. Transactions of the ASAE 18:370-375.

Sweat, V.E. 1986. Thermal properties of foods. In: *Engineering Properties of Foods*. eds. M.A. Rao and S.S.H. Rizvi. 49. New York, NY: Marcel Dekker, Inc.

Tabil, L.G., Jr. 1996. Binding and Pelleting Characteristics of Alfalfa. Unpublished Ph.D. dissertation, Department of Agricultural Engineering, University of Saskatchewan, Saskatoon, SK, Canada.

Tabil, L.G., Jr. and S. Sokhansanj. 1992. Pelleting of animal feeds: a review on the factors affecting physical quality. In: Research in Feed Processing and Storage. Ed. S. Sokhansanj. Saskatoon, SK: Department of Agricultural and Bioresource Engineering, University of Saskatchewan.

Tabil, L.G., Jr. and S. Sokhansanj. 1993. Project on effect of process and material parameters on pellet durability. Saskatoon, SK: Department of Agricultural and Bioresource Engineering, University of Saskatchewan.

Tang, J., S. Sokhansanj, S. Yannacopoulos and S.O. Kasap. 1991. Specific heat capacity of lentil seeds by differential scanning calorimetry. Transactions of the ASAE 34(2):517-522.

Tao, Y.-X., R.W. Besant, and K.S. Rezkallah. 1992a. The transient thermal response of a glass-fiber insulation slab with hygroscopicity effects. International Journal of Heat and Mass Transfer 35:1155-1167.

Tao, Y.-X., R.W. Besant, and C. J. Simonson. 1992b. Measurement of the heat of adsorption for a typical fibrous insulation. ASHRAE Transactions 98:495-501.

Toledo, R.T. 1991. *Fundamentals of Food Process Engineering*. 134-136. New York, NY: Van Nostrand Reinhold.

Troelsen, J.E. and J.B. Campbell. 1968. Voluntary consumption of forage by sheep and its relation to the size and shape of particles in the digestive tract. Animal Production 10:289-296.

Van der Held, E.F.M. and F.G. Van Drunen. 1949. A method of measuring the thermal conductivity of liquids. Physica 15:865.

Violante, A. and P.M. Huang. 1992. Effect of tartaric acid and pH on the nature and physicochemical properties of short-range ordered aluminum precipitation products. Clays and Clay Minerals 40(4):462-469.

Wang, J. and K. Hayakawa. 1993. Maximum slope method for evaluating thermal conductivity probe data. Journal of Food Science 58(6):1340-1345.

Winowiski, T. 1985. Optimizing pelleting temperature. Feed Management 36(7):28-35.

Woodcock, C.R. and J.S. Mason. 1986. Bulk Solids Handling. An Introduction to the Practice and Technology. New York: Chapman and Hall. p5, p26.

Woodford, S.T. and M.R. Murphy. 1988. Dietary alteration of particle breakdown and passage from the rumen in lactating dairy cattle. Journal of Dairy Science 71:687-696.

Yang, W. and S. Cenkowski. 1993. Enhancement of the Halsey equation for canola isotherms. Canadian Agricultural Engineering 37(3):169-182.

Yang, W., S. Sokhansanj, S. Cenkowski, J. Tang and Y. Wu. 1995a. A general model for sorption hysteresis in food materials. Journal of Food Engineering (In press).

Yang, W., S. Sokhansanj, L. Tabil, Jr., J. Tang and S. Yannacopoulos. 1995b. Specific heat measurement for borage seeds by differential scanning calorimetry. Journal of Food Processing and Preservation (In press).

Yang, W., S. Sokhansanj, Y. Wu and J. Tang. 1996a. Quantification of sorption hysteresis loops. CSAE Paper No. 96-312. Saskatoon, SK: Canadian Society of Agricultural Engineering.

Yang, W., S. Sokhansanj, L. Tabil, Jr. and J. Tang. 1996b. Specific heat capacity and thermal conductivity of borage seeds by DSC and maximum slope methods. ASAE Paper No. MANSASK 96-110. St. Joseph, MI: ASAE.

Young, J.H. and G.L. Nelson. 1967. Theory of hysteresis between sorption and desorption isotherms in biological materials. Transactions of the ASAE 10:260-263.

Zsigmondy, R. 1911. Structure of gelatious silicic acid. Theory of dehydration. Z. Anorg. Chem. 71:356.

Appendix A

Principle of the helium-operated pyconometer for solid density measurement

In principle, the pycnometer consists of one reference cell of precisely known volume and one sample cell connected to each other. It determines the solid density of alfalfa grind by measuring the pressure difference when a known quantity of helium under pressure is allowed to flow from the reference volume into the sample cell containing the alfalfa grind. At the beginning, the system is at ambient pressure and the gas law writes as follows for the helium in the sample cell:

$$P_a(V_c-V_p) = n_aRT_a \qquad \text{(i)}$$

where P_a is ambient pressure, V_c the sample cell volume, V_p the sample volume, n_a the number of moles of helium occupying the head-space of the sample cell, R the universal gas constant, and T_a the ambient temperature. When the reference cell is disconnected from the sample cell and pressurized to P_1 from P_a, the state of the reference volume (V_R) can be expressed as

$$P_1V_R = n_1RT_a \qquad \text{(ii)}$$

where n_1 is the number of moles of helium in the reference volume V_R.
when the reference cell is connected to the sample cell, the pressure drops to P_2 as given by

$$P_2(V_c-V_p+V_R) = n_aRT_a + n_1RT_a \qquad \text{(iii)}$$

Substituting Equations (i) and (ii) into Equation (iii) and rearranging gives

$$V_c - V_p = (P_1 - P_2)/(P_2 - P_a) * V_R \quad \text{(iv)}$$

If all the pressures are read relative to P_a, i.e., P_a is made to read zero on the digital meter, Equation (iv) becomes

$$V_p = V_c - V_R[(P_1/P_2) - 1] \quad \text{(v)}$$

The solid density of alfalfa grind can be found by knowing the mass of the alfalfa grind in the sample cell and V_p.

Appendix B

Experimental data of the specific heat capacity of alfalfa grind by differential scanning calorimetry

Temperature	Moisture content (w/w, wb)											
	0.32		0.20		0.088			0.065			0.0054	
(°C)	#1	#2	#1	#2	#1	#2	#3	#1	#2	#3	#1	#2
10	1.71	1.82	1.49	1.42	0.95	1.05	1.10	1.06	0.86	0.89	0.97	1.00
15	1.73	1.82	1.62	1.47	1.02	1.14	1.12	1.17	0.96	0.94	1.05	1.08
20	1.78	1.83	1.64	1.59	1.08	1.15	1.21	1.21	1.01	1.00	1.14	1.14
25	1.86	1.96	1.73	1.65	1.17	1.29	1.29	1.27	1.06	1.06	1.16	1.16
30	1.94	1.95	1.79	1.68	1.23	1.33	1.32	1.33	1.08	1.12	1.15	1.16
35	2.00	2.02	1.82	1.67	1.25	1.35	1.40	1.38	1.18	1.15	1.22	1.24
40	2.02	2.01	1.87	1.76	1.35	1.44	1.43	1.40	1.24	1.20	1.25	1.26
45	2.05	2.07	1.86	1.83	1.41	1.50	1.49	1.47	1.24	1.24	1.31	1.28
50	2.04	2.11	1.92	1.89	1.48	1.51	1.52	1.50	1.30	1.33	1.30	1.31
55	2.05	2.07	1.95	1.87	1.50	1.56	1.70	1.57	1.39	1.37	1.36	1.37
60	2.09	2.09	1.93	1.93	1.55	1.62	1.72	1.72	1.49	1.47	1.33	1.40
65	2.09	2.16	1.98	1.90	1.65	1.74	1.73	1.74	1.57	1.62	1.35	1.39
70	2.08	2.15	1.98	1.95	1.74	1.78	1.84	1.81	1.63	1.69	1.35	1.40
75	2.14	2.23	2.00	1.94	1.83	1.89	1.88	1.90	1.75	1.73	1.39	1.46
80	2.13	2.23	2.01	1.93	1.84	1.90	1.93	2.02	1.84	1.84	1.31	1.43
85	2.15	2.22	2.03	1.98	1.82	1.84	1.88	2.02	1.82	1.82	1.41	1.46
90	2.16	2.20	2.01	1.99	1.82	1.86	1.90	2.06	1.85	1.81	1.41	1.44
95	2.16	2.18	2.01	1.97	1.84	1.86	1.92	2.02	1.86	1.81	1.44	1.49
100	2.14	2.17	2.00	1.91	1.84	1.81	1.89	2.03	1.83	1.78	1.41	1.46
105	2.15	2.13	1.98	1.92	1.89	1.85	1.91	2.03	1.84	1.83	1.47	1.46
110	2.11	2.07	1.94	1.95	1.93	1.80	1.91	2.05	1.85	1.82	1.47	1.51

Appendix C-1

Kinetic data for the whole dehy alfalfa grind

Test 1 (4.999 g)		Test 2 (5.036 g)		Test 3 (5.036 g)		Test 4 (5.003 g)		Test 5 (5.016 g)	
Time (s)	Gain (g)	Time (s)	Gain (g)	Time (s)	Gain (g)	Time (s)	Gain (g)	Time (s)	Gain (g)
2.13	0.198	1.53	0.146	1.55	0.164	1.13	0.163	1.13	0.154
6.56	0.319	4.61	0.255	5.55	0.261	5.36	0.28	5.17	0.291
10.76	0.437	10.74	0.369	10.52	0.38	10.14	0.375	11.41	0.401
20.5	0.553	21.21	0.491	19.54	0.526	20.49	0.486	20.41	0.498
30.44	0.626	36.17	0.615	30.15	0.612	30.12	0.573	30.45	0.569
40.36	0.782	50.3	0.751	40.17	0.737	40.2	0.723	40.34	0.773
51.48	0.873	70.58	0.891	50.17	0.842	50.09	0.772	50.29	0.805
61.16	1.029	90.47	1.065	60.09	0.946	59.92	0.918	60.18	0.937
80.6	1.123	110.39	1.208	80.22	1.029	80.17	1.046	80.55	1.078
100.17	1.284	140.43	1.369	101.5	1.231	120	1.32	100.17	1.261
120.18	1.406	160.28	1.588	120.5	1.336	140.35	1.436	121.21	1.397
150.38	1.619	180.08	1.751	140.32	1.545	180.2	1.633	150.04	1.566
180.26	1.774	210.13	1.941	160.23	1.654	210.15	1.884	180.33	1.721
210.85	2.021	240.44	2.145	180.23	1.819	239.99	2.064	210.24	1.951
240.53	2.235	270.04	2.315	211.42	2.025	270.98	2.281	240.12	2.167
270.12	2.388	300.36	2.467	240.16	2.228	299.8	2.499	270.11	2.345
300.48	2.593	330.31	2.701	269.94	2.357	330.06	2.649	301.28	2.538
330.23	2.721	360.12	2.908	300.06	2.621	360.08	2.784	335.71	2.777
360.13	2.917	390.11	3.064	330.38	2.736	389.85	3.045	360.18	2.975
391.13	3.114	420.28	3.323	360.24	2.95	420.04	3.202	390.18	3.137
420.44	3.334	450.38	3.538	389.91	3.229	450.23	3.427	420.03	3.296
450.37	3.6	480.14	3.761	421.31	3.386	480.02	3.589	450	3.539
480.32	3.76	510.84	3.955	450.19	3.617	509.94	3.799	480.34	3.737
511.64	3.936	540.23	4.159	480.22	3.779	540.12	4.018	510.15	3.983
543.22	4.159	570.35	4.335	510.28	4.031	569.91	4.249	540.1	4.163
557.52	4.333	601.43	4.553	539.97	4.199	600.17	4.399	570.1	4.394
				570.14	4.374				
				601.94	4.666				

Note: Initial moisture content 0.070 (w/w, db)

Appendix C-2

Kinetic data for the fractionated dehy alfalfa grind

Note: Initial moisture content 0.070 (w/w, db)

Sieve #18-#20		Sieve #20-#30		Sieve #30-#40		Sieve #40-#50		Sieve #50-#70		Sieve #70-#100		Sieve #100 & up	
Time (s)	Mass (g)	Time (s)	Mass (g)	Time (s)	Mass (g)	Time (s)	Mass (g)	Time (s)	Mass (g)	Time (s)	Mass (g)	Time (s)	Mass (g)
Test 1 (5.027 g)		Test 1 (5.012 g)		Test 1 (5.018 g)		Test 1 (5.023 g)		Test 1 (5.037 g)		Test 1 (5.043 g)		Test 1 (5.031 g)	
1.48	0.199	1.69	0.253	1.11	0.224	1.26	0.193	1.29	0.155	1.53	0.201	1.59	0.153
6.52	0.346	5.81	0.352	5.18	0.328	5.23	0.276	5.7	0.308	5.81	0.314	5.56	0.293
11.68	0.445	11.73	0.428	10.44	0.429	11.18	0.436	10.5	0.401	13.58	0.355	11.17	0.375
20.31	0.535	20.36	0.522	20.11	0.513	20.27	0.501	20.26	0.458	21.37	0.521	20.21	0.501
30.33	0.642	33.39	0.647	40.16	0.687	30.1	0.615	30.91	0.598	29.92	0.623	30.18	0.605
41.61	0.761	43.07	0.76	50.35	0.762	40.36	0.698	40.25	0.697	40.68	0.72	40.22	0.688
51.41	0.827	52.82	0.847	60.6	0.867	51.01	0.823	51.84	0.824	60.21	0.899	51.05	0.759
60.34	0.928	61.03	0.953	80.36	1.016	61.61	0.957	61.03	0.902	80.26	1.029	61.54	0.887
81.23	1.066	80.3	1.067	101.31	1.129	80.32	1.093	80.32	1.089	100.04	1.128	80.25	0.965
100.33	1.21	99.98	1.208	120.67	1.234	100.38	1.239	100.36	1.211	124.68	1.298	107.06	1.19
120.26	1.336	119.96	1.319	155.16	1.467	120.33	1.371	120.18	1.365	150.2	1.481	120.6	1.275
150.13	1.535	150.17	1.509	180.7	1.633	150.11	1.608	150.02	1.543	180.3	1.661	150.37	1.403
180.34	1.681	180.16	1.668	210.21	1.78	180.36	1.77	180.85	1.709	210.19	1.82	180.59	1.602
210.24	1.859	210.19	1.837	240.2	1.984	210.08	1.967	215.45	1.888	240.17	1.971	210.12	1.771
240.08	2.007	241.09	2.039	270.37	2.122	240.44	2.121	240.22	2.09	271.04	2.192	240.43	1.945
271.01	2.211	270.19	2.194	300.28	2.294	270.05	2.337	290.22	2.303	300.16	2.408	272.28	2.093
308.47	2.394	300.33	2.38	330.5	2.448	299.45	2.518	329.57	2.535	330.7	2.58	302.21	2.249
360.84	2.602	330.53	2.539	360.24	2.608	338.33	2.71	365.21	2.771	360.12	2.766	331.49	2.418
390.5	2.82	360.83	2.705	390.36	2.777	362.28	2.879	394.49	2.99	391.5	2.945	372.47	2.601
420.99	2.971	390.88	2.909	420.16	2.921	390.18	3.14	430.8	3.14	421.02	3.119	394.57	2.814
450.83	3.135	427.03	3.058	451.41	3.11	426.25	3.291	451.97	3.363	450.81	3.315	423.45	2.978
480.22	3.295	459.55	3.244	480.3	3.295	453.82	3.523	483.28	3.505	484.03	3.452	453.56	3.159
510.37	3.469	482.84	3.38	511.21	3.46	480.55	3.688	511.42	3.705	522.57	3.72	481.09	3.325
543.21	3.632	510.59	3.587	542.09	3.639	513.56	3.901	541.34	3.892	570.27	3.98	511.11	3.491
571.26	3.852	540.18	3.726	571.82	3.836	540.07	4.125	579.56	4.127	601.77	4.165	540.78	3.643
601.96	4.016	570.72	3.896	600.19	3.96	581.31	4.321	601.33	4.276			570.38	3.83
		605.15	4.111			601.47	4.492					601.17	4.033
Test 2 (5.022 g)		Test 2 (5.039 g)		Test 2 (5.022 g)		Test 2 (5.043 g)		Test 2 (5.031 g)		Test 2 (5.037 g)		Test 2 (5.036 g)	
1.55	0.171	1.35	0.215	1.38	0.277	1.53	0.22	1.42	0.187	1.57	0.209	1.45	0.144
5.41	0.250	5.59	0.324	5.42	0.334	5.31	0.376	6.02	0.342	5.4	0.317	5.87	0.265
10.28	0.332	10.3	0.377	10.55	0.385	13.08	0.472	10.85	0.396	10.5	0.407	12.59	0.323
20.15	0.471	20.18	0.516	20.38	0.476	21.68	0.564	20.11	0.490	20.4	0.513	22.45	0.426
30.18	0.592	30.71	0.619	30.25	0.560	31.7	0.662	30.28	0.585	40.32	0.658	29.62	0.513
41.05	0.710	40.1	0.701	40.97	0.646	40.35	0.779	40.97	0.679	60.77	0.839	40.58	0.634
50.69	0.806	50.04	0.799	50.36	0.718	50.4	0.869	50.15	0.756	83.43	0.996	60.55	0.830
61.54	0.907	61.11	0.897	60.85	0.796	63.02	1.024	60.32	0.839	110.8	1.132	80.12	1.002
80.55	1.071	80.09	0.993	80.47	0.936	85.08	1.152	80.46	0.996	140.31	1.336	101.14	1.171
100.49	1.229	100.16	1.157	100.21	1.072	101.32	1.308	99.58	1.139	176.96	1.51	120.69	1.318
120.91	1.380	121.92	1.335	120.09	1.204	120.31	1.46	120.47	1.291	221.08	1.709	150.3	1.525
150.36	1.583	161.06	1.582	150.38	1.400	150.5	1.618	150.02	1.497	246.77	1.913	180.37	1.720
180.66	1.777	182.63	1.733	181.22	1.593	181.62	1.861	180.33	1.702	274.7	2.081	210.19	1.903
211.37	1.962	210.16	1.865	210.17	1.770	209.99	2.025	210.45	1.899	301.17	2.267	240.22	2.077
240.56	2.129	240.23	2.028	240.33	1.950	240.2	2.218	240.59	2.092	337.67	2.432	270.91	2.248
270.43	2.292	271.21	2.199	270.2	2.126	270.38	2.355	270.62	2.280	365.4	2.627	300.29	2.404
300.09	2.448	301.38	2.321	300.82	2.303	302.68	2.618	300.44	2.463	390.42	2.802	330.07	2.557
330.78	2.603	330.16	2.551	330.54	2.473	330.75	2.798	330.59	2.646	420.67	3.015	360.52	2.709
372.44	2.806	360.43	2.716	371.29	2.702	360.25	3.021	370.01	2.880	450.2	3.178	390.44	2.853
390.16	2.889	390.26	2.911	400.59	2.865	390.07	3.188	400.61	3.058	480.6	3.319	423.52	3.007
420.38	3.028	424.1	3.018	423.28	2.990	420.44	3.388	443.25	3.303	510.47	3.538	450.09	3.128
450.69	3.164	450.28	3.209	450.16	3.137	491.17	3.658	480.5	3.514	540.2	3.716	480.66	3.264
480.11	3.293	492.7	3.462	480.15	3.300	510.42	3.893	510.12	3.680	570.51	3.843	510.47	3.393
510.23	3.422	540.55	3.693	510.03	3.460	555.04	4.13	540.37	3.848	603.96	4.139	554.15	3.577
540.87	3.550	570.19	3.847	540.78	3.624	602.13	4.353	570.66	4.014			600.07	3.765
570.38	3.670	600.59	4.063	570.66	3.782			600.08	4.174				
600.92	3.793			600.64	3.940								

Appendix C-3 (Part 1)

Kinetic data for the fractionated sun-cured alfalfa grind

Note: Initial moisture content 0.070 (w/w, db)

Sieve #14-#18		Sieve #18-#20		Sieve #20-#30		Sieve #30-#40		Sieve #40-#50		Sieve #50-#70		Sieve #70-#100		Sieve #100 & up	
Time (s)	Mass (g)	Time (s)	Mass (g)	Time (s)	Mass (g)	Time (s)	Mass (g)	Time (s)	Mass (g)	Time (s)	Mass (g)	Time (s)	Mass (g)	Time (s)	Mass (g)
Test 1 (5.022 g)		Test 1 (5.023 g)		Test 1 (5.045 g)		Test 1 (5.047 g)		Test 1 (5.035 g)		Test 1 (5.028 g)		Test 1 (5.047 g)		Test 1 (5.053 g)	
1.49	0.223	1.45	0.244	1.57	0.226	1.55	0.262	1.62	0.236	1.27	0.2	1.52	0.176	1.38	0.162
5.29	0.335	5.95	0.345	5.27	0.345	6.01	0.358	5.22	0.336	5.58	0.314	5.53	0.291	5.16	0.266
10.5	0.416	11.88	0.443	10.43	0.433	20.1	0.547	10.44	0.443	11.19	0.419	10.45	0.388	10.3	0.352
20.22	0.543	20.36	0.592	20.31	0.576	30.11	0.647	22.22	0.565	20.47	0.554	20.49	0.496	28.22	0.489
30.41	0.645	30.12	0.687	30.48	0.707	40.07	0.804	31.41	0.703	30.33	0.649	30.34	0.601	40.35	0.623
40.39	0.789	40.32	0.732	41.04	0.743	50.78	0.932	41.75	0.803	40.45	0.728	40.39	0.698	60.29	0.699
50.26	0.884	49.97	0.909	50.14	0.916	60.29	1.035	50.14	0.893	50.36	0.847	50.25	0.813	80.34	0.841
60.29	1.004	60.52	1.008	60.25	0.943	80.21	1.202	61.11	1.023	60.8	0.953	60.42	0.92	100.64	0.997
80.06	1.143	80.3	1.198	80.64	1.093	94.67	1.3	81.43	1.109	80.59	1.064	80.22	1.057	120.18	1.103
100.46	1.263	100.43	1.353	102.54	1.319	110.35	1.465	100.27	1.27	100.45	1.236	100.51	1.13	150.52	1.251
120.52	1.446	121.14	1.499	127.3	1.501	141.19	1.645	120.17	1.341	120.74	1.343	120.25	1.324	180.24	1.395
150.62	1.658	151.17	1.689	150.41	1.615	180.34	1.913	150.31	1.623	150.17	1.528	153.8	1.466	220.17	1.571
180.3	1.798	199.53	1.932	180.05	1.837	210.39	2.073	180.17	1.794	181.3	1.71	180.36	1.657	260.28	1.789
210.39	1.973	240.27	2.104	210.56	2.097	240.48	2.202	210.07	1.953	210.42	1.854	211.07	1.812	320.51	2.02
240.2	2.16	270.41	2.318	240.22	2.241	270.51	2.478	240.55	2.171	240.27	2.043	240.5	2.003	360.27	2.204
270.37	2.361	300.31	2.6	270.28	2.484	301.5	2.644	272.4	2.335	271.39	2.206	270.57	2.153	420.29	2.48
300.05	2.583	330.46	2.763	300.35	2.6	330.23	2.856	303.41	2.52	305.11	2.406	300.04	2.324	480.43	2.721
330.48	2.754	361.01	2.94	335.32	2.853	360.26	3.023	333.45	2.713	330.4	2.528	331.59	2.473	543.4	2.977
362.01	2.964	390.7	3.143	360.66	2.945	390.21	3.182	361.94	2.892	365.52	2.762	369.76	2.638	600.32	3.264
390.19	3.152	420.68	3.357	390.42	3.257	421.24	3.448	390.24	3.095	395.91	2.93	397.39	2.875		
420.15	3.308	450.24	3.489	420.22	3.466	451.37	3.615	426.57	3.278	420.51	3.11	421.63	2.996		
450.28	3.521	480.24	3.661	451.02	3.651	480.18	3.824	450.91	3.447	450.29	3.253	457.38	3.202		
480.23	3.64	510.98	3.864	480.01	3.766	510.27	4.031	480.2	3.648	481.95	3.43	484.57	3.321		
512.81	3.783	541.91	4.13	510.49	4.015	540.83	4.281	511.16	3.813	511.97	3.624	540.11	3.634		
550.66	4.108	570.69	4.281	540	4.225	570.6	4.452	542.71	3.953	549.45	3.773	600.99	3.884		
601.1	4.362	601.49	4.43	570.56	4.308	600.16	4.581	571.42	4.199	572.43	3.991				
				600.96	4.691			605.88	4.397	600.57	4.181				
										631	4.355				

Appendix C-3 (Part 2)

Kinetic data for the fractionated sun-cured alfalfa grind

Note: Initial moisture content 0.070 (w/w, db)

Sieve #14-#18		Sieve #18-#20		Sieve #20-#30		Sieve #30-#40		Sieve #40-#50		Sieve #50-#70		Sieve #70-#100		Sieve #100 & up	
Time (s)	Mass (g)	Time (s)	Mass (g)	Time (s)	Mass (g)	Time (s)	Mass (g)	Time (s)	Mass (g)	Time (s)	Mass (g)	Time (s)	Mass (g)	Time (s)	Mass (g)
Test 2 (5.047 g)		Test 2 (5.019 g)		Test 2 (5.034 g)		Test 2 (5.041 g)		Test 2 (5.050 g)		Test 2 (5.049 g)		Test 2 (5.035 g)		Test 2 (5.044 g)	
1.59	0.234	1.34	0.279	1.44	0.228	1.37	0.203	1.84	0.239	1.59	0.258	1.32	0.176	1.44	0.220
5.22	0.344	5.11	0.395	5.68	0.339	5.14	0.318	5.5	0.359	5.01	0.301	5.33	0.291	5.2	0.271
10.29	0.427	11.19	0.469	10.3	0.374	10.31	0.445	10.26	0.458	10.44	0.413	10.45	0.388	10.51	0.329
20.43	0.537	20.47	0.570	20.28	0.563	27.55	0.589	20.35	0.561	20.38	0.529	20.5	0.496	20.69	0.422
30.85	0.669	31.02	0.674	30.17	0.762	40.39	0.742	30.92	0.698	31.28	0.626	30.61	0.601	31.42	0.509
40.9	0.74	40.45	0.761	50.45	0.849	61.28	0.990	41	0.833	40.59	0.704	40.37	0.698	40.69	0.579
50.07	0.865	50.36	0.849	70.16	1.002	80.69	1.187	50.49	0.942	51.3	0.790	50.98	0.813	50.21	0.646
62.18	0.932	60.95	0.940	90.4	1.228	100.64	1.372	60.35	1.001	60.62	0.863	60.37	0.92	60.98	0.719
80.43	1.124	80.59	1.101	120.59	1.405	120.88	1.547	90.3	1.213	81.06	1.016	80.32	1.057	81.29	0.848
100.36	1.298	103.42	1.279	150.92	1.601	151.47	1.793	121.39	1.386	100.55	1.156	100.24	1.13	100.33	0.963
120.21	1.418	120.74	1.409	180.27	1.817	183.99	2.036	151.35	1.576	120.03	1.292	120.12	1.324	120.39	1.078
151.07	1.617	153.16	1.645	214.04	1.986	218.36	2.276	180.19	1.803	155.89	1.533	155.82	1.466	151.87	1.249
180.77	1.798	185.09	1.867	240.21	2.132	260.54	2.553	221.34	2.029	180.49	1.693	182.02	1.657	180.29	1.379
210.41	1.986	210.42	2.039	270.13	2.306	320.51	2.920	270.35	2.268	210.63	1.884	221.28	1.812	210.63	1.549
240.07	2.157	239.33	2.230	300.09	2.561	361.55	3.156	300.35	2.456	241.61	2.076	250.93	2.003	240.55	1.693
270.26	2.363	271.39	2.437	350.2	2.772	420.39	3.478	330.24	2.647	270.68	2.253	299.98	2.153	270.91	1.836
300.64	2.553	300.85	2.624	390.19	3.032	480.28	3.788	360.25	2.834	300.59	2.431	330.25	2.324	302.47	1.980
334.55	2.724	330.4	2.807	420.25	3.249	543.11	4.099	390.54	3.028	330.93	2.609	360.35	2.473	330.53	2.105
360.21	2.824	360.28	2.990	450.78	3.334	600.57	4.371	420.36	3.207	360.78	2.782	390.22	2.638	360.43	2.235
390.42	3.089	395.91	3.204	480.23	3.547			450.52	3.336	390.54	2.952	420.5	2.875	390.17	2.362
420.33	3.238	421.98	3.359	510.18	3.788			480.56	3.622	420.11	3.118	450.22	2.996	420.28	2.489
450.25	3.398	455.21	3.553	540.2	4.063			510.36	3.817	451.39	3.292	494.52	3.202	450.08	2.612
480.14	3.551	480.77	3.701	570.22	4.197			541.21	3.974	480.09	3.450	551.77	3.321	480.96	2.737
510.38	3.764	507.12	3.852	600.04	4.417			570.59	4.177	510.24	3.615	600.45	3.634	510.77	2.856
540.25	3.911	550.59	4.097					605.83	4.377	540.38	3.778			550.64	3.013
570.41	4.098	580.62	4.265							570.07	3.936			600.95	3.207
616.5	4.387	600.57	4.375							601.49	4.103				

Appendix D

Moisture content of the whole alfalfa grind in the rings

Test #1 Time: 14520 s		Test #2 Time: 18360 s		Test #3 Time: 35340 s	
X (mm)	M.C. (w/w, db)	X (mm)	M.C. (w/w, db)	X (mm)	M.C. (w/w, db)
7.5	0.285	7.5	0.256	7.5	0.279
22.5	0.176	22.5	0.174	22.5	0.221
37.5	0.163	37.5	0.139	37.5	0.175
52.5	0.125	52.5	0.117	52.5	0.147
67.5	0.106	67.5	0.104	67.5	0.124
82.5	0.088	82.5	0.096	82.5	0.114
97.5	0.081	97.5	0.093	97.5	0.109
112.5	0.081	112.5	0.086	112.5	0.096
127.5	0.074	127.5	0.083	127.5	0.093
142.5	0.073	142.5	0.082	142.5	0.083
157.5	0.071			157.5	0.075
172.5	0.071				

Note: X - the mid-point location of rings.

M.C. - Average moisture content of alfalfa grind in each ring.

Appendix E

Moisture content of the fractionated dehy alfalfa grind in the rings

Sieve #18-#20		Sieve #20-#30		Sieve #30-#40		Sieve #40-#50		Sieve #50-#70		Sieve #70-#100		Sieve #100 & up	
X (mm)	M.C.	X (mm)	M.C.	X (mm)	M.C.	X (mm)	M.C.	X (mm)	M.C.	X (mm)	M.C.	X (mm)	M.C.
7.5	0.429	7.5	0.469	7.5	0.475	7.5	0.427	7.5	0.368	7.5	0.410	7.5	0.527
22.5	0.199	22.5	0.248	22.5	0.224	22.5	0.180	22.5	0.180	22.5	0.191	22.5	0.260
37.5	0.159	37.5	0.196	37.5	0.169	37.5	0.143	37.5	0.135	37.5	0.144	37.5	0.200
52.5	0.136	52.5	0.170	52.5	0.141	52.5	0.119	52.5	0.114	52.5	0.123	52.5	0.154
67.5	0.121	67.5	0.149	67.5	0.130	67.5	0.105	67.5	0.106	67.5	0.097	67.5	0.150
82.5	0.100	82.5	0.134	82.5	0.115	82.5	0.097	82.5	0.093	82.5	0.092	82.5	0.127
97.5	0.092	97.5	0.122	97.5	0.098	97.5	0.108	97.5	0.086	97.5	0.173	97.5	0.128
112.5	0.098	112.5	0.113	112.5	0.092	112.5	0.084	112.5	0.084	112.5	0.073	112.5	0.105
127.5	0.086	127.5	0.109	127.5	0.070	127.5	0.073	127.5	0.074	127.5	0.067	127.5	0.097
142.5	0.085	142.5	0.102	142.5	0.077	142.5	0.073	142.5	0.070	142.5	0.068	142.5	0.092
						157.5	0.069	157.5	0.073	157.5	0.077	157.5	0.083
								172.5	0.065				

Note: X - the mid-point location of rings; M.C. - Mean moisture content of alfalfa grind in a ring in w/w, db; Two periods of exposure time were involved: 7.6107 h and 8.5605 h.

Appendix F

Moisture content of the dehy alfalfa grind in the rings at four different packing densities

ρ = 471.1 kg/m^3		ρ = 663.5 kg/m^3		ρ = 1163.5 kg/m^3		ρ = 1396.4 kg/m^3	
X (mm)	M.C.	X (mm)	M.C.	X (mm)	M.C.	X (mm)	M.C.
7.5	0.503	7.5	0.338	7.5	0.475	7.5	0.349
22.5	0.135	22.5	0.096	22.5	0.224	22.5	0.110
37.5	0.093	37.5	0.079	37.5	0.169	37.5	0.098
52.5	0.081	52.5	0.075	52.5	0.141	52.5	0.095
67.5	0.075	67.5	0.069	67.5	0.130	67.5	0.097
82.5	0.071	82.5	0.074	82.5	0.115	82.5	0.096
97.5	0.068	97.5	0.074	97.5	0.098	97.5	0.096
112.5	0.066	112.5	0.080	112.5	0.092	112.5	0.096
127.5	0.065	127.5	0.084	127.5	0.070	127.5	0.096
142.5	0.065	142.5	0.088	142.5	0.077		
157.5	0.063	157.5	0.084				

Note: X - the mid-point location of rings; M.C. - Mean moisture content in a ring (w/w, db); ρ - packing density of alfalfa grind.
The exposure time were 8.8647 h, 9.3433 h, 11.0964 h and 9.1138 h, respectively.

Appendix G-1

Hysteresis model parameters and statistics as Equation 6.29 applied to food products

Isotherm Equation	R^2	S.D.	C.V.%	RUN	A	B	C	D	E
I. Hysteresis loop peaked in the monolayer sorption area									
1. Air-dried apple (Wolf et al., 1972), data points: 13									
Kuhn	0.991	0.225	3.53	4	3.3318	0.8029	-5.6859	0.4245	
Smith	0.988	0.249	4.01	5	5.0166	0.8548	41.1403		
Halsey	0.986	0.283	4.70	5	16.1592	0.7775	1.2214	1.2087	
Mizrahi	0.985	0.283	5.40	5	35.6754	0.9288	-5.2087		
Chung-Pfost	0.955	0.519	10.33	4	8.4778	0.6244	1.5370	1.7374	
2. No. 1 Garnet wheat (Babbitt, 1945), data points: 12									
Chung-Pfost	0.991	0.220	9.44	6	5.9466	0.4475	1.4641	1.7852	
Oswin	0.990	0.221	9.61	6	9.5347	0.4359	4.6398	1.7852	
Henderson	0.989	0.240	12.23	6	7.9389	0.4152	0.4080		
Halsey	0.988	0.255	19.95	5	12.0817	0.5642	0.9120		
BET	0.966	0.401	12.97	6	5.6268	0.4862	690.8300		
3. Haddock (Wolf et al., 1972), data points: 13									
Hailwood-Harrobin	0.947	0.294	14.92	6	8.9898	0.7524	0.6637	-1.5279	0.2997
Langmuir	0.935	0.291	13.09	5	30.3707	0.2916	4.9932		
Henderson	0.898	0.386	17.66	6	5.9774	0.3565	0.8927	2.1094	
BET	0.891	0.378	19.18	5	3.7123	0.4397	10.5199		
Chung-Pfost	0.888	0.404	16.92	6	3.7240	0.3213	1.0649	1.8628	
II. Hysteresis loop peaked in the multilayer sorption region									
1. Flour (Bushuk and Winkler, 1957), data points: 10									
Hailwood-Harrobin	0.954	0.188	5.98	5	4.5512	0.3215	2.8228	-3.1062	0.0549
BET	0.953	0.161	5.69	5	1.5813	0.2963	43.9486		
Oswin	0.939	0.182	5.41	4	2.7691	0.2483	3.0605		
Halsey	0.939	0.198	6.31	5	5.6117	0.2850	0.2811	1.4905	
Henderson	0.934	0.205	5.54	5	3.6096	0.2320	1.5841	2.7108	
2. Freeze-dried gluten (Bushuk and Winkler, 1957), data points: 10									
Hailwood-Harrobin	0.985	0.111	4.49	5	8.0695	0.3091	2.5485	-1.5067	0.3944
Langmuir	0.983	0.099	3.50	5	16.5462	0.2814	3.7296		
Henderson	0.983	0.110	5.62	5	4.3967	0.3185	1.3366	2.1155	
Oswin	0.982	0.105	6.25	5	3.3875	0.3371	2.4126		
BET	0.981	0.106	7.06	5	2.0325	0.3778	14.0529		
3. Unstored beef (Wolf et al., 1972), data points: 13									
Mizrahi	0.986	0.116	8.33	8	5.4448	0.4291	-0.6894		
Smith	0.979	0.144	14.12	8	0.5955	0.3637	7.1534		
Halsey	0.962	0.203	10.89	8	11.3579	0.4424	0.4835	0.7540	
Oswin	0.926	0.269	15.70	6	5.8197	0.3802	1.4610		
BET	0.919	0.297	18.57	4	6.8952	0.3471	0.9770	1.2990	
III. Hysteresis loop peaked in the capillary condensation region									
1. Millet (Ajisegiri and Sopade, 1990), data points: 11									
Oswin	0.980	0.194	8.22	6	2.6230	0.1450	1.1259		
BET	0.980	0.196	8.81	6	2.1746	0.1492	1.5514		
Halsey	0.980	0.205	10.85	6	5.8302	0.1774	0.3939	0.7434	
Mizrahi	0.978	0.199	10.59	6	2.4113	0.1581	-0.1208		
Henderson	0.976	0.225	7.61	6	4.4042	0.1223	1.0799	0.8210	
2. Rice (Wolf et al., 1972), data points: 9									
Halsey	0.967	0.276	6.39	5	8.6658	0.2677	0.4047	1.0156	
Hailwood-Harrobin	0.965	0.317	7.61	6	3.3554	0.3192	1.2051	-1.5098	0.0733
BET	0.962	0.272	7.59	5	2.4922	0.2425	15.5463		
Oswin	0.948	0.318	9.07	5	4.6372	0.2246	1.9044		
Henderson	0.932	0.398	10.17	5	5.7611	0.2008	1.0715	1.6400	
3. Unstored potato (Wolf et al., 1972), data points: 12									
GAB	0.958	0.414	12.00	4	21.6996	0.3485	1.1104	0.0855	
Smith	0.952	0.421	10.78	7	1.1911	0.1884	8.0867		
Mizrahi	0.942	0.461	12.54	7	5.2612	0.2575	-1.3686		
Halsey	0.941	0.493	12.89	6	10.7458	0.2361	0.4807	1.0140	
Henderson	0.927	0.548	17.07	6	7.1792	0.1359	0.9781	1.7996	

Appendix G-2

Hysteresis model parameters and statistics for inorganic, orgainic and biological materials*

Sorbate	Sorbent	Temp (°C)	Best-fit Model	R^2	Std. Err.	A	B	C	D	Type
Argon	Porous glass	25.3	Henderson	0.876	0.245	12.9261	0.8596	0.7144	0.1251	1
Argon	Chromia gel	25.2	Chung-Pfost	0.917	0.101	0.2791	0.1003	0.9663		1
Nitrogen	Silica gel (Davidson 81)	25.3	Iglesias&Chirife	0.966	4.270	10.8686	0.2398	-1.9756	211.8436	1
Ethanol	Egg Albumin	25	Langmuir	0.982	0.041	11.4514	0.1001	8.9229		2
Diethyl ether	Egg Albumin	25	Langmuir	0.951	0.018	2.0950	0.1000	6.1898		2
Water	Cellulose	25	Iglesias&Chirife	0.989	0.069	2.1646	0.0110	-0.3602	-0.3840	3
Water	Agar	25	Iglesias&Chirife	0.970	0.223	0.9006	0.0419	-2.2059	-1.2376	3
Water	Egg Albumin	25	Chung-Pfost	0.899	0.135	1.0366	0.1004	0.7046		3
Water	Potato starch	25	Chung-Pfost	0.819	0.264	2.4071	0.1001	1.1085		3
Water	Rapeseed	25	BET	0.970	0.046	3.1167	0.3534	5.0197		3
Water	Corn	5	Iglesias&Chirife	0.927	0.144	1.5799	0.0429	0.5194	-0.5068	3
Water	Corn	25	Iglesias&Chirife	0.999	0.020	0.4230	0.0699	1.9135	46.2948	3
Water	Corn	45	Chung-Pfost	0.930	0.081	5.8177	1.3894	5.2929		3

Note: Temp - The temperature at which hysteresis data were obtained.

A, B, C, D - The constants contained in the hysteresis models.

Type - Sorption types: 1-inorganic gas in inorganic sorbent; 2-organic gas in organic sorbent; 3-inorganic gas in organic or biological materials.

* Refer to Yang et al. (1996a) for details.

IMAGE EVALUATION
TEST TARGET (QA-3)

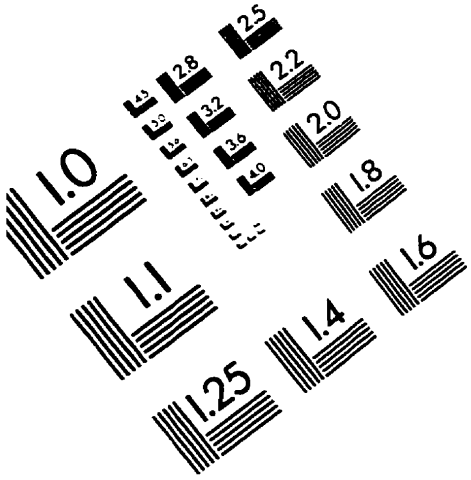

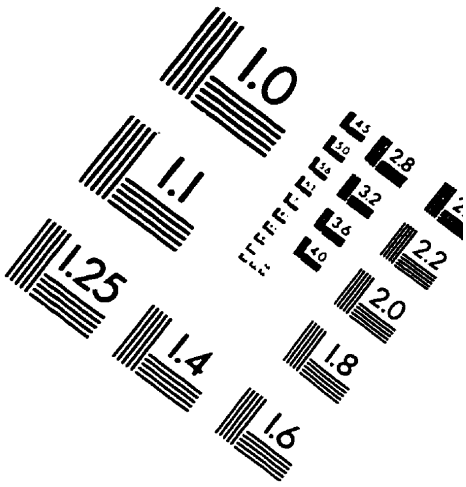

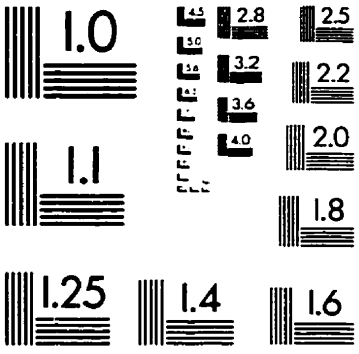

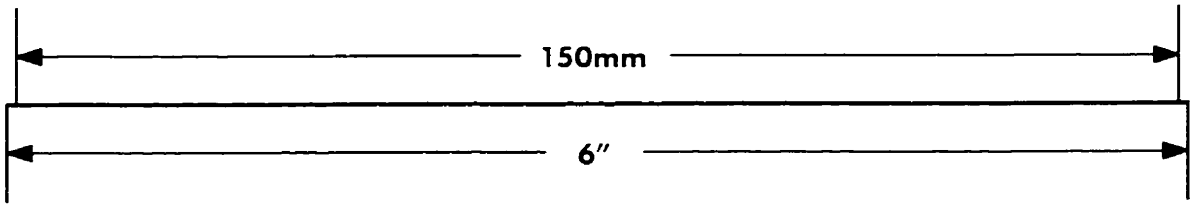

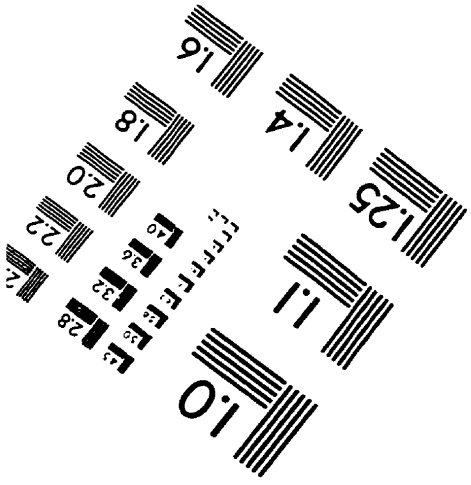

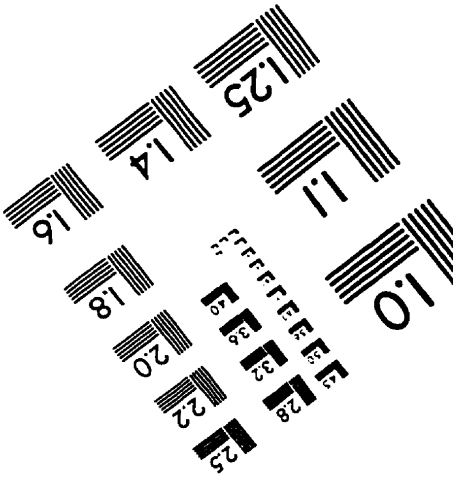

APPLIED IMAGE, Inc
1653 East Main Street
Rochester, NY 14609 USA
Phone: 716/482-0300
Fax: 716/288-5989